

TECHNISCHE UNIVERSITÄT MÜNCHEN

Max-Planck-Institut für Biochemie

Genetic code engineering with methionine analogs for synthetic biotechnology

Carlos Guillermo Acevedo Rocha

Vollständiger Abdruck der von der Fakultät für Chemie der Technischen Universität München zur Erlangung des akademischen Grades eines

Doktors der Naturwissenschaften

genehmigten Dissertation.

Vorsitzender:

Univ.-Prof. Dr. Michael Groll

Prüfer der Dissertation:

1. Univ.-Prof. Dr. Nediljko Budisa
2. Univ.-Prof. Dr. Thomas Kiefhaber

Die Dissertation wurde am 24.06.2010 bei der Technischen Universität München eingereicht und durch die Fakultät für Chemie am 23.07.2010 angenommen.

To my lovely family

“To put the world right in order, we must first put the nation in order; to put the nation in order, we must first put the family in order; to put the family in order, we must first cultivate our personal life; we must first set our hearts right.”

Confucius

Parts of this work are planned to be, or have been submitted to publication:

Nehring S*, **Acevedo-Rocha CG***, Hoesl MG*, et al. Lipase congeners with enhanced resistance toward additives. (*contributed equally; in preparation)

Hoesl MG*, **Acevedo-Rocha CG***, Nehring S*, et al. Lipase congeners designed by genetic code engineering. (*contributed equally; submitted)

Poster presentations:

Acevedo-Rocha CG, Merkel L, and Budisa N. "Translation initiation by means of β -Cyclopropylalanine" 2008. International Conference on aminoacyl-tRNA synthetases: From basic mechanisms to systems biology, Veyrier-du-Lac, France

Other scientific publications:

Acevedo-Rocha CG, et al. Synthetic cells and genomes (in preparation)

Acevedo-Rocha CG, Geiermann AS, Budisa N, Merkel L. *In vivo* unnatural translation initiation. (in preparation)

Sharp L and **Acevedo-Rocha CG**. New Frontiers in Science. *Offspring* (Official magazine from the Max Planck PhDnet; in press)

Acevedo-Rocha CG, Yu J y Dobay A. Entgrenzung – transcending boundaries across scientific disciplines. *Arkhai* 2010; (14)23-40

Acevedo-Rocha CG and Steinbach J. The Art of Science and the Science of Art. *Offspring* 2009; (4)8-13

Acknowledgments

I would like to thank very much the following people:

- Prof. Dr. Nediljko Budisa for his kindness, openness, support, motivation, originality, good sense of humour, priceless freedom, exciting discussions about science, history, politics, and the world. He provided me a solid ground where I could grow as a person and as an open-minded scientist.
- Prof. Dr. Michael Groll and Prof. Dr. Thomas Kiefhaber for allowing me to present them my dissertation.
- Prof. Dr. Thomas Kiefhaber, Prof. Dr. Elena Conti, Dr. Daniel Wilson, and Dr. Birgit Wiltschi for being part of my thesis advisory committee.
- Prof. Dr. Dieter Oesterhelt and his incredible friendly group of people for permitting me to work in his department of “Membrane Biochemistry”.
- Prof. Dr. Garabed Antranikian and Dr. Maryna Royter for allowing me to cooperate and to learn new things about the exciting field of biocatalysis.
- Prof. Dr. Zoya Ignatova for her motivation and input with my thesis work, and for the original scientific cooperations.
- Prof. Dr. Yves Mechulam and Prof. Dr. Peter Schultz for sending kindly some of the plasmids used in this work.
- Prof. Dr. Robert Huber for giving me the great chance to meet his student.
- Dr. Caroline Koehrer for her technical help and nice scientific discussions.

- Dr. Harald Huber, Prof. Dr. Nick Talbot, Dr. Michael Kershaw, Dr. Gaia Travosanis, Mrs. Tatjana Kleine, Mr. Christian Hoffman, and Mrs. Sylvia Reddehase for giving me genomic DNA or cDNA from different organisms.
- Dr. Joerg Tittor, Dr. Gong Zhang, and Mr. Wolfgang Schloegl for their special help with radioactive experiments.
- Mrs. Elisabeth Weyher-Stingl, Mr. Snezan Marinkovic and Mr. Reinhard Mentele for their great expertise and help concerning scientific issues.
- Mrs. Petra Birle, Mrs. Tatjana Krywcun, and Mrs. Traudl Wenger for her invaluable technical assistance and help, especially for the cloning work and the purification of alloproteins.
- Dr. Birgit Wiltschi for her great supervision, exciting scientific discussions, and helpful manners to make me think differently about science, as well as her feedback with the thesis and her organized way of working.
- Dr. Yuri Cheburkin for his supervision during my first internship at the Budisa lab, and for his technical aid and advises.
- Dr. Lars Merkel for his cordial support in the lab, synthesis of amino acids, great input with my thesis, and for this great teachings in chemistry and art.
- Prof. Dr. Shouliang Dong for his great support with the synthesis of amino acids.
- Mr. Martin Turk for his great help and expertise related to enzyme modeling.
- Mrs. Pamela David for her exact and great proof-reading quality of my thesis.

- Dr. Maud Larregola, Thomas Steiner, and Michael Hoesl for their great input in my thesis and their cordiality in the last weeks of this voyage.
- My easy-going colleagues Michael Hoesl, Dr. Christina Wolschner, Dr. Sandra Lepthien, Sebastian Nehring, Lena Strube, Anna Skrollan-Geiermann, Dr. Hamid Heidary, Dr. Maud Larregola, and Thomas Steiner for their great support and exciting moments during the PhD.
- My hard-working students Alessandro de Simone, Franziska Benedikter, Harini Venkataraman, Kathy Schmohl, Julia Kobuch, Tian Tian, and Katharina von Roman for their special help and fun in the lab.
- Mr. Konrad Frischeisen for giving me the great opportunity to start a scientific career in Germany, and for his influential discussions on epistemology.
- Dr. Hans-Joerg Schaeffer, Dr. Ingrid Wolf, and Mrs. Maximiliane Reif for their great support and dedication on having an amazing IMPRS office.
- My dearest friends Rosy Elena Yañez García, Ernesto Arturo Márquez Waldthausen, Leonie Waanders, Andreas Kopp, Marisaura López, Konrad Hoenl, Ákos Dobay, and Jerry Yu for their friendship, support, and good moments of joy.
- My wonderful parents Yolanda and Guillermo, as well as my priceless siblings Eyra Angélica, Luis Guillermo, and Braulio for their love, care support, motivation, advises, and guidance during all my life.
- My beloved girlfriend Friederike for her precious love, enormous care, great support, invaluable help, incredible good sense of humour, amazing dedication, and unique patience, among many other great qualities.

Abbreviations

Abbreviations are used according to the International Union of Pure and Applied Chemistry (IUPAC) and the joint commission for biochemical nomenclature (IUPAC-IUB).

A

AA	Amino Acid
AA-AMP	Aminoacyladenylate
AARS	Aminoacyl-tRNA synthetase
AaMetRS	<i>Aquifex aeolicus</i> methionyl-tRNA synthetase
Aha	L-Azidohomoalanine
Ala	L-Alanine
Amp	Ampicillin
Anl	L-Azidonorleucine
approx.	approximately
APS	Ammonium persulfate
Arg	L-Arginine
Asn	L-Asparagine
Asp	L-Aspartate or aspartic acid
ATP	Adenosine triphosphate
AUG	Starting codon

B

b*1M	barstar mutant P28A/C41A/C83A containing one AUG codon
b*2M	barstar mutant P28A/C41A/E47M/C83A with two AUG codons
BLA	Basal Lipase Activity
BME	β -Mercaptoethanol

C

CAI	Codon Adaptation Index
CHAPS	3-[(3-Cholamidopropyl)dimethylammonio]-1propanesulfonate
Cpa	L-Cyclopropylalanine
CD	Circular Dichroism
CV	Column Volume
Cys	L-Cysteine

D

Da	Dalton
Dpg	L-Dihomopropargylglycine
DMSO	Dimethyl sulfoxide
Don	L-6-diazo-5-oxo-norleucine
DNA	Deoxyribonucleic acid
DTT	Dithiothreitol

E

<i>E. coli</i>	<i>Escherichia coli</i>
<i>EcMetRS</i>	<i>E. coli</i> methionyl-tRNA synthetase
EDTA	Ethylenediaminetetraacetic acid
ϵ M	Molar extinction coefficient
ESI-MS	Electrospray ionization mass spectrometry
Eth	L-Ethionine
EtOH	Ethanol

F

fMet	formylmethionine
------	------------------

G

GdnCl	Guanidine hydrochloride
Gln	L-Glutamine
glnS	glutamine-tRNA synthetase promoter

glnS'	glutamine-tRNA synthetase mutated promoter
Glu	L-glutamate or glutamic acid
Gly	L-Glycine

H

h	hour
His	L-Histidine
His-Tag	6x histidine tag
Hpg	L-Homopropargylglycine

I

I	Induced cells
IF	Insoluble Fraction
IEX	Ion Exchange Chromatography
IPTG	Isopropyl- β -D-thiogalactopyranosid
Ile	L-Isoleucine

K

Kan	Kanamycin
kDa	kilo Dalton = 1000 Daltons

L

LB medium	Luria Bertani medium
L	Liter
Leu	L-Leucine
Lys	L-Lysine

M

M	Molar
Met	L-Methionine
min	minute(s)

MjMetRS	<i>Methanocaldococcus jannaschii</i> methionyl-tRNA synthetase
Mox	L-Methoxinine
MS	Mass Spectrometry
mRNA	messenger ribonucleic acid
MW	Molecular Weight

N

Nhm	N-hydroxy-methionine
NI	None-Induced cells
Ni-NTA	Nickel nitrilo-acetic acid
Nle	L-Norleucine (L-6-aminohexanoic acid)
NMM	New Minimal Medium
NpMetRS	<i>Natronomonas pharaonis</i> methionyl-tRNA synthetase

O

OD ₆₀₀	Optical density at 600 nm
Omd	L-aspartic acid β-methyl ester
Ome	L-gutamic acid γ-methyl ester
ON	Overnight

P

PaMetRS	<i>Pyrobaculum aerophilum</i> methionyl-tRNA synthetase
PabMetRS	<i>Pyrococcus abyssi</i> methionyl-tRNA synthetase
PAGE	Polyacrylamide gel electrophoresis
PBS	Phosphate buffered saline
PCR	Polymerase chain reaction
PDB	Protein data bank
Pefabloc	4-(2-aminoethyl)-benzenesulfonyl fluoride hydrochloride
pH _{opt}	pH optimum
Phe	L-Phenylalanine
PMSF	Phenylmethylsulfonyl fluoride

pNPP	<i>p</i> -nitrophenyl palmitate
PPi	Pyrophosphate
Pro	Proline
pTEc	plasmids for Tandem expression in <i>E. coli</i>
PVA	Polyvinylalcohol
Pyr	Pyrrolysine

R

<i>rho T</i>	rho T terminator
RNA	Ribonucleic acid
rpm	rotations per minute
RP-HPLC	Reversed phase high pressure liquid chromatography
RT	Room temperature

S

SaMetRS	<i>Sulfolobus acidocaldarius</i> methionyl-tRNA synthetase
Sa-tRNA ^{Met1}	<i>S. acidocaldarius</i> elongator transfer RNA for methionine No. 1
<i>S. cerevisiae</i>	<i>Saccharomyces cerevisiae</i>
ScMetRS	<i>Saccharomyces cerevisiae</i> methionyl-tRNA synthetase
Sel	L-Selenomethionine
Ser	L-Serine
SCS	Stop Codon Suppression
SDS	Sodium Dodecyl Sulphate
SF	Soluble Fraction
SPI	Supplementation-based Incorporation
Strep-Tag II	Streptavidine tag II

T

TEMED	<i>N,N,N',N'</i> -Tetramethylethyldiamine
TaMetRS	<i>Thermoplasma acidophilum</i> methionyl-tRNA synthetase
TFA	Trifluoroacetic acid

Abbreviations | X

Tel	L-Telluromethionine
Tfm	5,5,5-trifluoromethionine
Tfn	6,6,6,-trifluoronorleucine
Thr	L-Threonine
T _{opt}	Temperature optimum
Tris	Tris(hydroxymethyl)aminomethane
Triton	Polyethylene glycol p-(1,1,3,3-tetramethylbutyl)-phenyl ether
tRNA	transfer ribonucleic acid
tRNA ^{fMet}	Bacterial initiator tRNA for methionine
tRNA ^{Met}	Bacterial/Eukaryotic/Archaeal elongator tRNA for methionine
tRNA _i ^{Met}	Eukaryotic/Archaeal initiator tRNA for methionine
Trp	L-Tryptophan
TTL	<i>Thermoanaerobacter thermohydrosulfuricus</i> Lipase
TTL[Aha]	Methionine residues replaced by azidohomoalanine in TTL
TTL[Nle]	Methionine residues replaced by norleucine in TTL
Tween 20	Polyoxyethylene (20) sorbitan monolaurate
Tween 80	Polyoxyethylen (20) sorbitan monooleat
Tyr	L-Tyrosine

U

UAA	Ochre stop codon
UAG	Amber stop codon
UGA	Opal stop codon

V

Val	L-Valine
v/v	volume per volume

W

WT	Wild Type
w/v	weight per volume

Summary

In this work, the lipase from the thermophilic anaerobic bacterium *Thermoanaerobacter thermohydrosulfuricus* expressed in *E. coli* was used as model protein to engineer the genetic code. Two methionine analogs with opposite polarities, the strictly hydrophobic norleucine and the highly hydrophilic azidohomoalanine, were used to globally replace all methionine residues in lipase. The substitution yielded lipase congeners with remarkable differences in enzyme activity when compared to the parent protein. The novel and emergent features of the lipase congeners are reflected in changes in optimal temperature and pH, thermostability, substrate access and specificity, as well as resistance toward additives of diverse nature.

Additionally, the first efforts toward the development of a method for the position-specific replacements of Met residues in *E. coli* are also presented. To this end, the host methionyl-tRNA synthetase (MetRS) along its cognate initiator tRNA^{fMet} can be used to initiate protein synthesis, while an exogenous MetRS imported with its cognate elongator tRNA^{Met} is left to decode internal positions more efficiently. The fact that *S. acidocaldarius* MetRS is orthogonal in *E. coli*, and that it prefers activating ethionine over azidohomoalanine while *E. coli* MetRS displays an opposite amino acid preference, serves as a starting point to reprogram protein translation *in vivo*. In this context, it is intended that the N-terminus is translated with one Met analog and the internal positions with another one. In the future, this platform could allow engineering the genetic code of important biocatalysts for synthetic biotechnology.

Table of contents

1	Introduction	1
1.1	Synthetic biology	2
1.1.1	Genetic code engineering	5
1.1.2	Incorporation of methionine analogs into proteins <i>in vivo</i>	9
1.2	The role of methionine in proteins	13
1.2.1	Methionine as key residue of protein oxidation	14
1.2.2	The Janus face of protein synthesis	14
1.3	Industrial biotechnology	19
1.3.1	The search for the ideal biocatalyst	19
1.3.2	The most versatile biocatalyst: Lipase	20
2	Goal	25
3	Results and discussion	27
3.1	Engineering lipase with methionine analogs	27
3.1.1	Expression and purification	28
3.1.2	Incorporation efficiency	29
3.1.3	Basal lipase activity	30
3.1.4	Optimal temperature and pH	30
3.1.5	Thermostability	32
3.1.6	Thermal activation	33
3.1.7	Substrate specificity	37
3.1.8	Influence of additives on lipase activity	40

3.2	Making up the faces of Janus.....	49
3.2.1	Searching for an orthogonal pair of methionine	49
3.2.2	Incorporation of Aha and Eth into barstar 1M	63
3.2.3	Incorporation of Aha and Eth into barstar 2M	68
3.2.4	Cloning of orthogonal pair and SaMetRS expression	73
4	Conclusions	83
5	Outlook	85
6	Experimental section	87
6.1	Materials	87
6.1.1	Equipment	87
6.1.2	Extendable materials	88
6.1.3	Chemicals.....	88
6.1.4	Commercial reagents.....	89
6.1.5	Buffers and solutions	90
6.1.6	Media and supplements.....	91
6.1.7	Bacterial strains	92
6.1.8	Plasmids	93
6.1.9	Software	102
6.2	Methods	102
6.2.1	Molecular biology.....	102
6.2.2	Microbiology.....	104

6.2.3	Biochemistry	108
6.2.4	Spectroscopy and spectrometry	109
6.2.5	Informatics	113
7	List of figures	115
8	List of tables.....	116
9	Appendix.....	117
9.1	Primary amino acid sequence of TTL.....	117
9.2	Primary sequence of barstar 1M (P28A/C41A/C83A)	117
9.3	Primary sequence of barstar 2M (P28A/C41A/E47M/C83A).....	117
9.4	MetRS alignment.....	117
9.5	pTEc0 sequence	119
9.6	pTEc1 sequence	125
9.7	pTEc1.1G-R/L sequence.....	134
9.8	pTEc2 sequence	144
10	References.....	155

1 Introduction

Biology is changing: During the half-century between the deciphering of the genetic code and the sequencing of the human genome, it became clear that biology is essentially an information science with deoxyribonucleic acid (DNA) as a storage device. Systems biology has latterly emerged fuelled by the generation of enormous amounts of data from large-scale top-down profiling 'omics' technologies (genomics, transcriptomics, proteomics, metabolomics, lipidomics, glycomics, interactomics, fluxomics, biomics) and its subsequent analysis using refined computational tools. The volume of these data is indicative of the complexity of biological systems. It is thus necessary to generate tools and methods that will help us to characterize and manipulate any biological molecule as it works in its native habitat. In order to achieve this, the crosstalk between systems biology and the emerging field of synthetic biology will be of primary importance in expanding our understanding of biological phenomena and in finding applications for societal benefit.

1.1 Synthetic biology

Synthetic biologists seek to build well-characterized, nature-inspired complex devices that perform desired tasks. There are two main approaches to engineer artificial biological systems. The best known is the top-down approach where a living system is re-designed for particular purposes. For instance, the genome of *Mycobacterium genitalium* was synthesized and assembled *de novo* through the use of nucleic acid synthesis and recombinant DNA technology.¹ This challenging experiment showed that it is, in principle, feasible to artificially clone and, thus, manipulate a whole genome of an organism. These cells could ultimately be used for numerous applications e.g. efficient production of pharmaceuticals, biofuels, or even extraction of useful genomic information from microorganisms that are difficult to cultivate, given that the majority of microbes are difficult or almost impossible to cultivate. On the other hand, the bottom-up strategy involves the small-scale synthesis of nucleic acids, metabolites, and protocells, which are artificial self-assembling and self-reproducing chemical systems. One example is the concept of 'BioBricks', which are standard DNA parts encoding basic biological functions. There is hope that it will be possible to program living organisms in the same way that a computer scientist can program a computer.²

Similarly, living systems have already been designed to stimulate pattern formation³, disperse biofilms⁴, produce drugs⁵, or target cancer cells⁶. Furthermore, the subfield of synthetic metabolism, defined as engineering biology at the protein and pathway scales⁷, will also play a significant role in the consolidation of synthetic biology. This subfield focuses on the production of valuable and useful compounds for which there are no known natural biochemical synthesis pathways. The design and assembly of synthetic metabolic pathways has much potential for optimizing the current enzyme-catalyzed industrial processes used in the production of fine chemicals. The integration between synthetic pathways and proteins will be of utmost importance for synthetic biology.⁸

The generation of synthetic proteins can be done either by the expansion or the engineering of the genetic code. The expansion of the genetic code refers to methods where DNA mutagenesis is required to consider some termination triplets (e.g. amber) or quadruplets as blank codons for expansion of protein functions. Synthetic amino acids are incorporated into single recombinant proteins by means of a nonsense or frameshift suppression using genetically engineered components of the translational machinery including aminoacyl-tRNA synthetases, transfer RNAs, or ribosomes.

On the other hand, the genetic code engineering relies on the substrate tolerance of cellular uptake and endogenous translation systems, which allows synthetic amino acids to be successfully incorporated into proteins. This methodology allows the residue-specific replacement of a particular amino acid at all positions via sense codon reassignment in a target protein without the need for DNA mutagenesis. Proteins produced in this manner are typically referred to congeneric (from old Latin), meaning 'born together' or 'belonging to the same race or kind' since they are encoded by the same gene but contain only a small fraction of amino acids exchanged with analogs in a residue-specific manner.

The final goal of these bottom-up approaches in the framework of synthetic biology is to extend the synthetic capacities of the protein translation machinery. In this way, the coding capacities of the genetic code will also be enhanced either by including reassignment of existing coding units or the introduction of novel ones. In the long-term, these efforts will help in controlling cellular processes and synthetic cellular systems.

To summarize, the long term goal for synthetic biology is that the bottom-up and top-down approaches meet and contribute to produce 'encapsulated complex systems' that would be the starting point for a wide range of genetic programming applications (**Figure 1**).

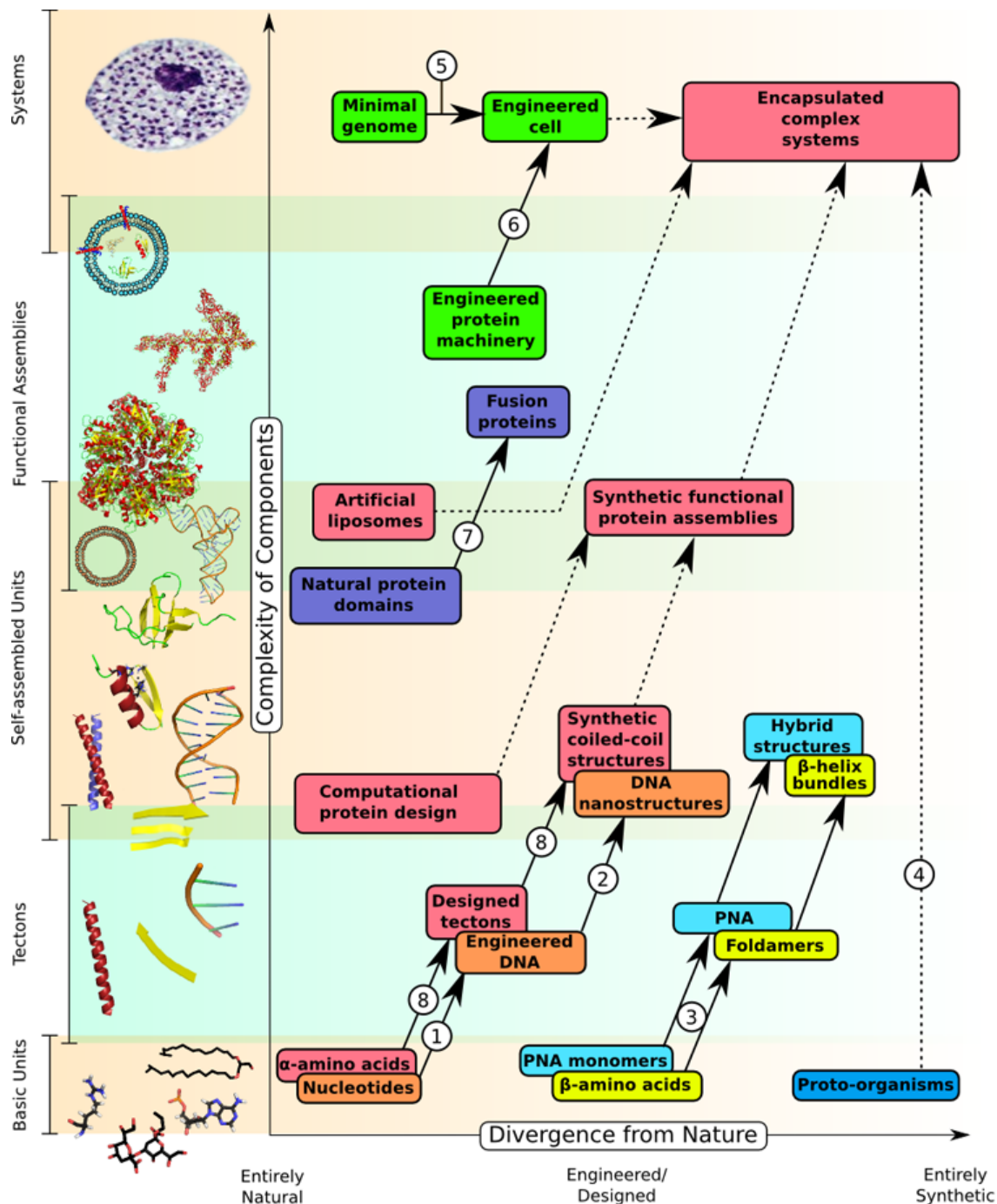


Figure 1. Synthetic biology. Nucleic acids, amino acids or protocells (basic units) of diverse chemistry (entire/partial natural/synthetic) can be linked to form polymers (tectons) whose self-assembly into defined structures will allow functional modules to design a synthetic system that performs a specific task. The efforts in the bottom-up and top-down research approaches (indicated by numbers) to engineer components display different levels of complexity (copyright-free image taken from the Synthetic Components Network at the University of Bristol, UK). PNA = Peptide Nucleic Acid

1.1.1 Genetic code engineering

The genetic code is comprised of 61 codons encoding twenty canonical amino acids. As a rule, each codon is translated unambiguously. Of these 20 amino acids, methionine (Met) and tryptophan (Trp) are encoded by a single codon each, while the rest is encoded by at least two degenerate codons. Theoretically, each of the 61 coding triplets should be decoded by specific transfer RNAs (tRNA), the adapter molecule that translates the nucleotide sequence into the amino acid sequence via anticodon-codon recognition. In practice, this number is usually smaller e.g. there are 46 functional tRNAs in *Escherichia coli*⁹ because different tRNAs are capable of reading degenerate (i.e. synonymous) codons that encode only one amino acid type. These tRNAs are termed isoacceptors, and are strictly recognized by their cognate aminoacyl-tRNA synthetase (AARS).

There are generally twenty different AARSs, each one specific for the twenty canonical amino acids. The AARSs recognize their cognate isoacceptor tRNA(s) through several identity elements.¹⁰ For most tRNAs, the determinants are located at the two distal extremities: the amino acid acceptor stem and the anticodon loop. The process of protein synthesis is highly regulated because it involves the precise interplay of a great number of molecules. First, each of the 20 canonical amino acids has to be activated in an ATP-dependent manner by its cognate AARS. Then, the enzyme-bound aminoacyladenylate (AA-AMP) intermediate binds its cognate tRNA(s), and the amino acid is covalently linked to the terminal 2' or 3' hydroxy group of the adenosine in its respective tRNA. Consequently, the charged tRNAs are ready to participate in protein synthesis.

In general, proteins are composed of 'diverse' building blocks, but from the point of view of synthetic biology, the chemical functionalities introduced by the canonical aliphatic, aromatic, basic, acidic, hydroxyl-, and sulfur-containing amino acids are somewhat limited. In fact, to achieve full protein functionality, Nature expands the genetic code by introducing posttranslational modifications (**Figure 2**).¹¹

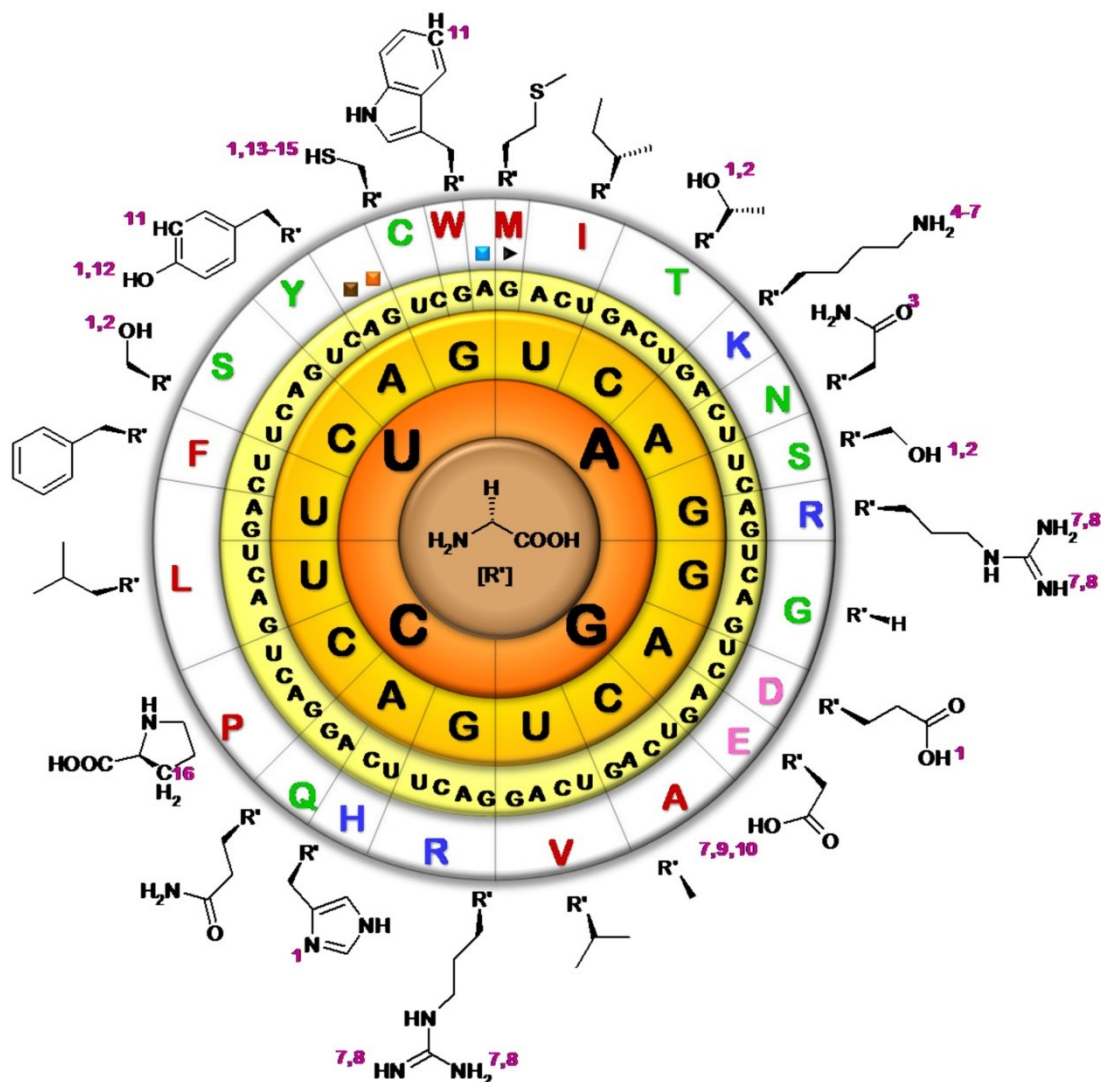


Figure 2. Radial presentation of the universal genetic code in RNA format (previous page). The twenty canonical amino acids are encoded by 61 degenerate codons. M, methionine; I, isoleucine; T, threonine; K, lysine; N, asparagine; S, serine; R, arginine; G, glycine; D, aspartate or aspartic acid; E, glutamate or glutamic acid; A, alanine; V, valine; H, histidine; Q, glutamine; P, proline; L, leucine; F, phenylalanine; Y, tyrosine; C, cysteine; and W, tryptophan. Amino acids are arranged with reference to their physicochemical properties; polar residues are shown in green; nonpolar in red; basic in blue and acidic in pink. Translation initiation and termination are represented with the symbols ► (starting AUG codon) and ■ [stop codon UAA (ochre), UGA (opal), and UAG (amber)], respectively. Post-translational modifications are also indicated with numbers in violet near the specific residue to be modified: 1) Phosphorylation; 2) O-glycosylation; 3) N-glycosylation; 4) Acetylation; 5) Ubiquitination; 6) Biotinylation; 7) Methylation; 8) N-ADP-ribosylation; 9) Polyglycination; 10) Polyglutamylation; 11) Nitration; 12) Sulfation; 13) S-nitrosylation; 14) S-prenylation; 15) S-Acylation; and 16) C-hydroxylation.

Although the AARSs are crucial in the recognition of their cognate amino acids, they are often incapable of distinguishing between similar substrates. This phenomenon is known as substrate tolerance and permits AARSs to recognize and charge noncanonical amino acids onto tRNAs in lieu of the structurally-related canonical counterparts. Thus, it can be said that the fidelity of protein translation basically depends on the tRNA aminoacylation reaction (Figure 3).

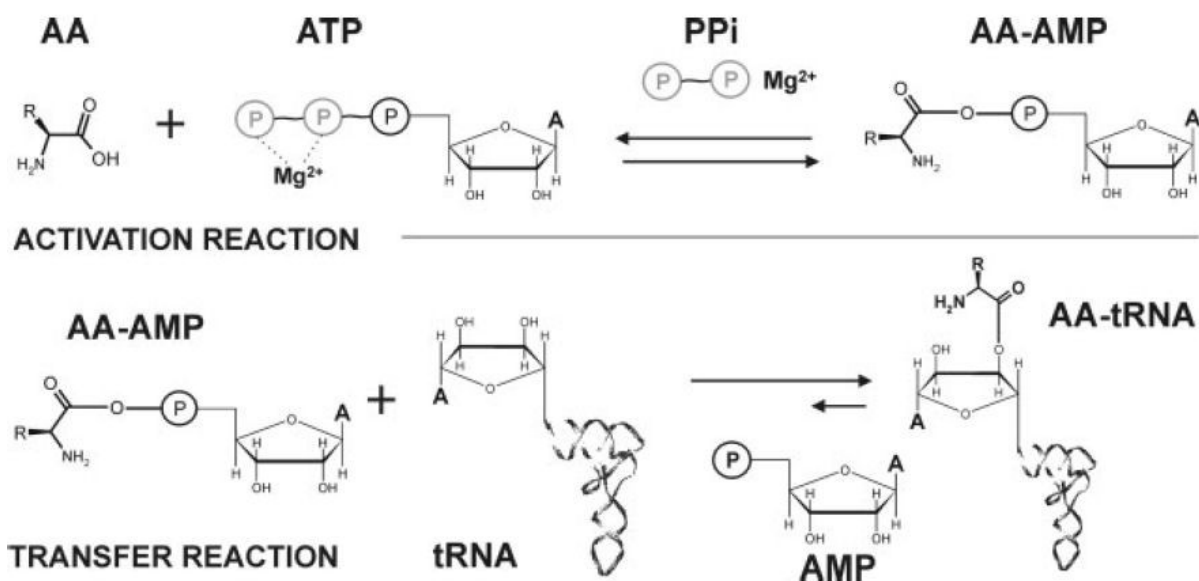


Figure 3. The aminoacylation reaction. In this two-step reaction, the amino acid (AA) is first activated with ATP and Mg²⁺ by the AARS to form an enzyme-bound aminoacyladenylate (AA-AMP) intermediate, accompanied by the release of pyrophosphate (PPi). This complex then binds the cognate tRNA, and the amino acid is covalently linked to the 3'-OH terminal adenosine of tRNA. AMP = adenosine monophosphate (image kindly provided by N. Budisa¹²)

Accordingly, the use of noncanonical amino acids, also termed unnatural, noncognate, or nonproteinogenic amino acids provides proteins with novel and even unexpected (emergent) properties due to the inclusion of new side-chains. Consequently, the addition of a vast array of chemical functionalities like halogeno, keto, cyano, azido, nitro, nitroso, and silyl groups, as well as alkenes and alkynes would permit the design of new protein fluorescent probes, photo-switches, redox markers, and also allow the elucidation of protein-protein interactions or enzyme mechanisms, the study of protein folding, or the determination of 3D protein

structures.¹³⁻¹⁸ As indicated previously, proteins produced in this way can be called congeners since they originate from the same gene sequence, but they contain only a small fraction of amino acids exchanged with synthetic amino acids.

The engineering of the genetic code permits the production of synthetic proteins through the incorporation of noncanonical amino acids not encoded by the standard genetic code. Supplementation-based Incorporation (SPI) is the predominant methodology for engineering the genetic code. SPI allows the residue-specific incorporation of noncanonical amino acids in the resulting polypeptide sequence by reassigning one of the sense codons. This can be achieved through the use of specific amino acid auxotrophic strains and controlled fermentation conditions.¹⁹ While SPI allows the multiple residue-specific incorporation of noncanonical amino acids in response to sense codons, the stop codon suppression (SCS) method allows the addition of noncanonical amino acids at permissive sites of proteins but in a context-dependent manner. In this way, the incorporation of various useful aromatic analogs or extended aromatic systems is possible via orthogonal pairs e.g. *Methanocaldococcus jannaschii* TyrRS:tRNA^{Tyr} in *E. coli*.²⁰⁻²² Similarly, it is possible to incorporate a wide range of pyrrolysine (Pyr) analogs with aliphatic side chains equipped with versatile chemical properties and functionalities into proteins with other pairs such as *Methanosarcina maize* PylRS:tRNA^{Pyl} in response to stop codons in *E. coli*.²³⁻²⁵

Both SCS and SPI methods require the efficient cellular uptake of the desired amino acid analog, its efficient activation by the AARS and charging onto the tRNA, ribosome proofreading, and proper folding of the target protein. Nonetheless, the SPI method is more promising than SCS for designing enzymes with economically important applications for several reasons. First, many biological phenomena like enzymatic activity or folding properties are based on the synergistic effects of different amino acids at several positions in the context of folded protein structures. The SCS method is limited in this regard, since it only allows the insertion of only one, or at best, two analogs into the target sequence.²⁶ Furthermore, the efficiency of synthetic

amino acid incorporation using suppressor-based methodologies is affected by local protein structure, messenger RNA (mRNA) context, and competition with release factors. Third, the design and selection of orthogonal pairs is complex and time-consuming. Finally, the relative low protein yields produced using the SCS method prevents its use in many industrial applications. In contrast, the SPI method is reproducible, efficient, and has the added advantage of requiring a very simple experimental setup.

1.1.2 Incorporation of methionine analogs into proteins *in vivo*

The AUG sense codon has been reassigned to a large repertoire of Met analogs using the SPI method to study their effect in proteomes or target proteins. These experiments have been performed in their entirety in *E. coli* due to its simplicity as a model organism.

The landmark experiment using Met analogs was documented by Lewine and Tarver in 1951.²⁷ A few years later, Cowie and Cohen performed a quantitative replacement of Met by selenomethionine (SeMet; **Figure 4**) in proteins of a Met auxotrophic *E. coli* strain without impairing its cellular viability.²⁸ This was rather an exception since it was known that many noncanonical amino acids are bacteriostatic or bactericidal. In order to circumvent this problem and to enable labeling of single proteins, the translation capacity was resolved from metabolic toxicity. This concept could be experimentally verified only after advancements of recombinant DNA technology. In other words, by using heterologous gene expression systems, the production of fully-substituted single target proteins can be controlled with high efficiency.^{29,30} Three decades later SeMet emerged as an important tool in X-ray crystallography^{31,32} and NMR studies³³ of biological macromolecules. Similar applications can be obtained with the heavy metal-containing Met analog telluromethionine (Tel; **Figure 4**).^{30,34}

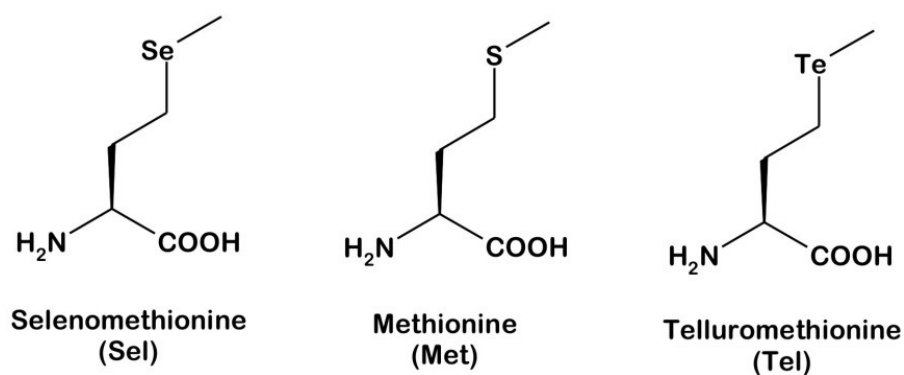


Figure 4. Methionine analogs useful in X-ray crystallography. Selenomethionine contains the heavy atom selenium instead of sulfur, whereas telluromethionine has tellurium.

Surprisingly, amino acids containing organic azides and terminal alkynes proved to be Met analogs (Figure 5).³⁵⁻³⁷ These are currently of particular interest due to the chemical nature of their moieties and their inertness under physiological conditions. These analogs can be used as chemical handles to mimic post-translational modifications using click chemistry.³⁸⁻⁴⁰ The Met analogs azidohomoalanine (Aha) and homopropargylglycine (Hpg), for example, have been used to artificially attach to proteins post-translational modifications like sugars⁴¹ or biotin.⁴² These Met analogs are referred to as bioorthogonal chemical reporters, and have been used in a wide-range of applications including cell biology⁴³, chemical proteomics⁴⁴, or selective modification of virus-like particles⁴⁵, among others.

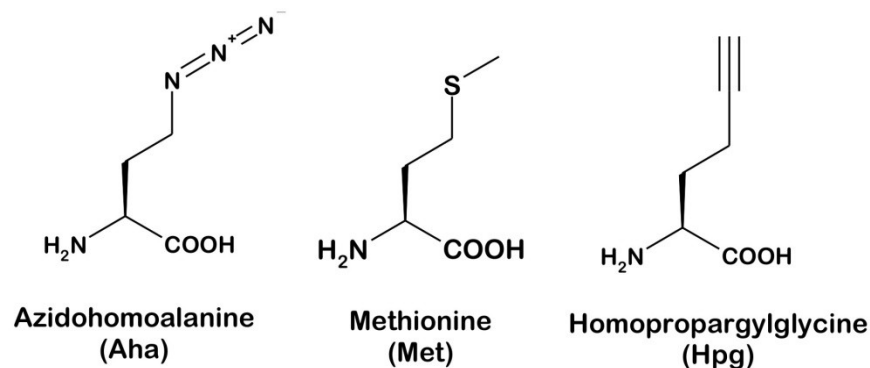


Figure 5. Methionine analogs useful as bioorthogonal reporters. The azide-containing Aha or alkyne-containing Hpg can be used in click chemistry to couple alkyne or azide groups, respectively.

The best approach for unraveling the interactions and relationships responsible for highly specific protein internal architecture and its folding process is by generating non-disruptive isosteric changes in the amino acid side-chains.⁴⁶ In the case of Met, these replacements are at the level of single atoms, as in Norleucine (Nle) and methoxinine (Mox). These Met analogs have already been used to design pro- and anti-aggregation congeners of the prion protein as models for investigating oxidative stress in prion-related neurodegenerative diseases.⁴⁷ In these substitutions, dramatic differences in physicochemical properties provided by the Met analogs were fully reflected in the related prion protein congeners. Mox and Nle have nearly identical chain lengths, the same number of single bonds and exhibit the same resistance to chemical oxidation; however, their polarities are extremely different. Mox is strictly hydrophilic whereas Nle is strongly hydrophobic (**Figure 6**).



Figure 6. Methionine analogs useful for probing protein hydropathy. Mox is strictly hydrophilic with a water solubility (Sol.) of 1000 mM⁴⁷ whereas Nle is neutral and strongly hydrophobic with a water solubility of 120 mM.⁴⁸ In comparison, Met solubility in water is 360 mM.⁴⁸

So far, most of the experiments using Met analogs have been for studying effects on protein architecture, folding, or stability. Its effects on enzymatic activity, however, have not been as extensively investigated, even though there are some reports on enzymes whose activities remain at the basal level or were even increased upon incorporation of the analogs. For example, the substitution of Met with Nle or the similar hydrophilic analog ethionine (Eth; **Figure 7**) often does not affect the enzymatic activity of calmodulin.⁴⁹ The same holds true when Nle was substituted in nuclease⁵⁰ or when trifluoromethionine (Tfm; **Figure 7**) was incorporated into phage lysozyme⁵¹ or

DNA polymerase.⁵² The advantage of using fluorinated analogs such as Tfm is that it can be used for the design of teflon-like or 'non-sticky' proteins.⁵³

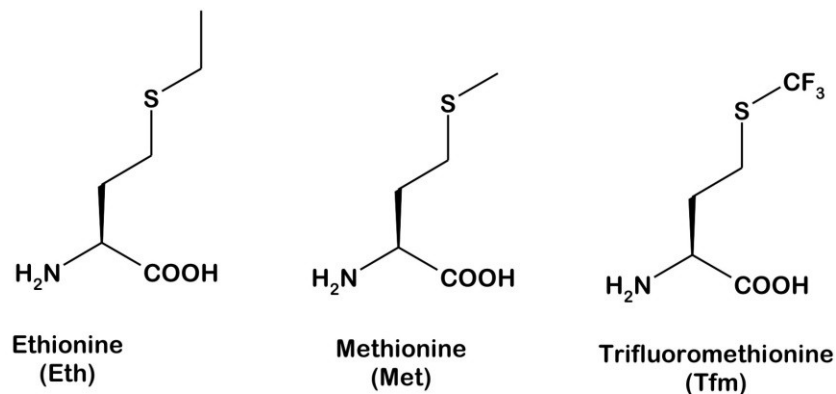


Figure 7. Methionine analogs useful to retain enzymatic activity. Eth and Tfm contain an extra methyl group and three fluorinated atoms, respectively, compared to Met.

There are also cases where the catalytic activity of enzymes is enhanced upon Met-substitution with particular analogs. For instance, the complete substitution of 13 Met residues with Nle in cytochrome P450 resulted in a nearly two-fold increase in peroxygenase activity.⁵⁴ A similar Met to Nle substitution in adenylate kinase results in a derivative with structural and catalytic properties similar to the original enzyme; nonetheless, it also exhibits much higher resistance to hydrogen peroxide inactivation under denaturing conditions.⁵⁵ These studies suggest that noncanonical amino acids could be used not only to retain, but also to enhance the enzymatic activity of proteins. None of these reports, however, systematically explored the impact of using isosteric analogs to manipulate the enzymatic activity of more important biocatalysts like nucleases, isomerases, proteases, amylases, or lipases.

A thorough survey of literature indicates that there are few studies with an intention to improve the catalytic performance of enzymes by incorporating noncanonical amino acids. For example, Tyr analogs have been incorporated into *E. coli* β galactosidase⁵⁶, *Pseudomonas* ketosteroid isomerase⁵⁷ and *Candida antarctica* lipase B.⁵⁸ There are also some reports where Met analogs have been documented.

The first experiment, for instance, was reported by Yoshida in 1959, where Eth as incorporated into *Bacillus subtilis* amylase⁵⁹; the second by Anfisen and Corley in 1969, where Nle was used in *Staphylococcus aureus* nuclease⁵⁰; the third by Cirino *et. al.* in 2003, where Nle was substituted in peroxygenase-active cytochrome P450⁶⁰; the fourth by Walasek and Honek in 2005 for the use of difluoromethionine in alkaline *Pseudomonas aeruginosa* protease⁶¹; the fifth by Schoffelen *et. al.* in 2008, where Aha is incorporated into *C. antarctica* lipase B; however, the main purpose in the last study was to investigate the potential of the click chemistry reaction⁶²; and finally Holzberger *et. al.* in 2010, where Tfm was used in *Thermus aquaticus* DNA polymerase.⁵² In all the aforementioned cases the enzymes remained active, but they were not further characterized. Therefore, understanding deeper the role of Met as well as extensively studying the effects of its replacement by synthetic analogs of such important biocatalysts should be very interesting for both academy and industry.

1.2 The role of methionine in proteins

In all known protein structures, Met comprises only 1.5% of all residues, and these are usually located in positions inaccessible to the bulk solvent, with only 15% of the Met being exposed to the surface.⁶³ There is clearly a link between the nature of Met and the fact that it is normally found inside the protein core. Met is classified as a nonpolar and modestly hydrophobic amino acid. Like cysteine, it contains sulfur; however, the Met sulfur is a part of the relatively inert thioether moiety. Indeed, the Met side-chain is polarizable and flexible, which is often a crucial feature in biological processes such as substrate recognition or packing at hydrophobic interiors of proteins. Furthermore, Met is also implicated in many cellular processes, including cofactor binding, functioning as a methyl donor in DNA methylation, and protein stabilization through its hydrophobic interactions and hydrogen bonding, as well as nonpolar molecular recognition processes.⁶⁴

1.2.1 Methionine as key residue of protein oxidation

Together with cysteine and tryptophan, Met is among the amino acids most prone to oxidation. The Met thioether moiety can be first oxidized to its sulfoxide form, Met(O), to become hydrophilic. The next oxidation step to sulfone is more drastic and rarely occurs in biological systems (Figure 8). Many proteins lose activity upon Met oxidation; in contrast, some proteins are functionally activated upon Met oxidation.⁶⁵

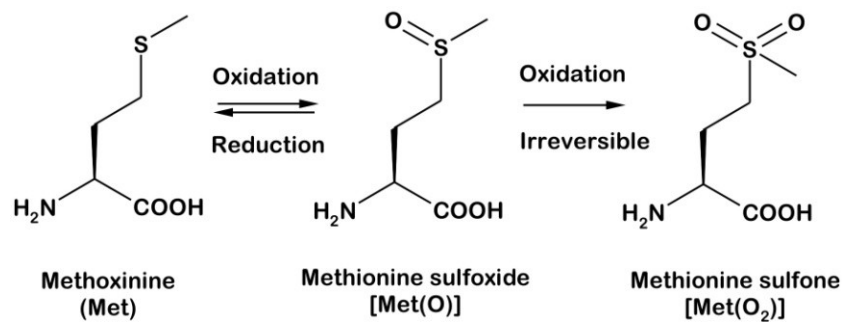


Figure 8. Methionine oxidation. Chemical structures of methionine and its oxidation products methionine sulfoxide and methionine sulfone.

The probability of Met oxidation varies based on its position in the protein structure. For instance, a Met residue near the surface is more easily accessible to oxidation, and would cause the protein to become more hydrophilic. A Met residue buried in a hydrophobic cluster is more protected from oxidation, although some reactive molecular species such as singlet-oxygen diffuse through the protein molecule and could cause oxidation at interior Met residues as well.⁶⁶ The oxidation or reduction of Met is therefore an important event that contributes to protein conformational changes and overall hydrophobicity. The physiological importance of Met oxidation is also gaining much attention because the presence of Met sulfoxide in particular proteins correlates with some pathological conditions like emphysema, arthritis, and cataracts.⁶⁷

1.2.2 The Janus face of protein synthesis

Janus was the Roman god of beginnings and ends. Since he is represented with two

faces looking opposite ways, the term Janus-faced is used to describe someone who is duplicitous. In relation to Met, it is encoded by the AUG codon, but participates in translation with two classes of adaptors, namely the initiator transfer RNA ($\text{tRNA}^{\text{fMet}}$ in prokaryotes and eukaryotic organelles, or $\text{tRNA}_i^{\text{Met}}$ in eukaryotes and in archaea), which is exclusively used for initiation of protein synthesis, and the elongator transfer RNA (tRNA^{Met}), which inserts Met in response to internal AUG codons in a protein sequence. Due to its double function, Met can be considered as the Janus-faced amino acid of protein translation.

In *E. coli*, Met is activated by the methionyl-tRNA synthetase (*EcMetRS*), whose functional form is a homodimer composed of two 76 kDa monomers. A 64 kDa monomeric *EcMetRS* fragment generated by a C-terminal trypsin cleavage was used to determine the 3D structure of the free enzyme (Figure 9).⁶⁸⁻⁷⁰ The crystal structures of *EcMetRS* confirm that the enzyme is organized into an N-terminal domain containing the active site and a C-terminal domain responsible for recognition of its cognate tRNAs. As a metalloenzyme, in addition, *EcMetRS* contains one tightly bound zinc ion for the correct folding of the enzyme.

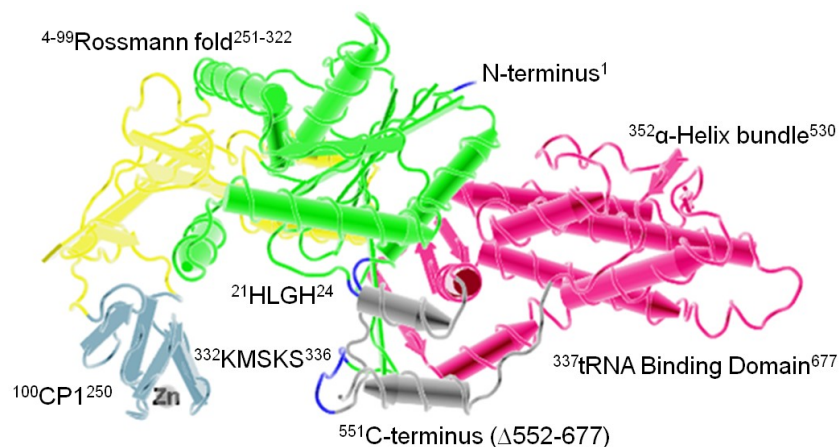


Figure 9. Ribbon diagram of the 3D crystal structure of monomeric *EcMetRS*. The *EcMetRS* (residues 1–551 with truncated C-terminus [$\Delta 552-677$]; PDB: 1QQT) shows three distinguishable domains: the Rossmann fold (green and yellow), the connective polypeptide-Zn-finger domain (light blue), and the α -helix bundle-anticodon binding domain (red and gray). The Class I Rossmann fold signature sequences HLGH and KMSKS responsible for ATP and Met binding are shown in blue.

EcMetRS methionylates the 2'-hydroxyl group of the terminal adenosine in both the initiator tRNA^{fMet} and elongator tRNA^{Met}, which have as common identity elements the A⁷³ base, the base pairs G²C⁷¹, C³G⁷⁰ and the CAU anticodon (Figure 10).

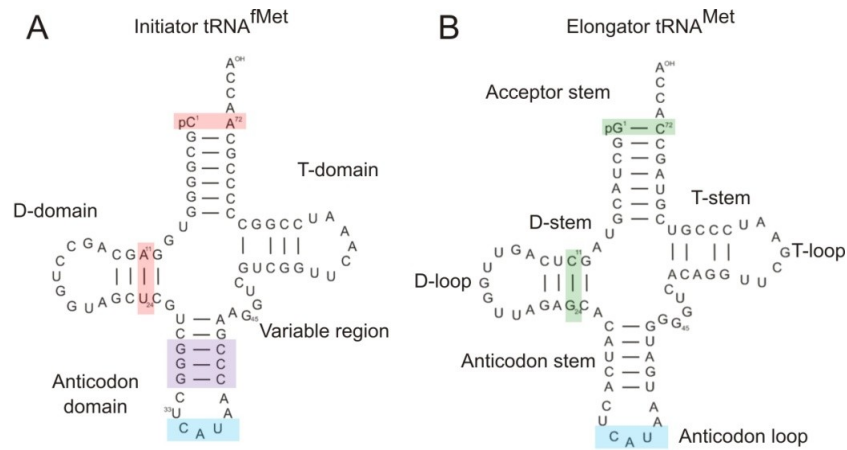


Figure 10. *E. coli* tRNAs^{Met}. Secondary structure of A) initiator tRNA^{fMet} and B) elongator tRNA^{Met} from *E. coli*.^{71,72} A tRNA molecule of canonical cloverleaf structure consists of four domains: The dihydrouridine (D), thymidine (T), anticodon and acceptor arm. Each domain has a stem and loop region. A variable arm occurs between the anticodon and T domains. The required identity elements for formylation (red), initiation (purple), elongation (green) and aminoacylation (blue) are shown.

Interestingly, there are approximately five times more internal AUG codons than initiator codons, but twice as much initiator tRNA^{fMet} than elongator tRNA^{Met} in *E. coli*.⁷³ This high intracellular concentration of tRNA^{fMet}, along with the participation of three initiation factors (IF1, IF2, and IF3), GTP, and the mRNA at the ribosome reflects the complexity of translation initiation.⁷⁴ In this event, the crucial step is when IF1 directs the formylmethionyl-tRNA^{fMet} (fMet-tRNA^{fMet}) to the peptidyl-site (P-site) of the small ribosomal subunit so that it could interact with the AUG initiation codon on the mRNA and form a stable complex with IF2 and IF3. Intriguingly, it is believed that Met starts translation because it is the most expensive amino acid to synthesize.⁷⁵ Additionally, 60% of the N-terminal Met residues in *E. coli* are subject to removal to provide proteins with further biological activity.⁷⁶ In this way, the cell would recycle a pool of Met and save energetic costs by coupling translation either to the intermediary metabolism or to its chemical environment.

In translation elongation, aminoacylated elongator tRNAs (aa-tRNAs), GTP, and three elongation factors (EF1A or EF-Tu, EF1B or EF-Ts, and EF2 or EF-G) are involved. The EFs transfer the aa-tRNA that corresponds to the next codon on the mRNA to the aminoacyl-site (A-site) of the ribosome. A peptide bond is then formed between the first and second amino acids, and the deacylated tRNA moves from the P-site to the exit-site (E-site), while the A-site-aa-tRNA translocates into the P-site with aid of the EFs. This cycle is repeated with the ribosome sliding along the mRNA as it is decoded into a polypeptide chain, which is synthesized at a rate of approximately 12 amino acids per second.⁷⁷ If an internal AUG is found, a Met will be incorporated by the elongator tRNA^{Met} in the growing polypeptide chain. Importantly, the initiator tRNA^{fMet} and elongator tRNA^{Met} isoacceptors have remarkable differences in their primary structure (Table 1), which serves as the basis for their accurate recognition during protein initiation or elongation.

Table 1. Identity elements that differentiate the *E. coli* initiator tRNA^{fMet} and elongator tRNA^{Met}.

Features	tRNA ^{fMet}	tRNA ^{Met}
Initial ribosomal binding site	P-site	A-site
Mismatch 1-72 in the acceptor stem	+	-
Purine11:Pyrimidine24 base pair in the dihydrouridine stem	+	-
3 consecutive paired guanosines and cytosines in the anticodon stem	+	-
Interaction of the anticodon loop (CAU) and stem (G-C) ₃ with the IF3	+	-
Recognition of fMet by IF2	+	-
Recognition by EF1A (EF-Tu)	-	+

+ = presence; - = absence

Figure 11 shows the scenario when the AUG triplet is decoded both at initiation and elongation of protein synthesis. Finally, translation is terminated when the ribosome encounters a stop codon on the mRNA and the protein is released.

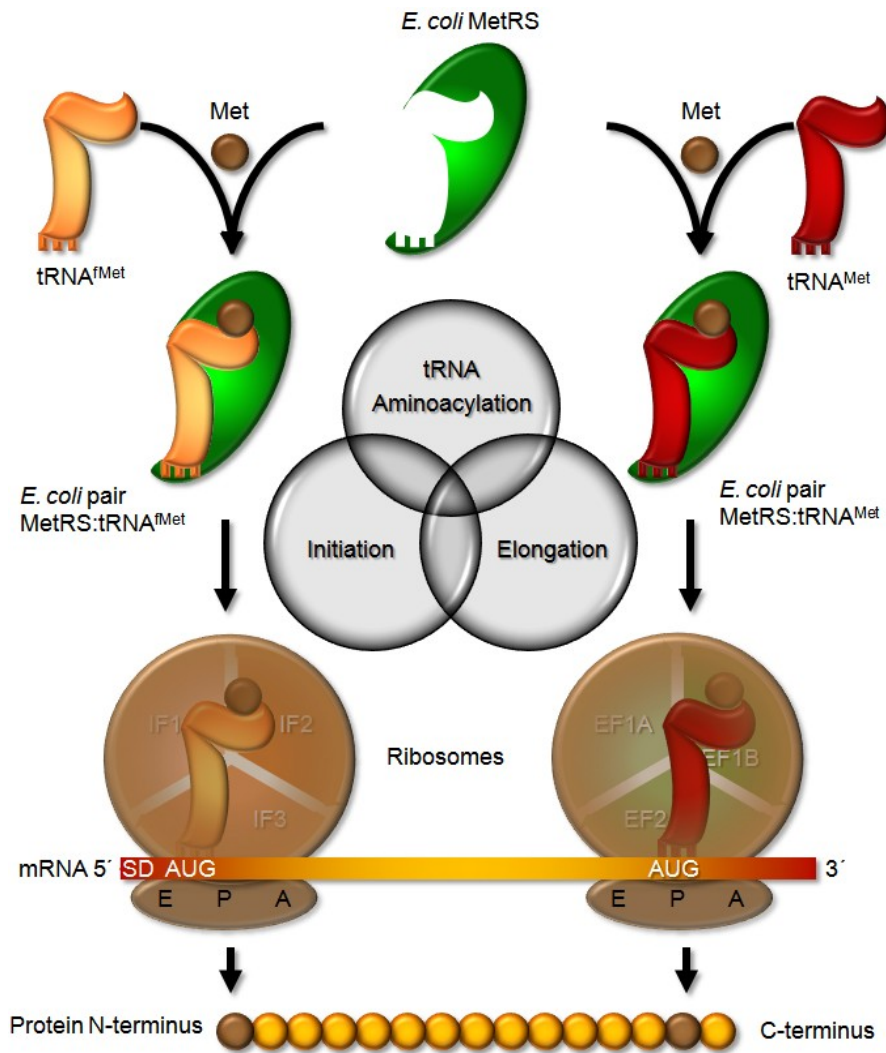


Figure 11. The Janus face of protein synthesis. In *E. coli*, the MetRS (green) normally activates methionine (brown) and charges it onto both the initiator tRNA^{Met} (orange) and elongator tRNA^{Met} (dark red). After tRNA aminoacylation and translation, the AUG sense codons present in a protein sequence will have an unambiguous meaning: Methionine. SD = Shine-Dalgarno sequence

1.3 Industrial biotechnology

Industrial or white biotechnology uses enzymes or organisms to sustainably produce chemicals, materials, and fuels from renewable sources. Driven by the global market economy, this field promises the optimization of processes at lower operating costs and capital expenditures. The achievements and promises of enzyme engineering, metabolic engineering, synthetic biology, and systems biology (including ‘omics’ and *in silico* approaches), are expected to speed up the development of white biotechnology as well. The engineering of strains or enzymes in combination with different procedures for the efficient production of biodiesel, for instance, could enable a paradigm shift from fossil fuel-based to bio-based production of value-added chemicals.⁷⁸ Last but not least, industrial biotechnology processes are nowadays very strong associated with reduced energy consumption, waste generation, and greenhouse gas emissions.

1.3.1 The search for the ideal biocatalyst

One of the most important tools for industrial biotechnology is protein engineering because enzymes isolated directly from nature rarely exhibit the ideal combination of traits and activities required for industrial use. Biocatalysts must be optimized to function in nonnative environments, such as extreme process conditions including exposure to solvents or additives over prolonged periods of time. In the early stages, developing suitable biocatalysts was generally limited to enzymes found in nature.⁷⁹

With the advent of recombinant DNA technology, enzyme optimization via rational and directed evolutionary approaches became the dominant route for the generation of sequence diversity.⁸⁰ However, the task of identifying beneficial diversity is nontrivial and mutations that span the entire structure of the enzyme usually cause detrimental effects. Directed evolution or random mutagenesis, for example, is like looking for a needle in a haystack, since billions of variants must be generated at the

DNA level, then functionally screened to bring a desired property.⁸¹ Moreover, complete protein sequences cannot be easily permuted because the generated libraries are limited in size. Finally, rational approaches often require structural information, which is not always available.

To fully realize the potential of customized enzymes in industrial applications, it is imperative to tailor catalyst properties optimal for both a given reaction and in the context of an industrial process.⁸² To this end, another alternative approach in finding the ideal biocatalyst could be by exploring the emergent effects generated by global replacements using the SPI-based residue-specific incorporation of noncanonical amino acids. Indeed, this method successfully combines the selectivity of *in vivo* co-translational sequence modifications with classical chemical approaches. The classical chemical approaches themselves are limited since modifications directed to the amino acid side-chains of biocatalysts are nonspecific and thus, it can result in heterogeneous mixtures of enzyme products.⁸³

1.3.2 The most versatile biocatalyst: Lipase

Lipases (triacylglycerol acylhydrolase, EC 3.1.1.3) possess the most common natural protein fold, the canonical α/β hydrolase fold, composed of a β sheet (and not a barrel) of eight beta-sheets connected by α -helices.⁸⁴ The canonical α/β hydrolase fold is characterized by the presence of a catalytic triad, formed of a nucleophile (Ser, Cys, or Asp), a strictly conserved His, and an acidic residue Asp or Glu in the case of lipases (**Figure 12A**). To promote catalysis, structural rearrangements around the active site are necessary. This process is characterized by the movement or 'opening' of a helical lid domain that covers the active site cleft of the enzyme. This flexible lid is attached to the enzyme core of many lipases and it is well conserved among organisms (**Figure 12B**). Hence, lipases have both an open and a closed conformation. However, in the aqueous phase, the equilibrium is shifted toward the inactive, closed form.

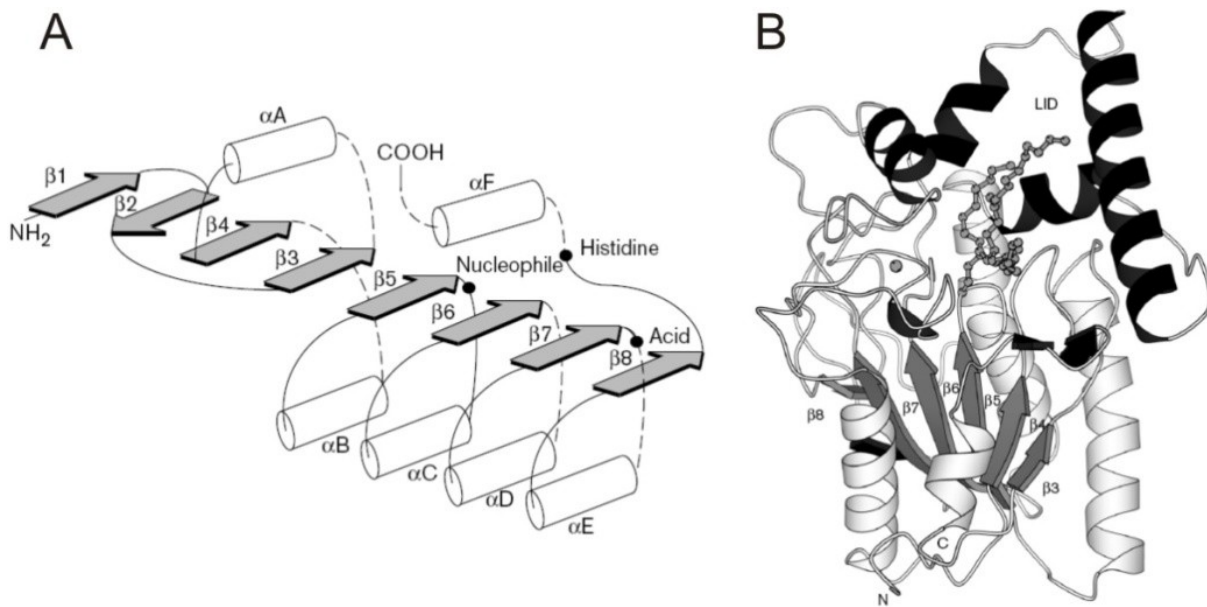


Figure 12. Structural features of lipases. A) Secondary structure diagram of the canonical α/β hydrolase fold: α -helices and β -strands are represented by white cylinders and gray arrows, respectively. The catalytic triad is indicated by black dots. The dashed lines indicate the location of possible insertions. B) Open conformation of *P. aeruginosa* lipase: α -helices, β -strands, and coils are represented by helical ribbons, arrows and ropes, respectively. α -helices and β -strands part of the hydrolase fold are shown in white and dark gray, respectively. Other secondary structure elements are in black. A phosphonate inhibitor covalently bound to the nucleophile and the calcium ion is represented in ball-and stick format. (Images taken from Marco Nardini⁸⁵)

Upon interfacial activation, which is defined as a sharp increase in lipase activity when acting at the lipid-water interface of micellar or emulsified substrates⁸⁶, the lid moves away, fully exposing the active site and activating the enzyme. Some lipases are likewise subject to an unusual feature called thermal activation; this refers to the phenomenon where enzymes are activated above 40 °C, as it is the case is with lipases from *Pseudomonas aeruginosa*⁸⁷⁻⁸⁹, *P. glumae*⁹⁰, or *Candida Antarctica*⁹¹ all of which nevertheless have an amphiphilic lid covering the active site.

Lipases hydrolyze triacylglycerols into glycerol and fatty acids, or catalyse the reverse reaction under low water conditions (Figure 13).

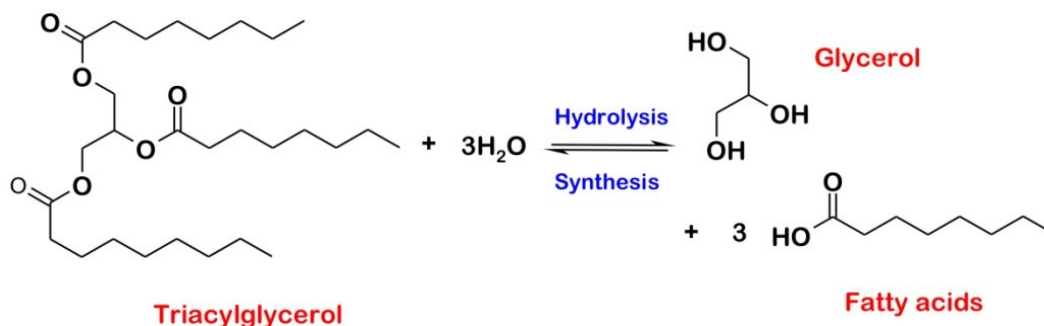


Figure 13. Lipase reactions. Lipases catalyze the hydrolysis or synthesis of triacylglycerols.

Lipolysis occurs exclusively at the lipid-water interface where the concentration of molecules directly determines the catalysis rate. However, the kinetics of a lipase reaction does not follow the classical Michaelis-Menten model, since it is valid only for soluble enzymes and substrates. Instead, when the solubility limit of the substrate is exceeded, there is a sharp increase in lipase activity as the substrate forms an emulsion. Esterase activity, in contrast, is a function of substrate concentration as described by Michaelis-Menten kinetics, with the maximal reaction rate being reached long before the solution becomes substrate-saturated.⁸⁹ Accordingly, a model for describing lipase kinetics has been proposed (Figure 14).⁹²

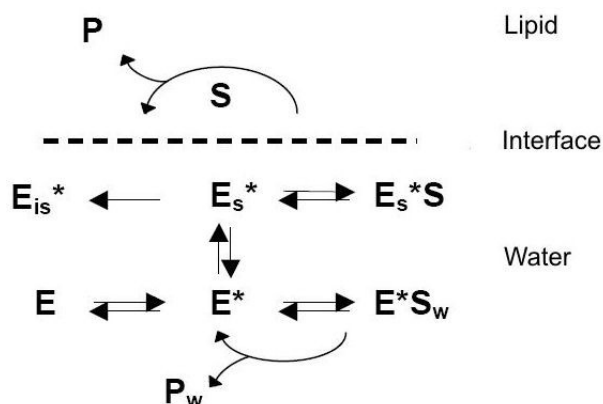


Figure 14. Model of lipase kinetics. The model is an extension of the one proposed by Verger.⁹³ In aqueous solution, upon activation, the inactive enzyme (E) becomes active (E*) and can either bind to the water-soluble substrate (S_w) and release the product in the water phase (P_w) or be absorbed at the interface (E_s*). Once absorbed, the enzyme can either lose its activity (E_{is}*) or catalyze the conversion of the water-insoluble substrate (S) to its product (P) (image modified from M. Royter⁹⁴).

The first step comprises the physical binding of the lipase, a step which may include the activation of the enzyme (i.e. lid opening). In the second step, the complex between the lipase and the substrate is formed, giving rise to the product, concurrent with the regeneration of the 'adsorbed' enzyme. **Figure 15** details the mechanism of the lipase reaction.⁹⁵

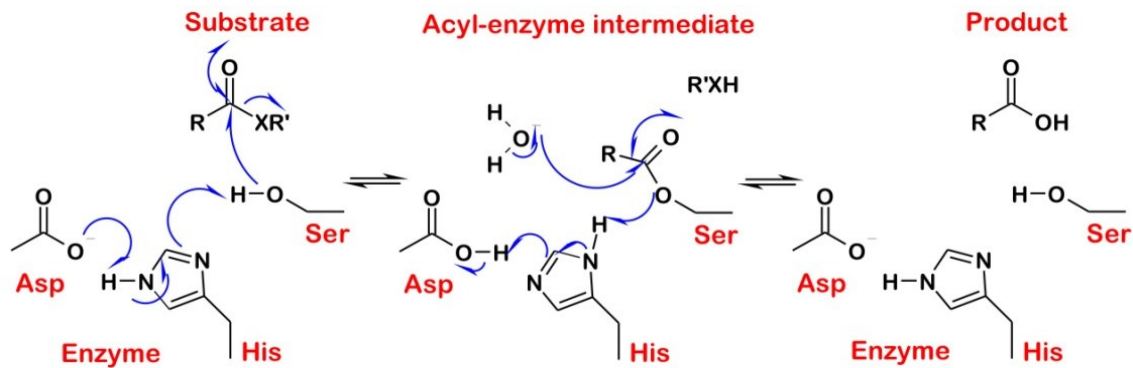


Figure 15. Mechanism of lipase catalysis. Left: Activation of serine and nucleophilic attack of the serine to the carbonyl group of the potential substrate to form an acyl-enzyme intermediate (center). In this step the charges are neutralizing, resulting in the formation of the oxyanion hole. Right: Release of the product and regeneration of the catalytic residues.

First, a serine is activated by proton transfer of the hydroxy proton to aspartate via the mediator histidine residue. As a nucleophile, the hydroxy group of serine attacks the carbonyl group of the potential substrate forming an acyl-enzyme intermediate (**Figure 15**). When a proton from the hydroxy group of the serine is accepted by the nitrogen of the histidine, its positive charge is neutralized with the negative charge of the aspartate, thereby forming the oxyanion hole. The oxyanion hole is important because it helps to stabilize the intermediate state, where the carbonyl oxygen of the substrate bears a partial negative charge. The deacylation step that follows is controlled by the electronegativity of the molecules populating the interface. The mechanism is repeated here, but using water or monoglyceride as a nucleophile instead. These then attack the acylated enzyme to form the tetrahedral intermediate. The intermediate collapses again, releasing the product and regenerating the catalytic residues which can be used in the next catalysis step.

Lipases are widely used to degrade fats and oils in food, flavor, leather, textile, cosmetic, fragrances, and detergent industry. The activity and stability of lipases can be influenced by the addition of surfactants and detergents when added to the reaction medium. However, when it was shown for the first time that they were active in almost 100% of organic solutions⁹⁶, lipases began developing as ideal tools for organic chemists.

Lipases can esterify an alcohol in the presence of an acid or transesterify an ester with a second alcohol (alcoholysis), an acid (acidolysis) or another ester. In this way, lipases are used for specific regioselective reactions in organic solvents to produce enantiomers.⁹⁷ The hydrolytic/synthetic versatility of lipases makes them the most attractive and widely-used biocatalysts. Commercially, the lipase sector is a million dollar business for which new applications in the areas of wastes management, biodegradation of oil, aliment development, specifically, the reduction of fats or the increase of flavor and fragrance; biofuels, biodegradable polymers, and pesticides production, are being sought for. Of course, there is a strong requirement for identifying new enzymes or optimizing existing ones, pushed forward by a rapidly demand for fine chemicals.⁹⁸ Finally, the pharmaceutical field is another important application area, with anticancer, antiviral, antihypertensive, anticholesterol, anti-Alzheimer, and anti-inflammatory drugs being produced in lipase-based procedures.⁹⁹

2 Goal

The basic goal of this thesis is to explore the perspectives of genetic code engineering in applications involving biocatalysts for industrial biotechnology. Here, the lipase from the thermophilic anaerobic bacterium *Thermoanaerobacter thermohydrosulfuricus* (TTL) expressed in *E. coli* was used as a model biocatalyst. The high number of 11 Met residues in TTL indicates that these could play an important role in its catalytic performance. Therefore, the Met side-chain conformational preferences were systematically varied by incorporating the isosteric analog norleucine and the surrogate azidohomoalanine globally. These have similar chain lengths but opposite polarities: Nle is strongly hydrophobic whereas Aha has a strictly hydrophilic side-chain. Accordingly, it is expected that the opposite physicochemical properties directly provided by the synthetic amino acids are fully reflected in the relative lipase congeners.

In order to distinguish between synergistic effects of multiple (all-or-none) replacements and individual effects of key Met residues in the enzyme structure, the first efforts toward the development of a method for the differential replacement of Met residues are also presented. Until now, stop codon suppression-based methods are not applicable to Met analogs. The basic idea behind these systems is to import aminoacyl-tRNA synthetases and tRNAs that show no cross-reactivity with endogenous components. For this, methionyl-tRNA synthetases (MetRSs) from different species should be tested for their cross-reactivity in *E. coli* and for their natural preference toward various Met analogs. This is an important starting point to later evolve the MetRS specificity. Moreover, the natural fact that MetRSs charge two different tRNAs suggests the next point for a differential decoding, i.e. initiator tRNA^{fMet} from *E. coli* is left to initiate translation whereas the imported elongator tRNA^{Met} should be capable to decode internal positions more efficiently. The final aim is to reprogram protein translation *in vivo* whereby the N-terminus is translated with one Met analog, and the internal positions with another one; thus serving as a platform to further engineer biocatalysts of industrial interest.

3 Results and discussion

3.1 Engineering lipase with methionine analogs

The lipase from the thermophilic anaerobic bacterium *Thermoanaerobacter thermohydrosulfuricus* (TTL) was chosen not only because it is efficiently expressed in *E. coli*, but also because it is thermostable, has broad substrate specificity, and exhibits resistance against various organic solvents and detergents.¹⁰⁰ These features make the use of TTL highly advantageous for biotechnological applications since it can be produced at low cost while exhibiting improved stability. In this way, TTL is considered an attractive biocatalyst for studying the effects of Met replacement with both the more hydrophobic analog Nle and the more hydrophilic, azide group-containing Aha (Figure 16).

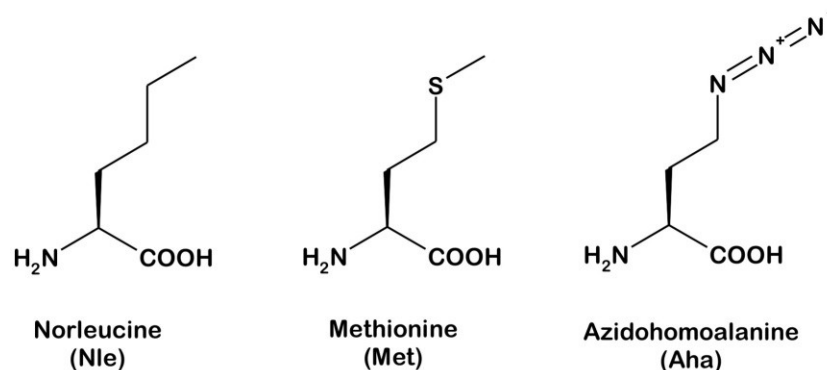


Figure 16. Probing the hydrophathy of lipase with two Met analogs. The role of conformational preferences of the Met side-chain in TTL is probed with Nle, which is more hydrophobic than Met, and Aha, that is more hydrophilic than Met.

The high number of Met residues in this particular lipase (11 residues, see Appendix 9.1 for sequence details) might indicate a functional importance. Therefore, it is expected that the TTL[Nle] congener would be more hydrophobic than the native TTL, whereas TTL[Aha] would be a more hydrophilic, 'clickable' lipase.

3.1.1 Expression and purification

All lipases were generated by culturing amino acid auxotrophic *E. coli* host strains with Met, Nle, and Aha supplementation during heterologous expression (see 6.2.2.4 for details). The expression of the three lipases was indicated by the presence of bands having an average MW of 30 kDa (Figure 17A). Subsequently, all the lipases were purified (close to 95%) by affinity chromatography (Figure 17B).

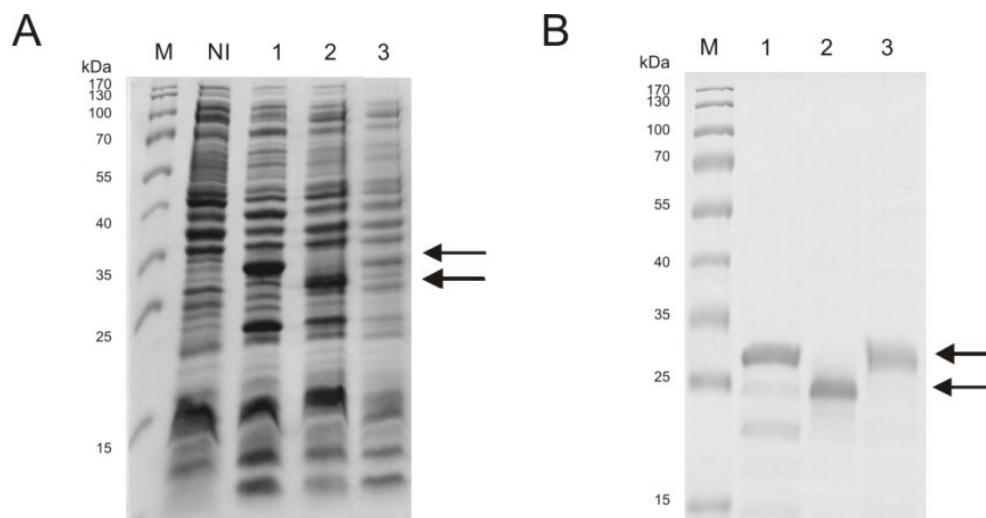


Figure 17. Lipase alloproteins. The TTL congeners were produced by supplementing the medium of auxotrophic *E. coli* strains with 1) Met, 2) Nle, and 3) Aha after expression (A) and purification (B) by using 12% SDS-PAGE and Coomassie staining (indicated with arrows). Note that TTL[Nle] (lane 2) is shifted compared to native TTL (lane 1) and TTL[Aha] (lane 3). M = MW standard marker; NI = Non-induced sample

Notable are the marked differences in the migration patterns observed for TTL[Nle] which moved faster than TTL and TTL[Aha] (Figure 17). In electrophoresis, SDS unfolds proteins and gives them a uniform negative charge such that these will migrate through the gel in the electric field based solely upon size. Hydrophobic proteins bind more SDS than hydrophilic ones. Since the lipase congeners have a very similar mass (not more than 100 Da difference; *vida infra*), the 5 kDa difference observed after electrophoresis might indicate that TTL[Nle] has a higher number of negative charges due to its hydrophobic nature compared to native and TTL[Aha].

In general, the SPI method allows the production in the order of milligrams of protein per liter of culture. The simple experimental set-up allows obtaining preparations with a yield of 20 mg/L, indicating the potential of using SPI for industrial applications.

3.1.2 Incorporation efficiency

In all incorporation experiments, comparatively high level of Met substitution is achieved using the SPI method. Here, a high incorporation level of all tested analogs into TTL was readily achieved, as indicated by ESI-MS results (Figure 18).

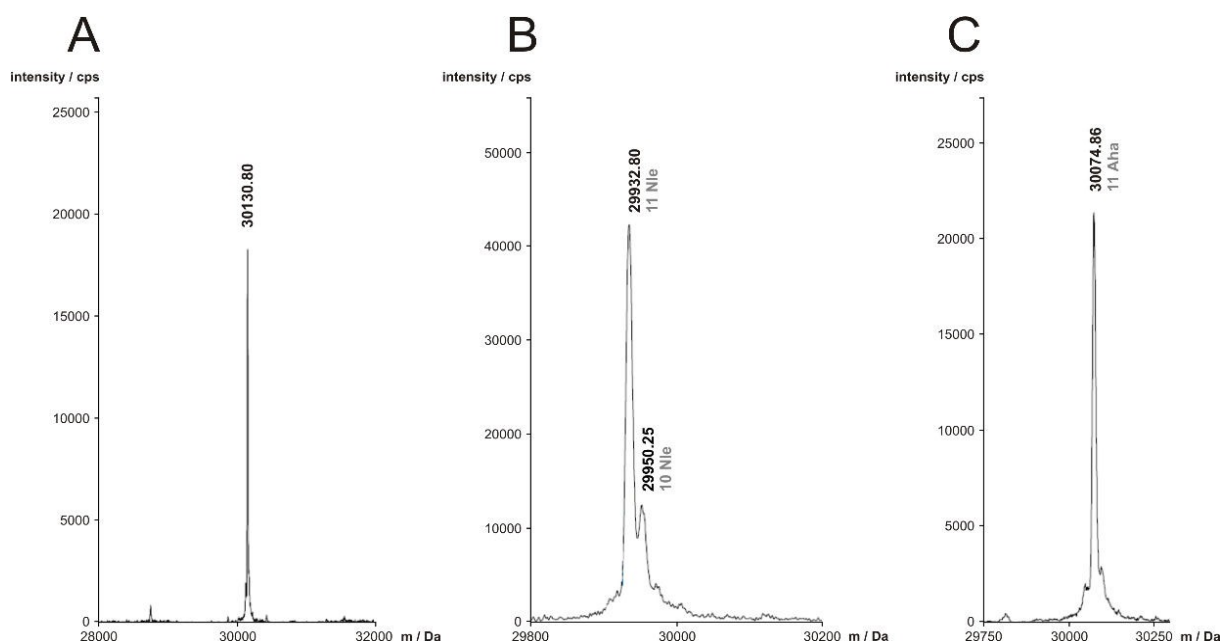


Figure 18. ESI-MS spectra of lipase congeners. Peaks corresponding to calculated masses are labeled accordingly. The theoretical calculated mass for TTL is 30130.2 Da (A), while for fully substituted TTL[Nle], it is 29932.8 Da and the congener with 10 Nle residues, 29950.8 (B); for fully labeled TTL[Aha], the theoretical calculated mass is 30074.6 Da (C).

In the case of TTL, a single peak corresponding to the expected mass was obtained (Figure 18A). For TTL[Nle], however, there was an additional mass species detected apart from the fully substituted congener containing only 10 Nle replacements (Figure 18B). Nonetheless, the preparation can generally be considered homogenous as the

dominant mass species is the fully Nle-substituted protein. In comparison, Aha was more successfully incorporated into TTL, since the spectra displays just a single peak (**Figure 18C**). In the both incorporations, no traces of native TTL were found.

3.1.3 Basal lipase activity

Lipase activity is normally determined by measuring the hydrolysis of *p*-nitrophenyl palmitate (*p*NPP). After the TTL congeners were characterized, cleavage of *p*NPP was measured at 70 °C in 25 mM Tris·HCl pH 8 according to the protocol of Winkler and Stuckmann (**Table 2**; see 6.2.4.4 for more details).¹⁰¹

Table 2. Enzymatic activity of lipase congeners.

Congener	Lipase activity (mU/μg)
TTL	2.3
TTL[Nle]	26.5
TTL[Aha]	0.5

TTL[Nle] displayed more than ten-fold enhanced activity in comparison to native TTL while TTL[Aha] showed almost 5 times lower lipase activity when compared to parent TTL (**Table 2**). The finding that the produced congeners have extremely different basal lipase activities indicates that the substitution of the Met by the more hydrophobic Nle, and the more hydrophilic Aha residues, caused the observed strike differences which can be better understood upon thermal activation (*vida infra*).

3.1.4 Optimal temperature and pH

Parent TTL is a thermoactive lipase that displays its highest enzymatic activity at an optimal temperature (T_{opt}) of ~70 °C and optimal pH (pH_{opt}) of 8.0.¹⁰⁰ In order to determine if the T_{opt} and pH_{opt} of the lipase congeners was affected, lipase activity was determined between 40 and 90 °C and pH 3-11 (**Figure 19**).

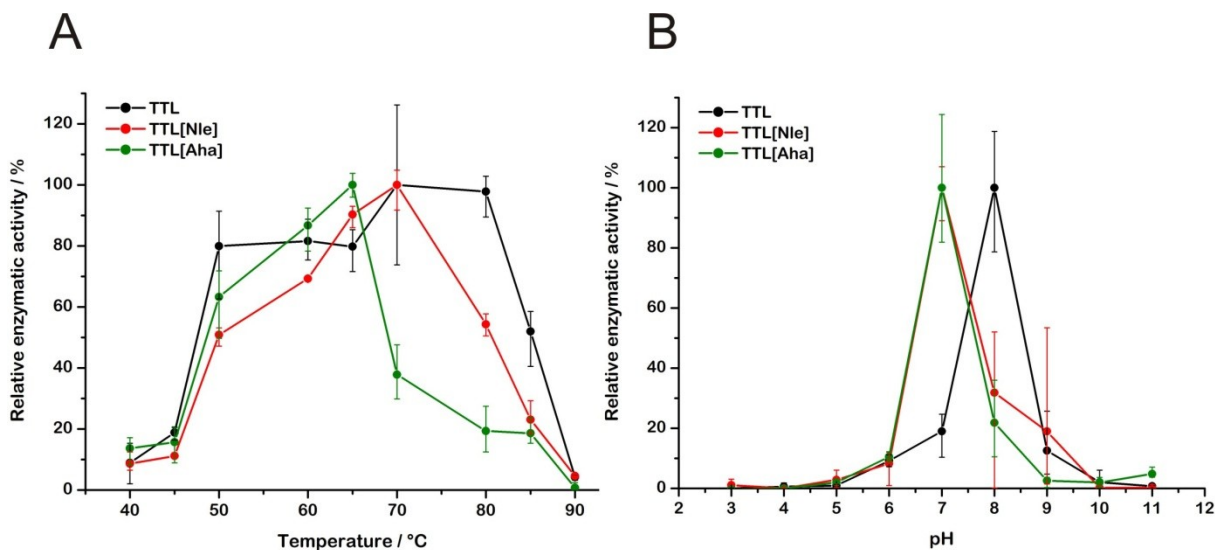


Figure 19. Temperature and pH profiles of lipase congeners. A) The optimal temperature for native TTL and TTL[Nle] is 70 °C, while for TTL[Aha], it is 65 °C. The reactions were performed using *p*NPP as substrate. B) The optimal pH for native TTL is 8, while for TTL[Nle] and TTL[Aha], it is 7. These reactions were carried out at T_{opt} overnight using tricaprylin as substrate. In both cases, enzymatic activity was measured in triplicate.

While the native TTL and TTL[Nle] congeners showed a T_{opt} of 70 °C, the TTL[Aha] exhibited better activity at 65 °C (**Figure 19A**). Note that 60% of TTL[Aha] activity is lost at 70 °C. These differences in the temperature profiles could be due to the acquired physicochemical properties of the lipase congeners. Once the T_{opt} for all lipases was found, these were then incubated at different pH values but using a tricaprylin assay (see 6.2.4.5 for details) given that *p*NPP is autohydrolyzed at extremely basic conditions; the standard lipase assay using *p*NPP as substrate is only reliable in the range of pH 6-9. Optimal lipase activity was observed at pH 8 for native TTL and at pH 7 for TTL[Nle] and TTL[Aha] (**Figure 19B**). These results reveal that all TTL congeners were mostly active between pH 7 – 9; however, the distinct maximum activity values are disproportionately high. Almost 70% of TTL[Nle] and TTL[Aha] activity is lost upon incubation at pH 8 whereas 80% activity of TTL appears to be lost at pH 7. These inconsistencies are intrinsic artifacts of the tricaprylin assay and have been described elsewhere.¹⁰² For this reason, *p*NPP was used in subsequent assays.

3.1.5 Thermostability

To compare thermal stability, the lipases were preincubated at different temperatures and times; thereafter the residual lipase activity was measured (Figure 20).

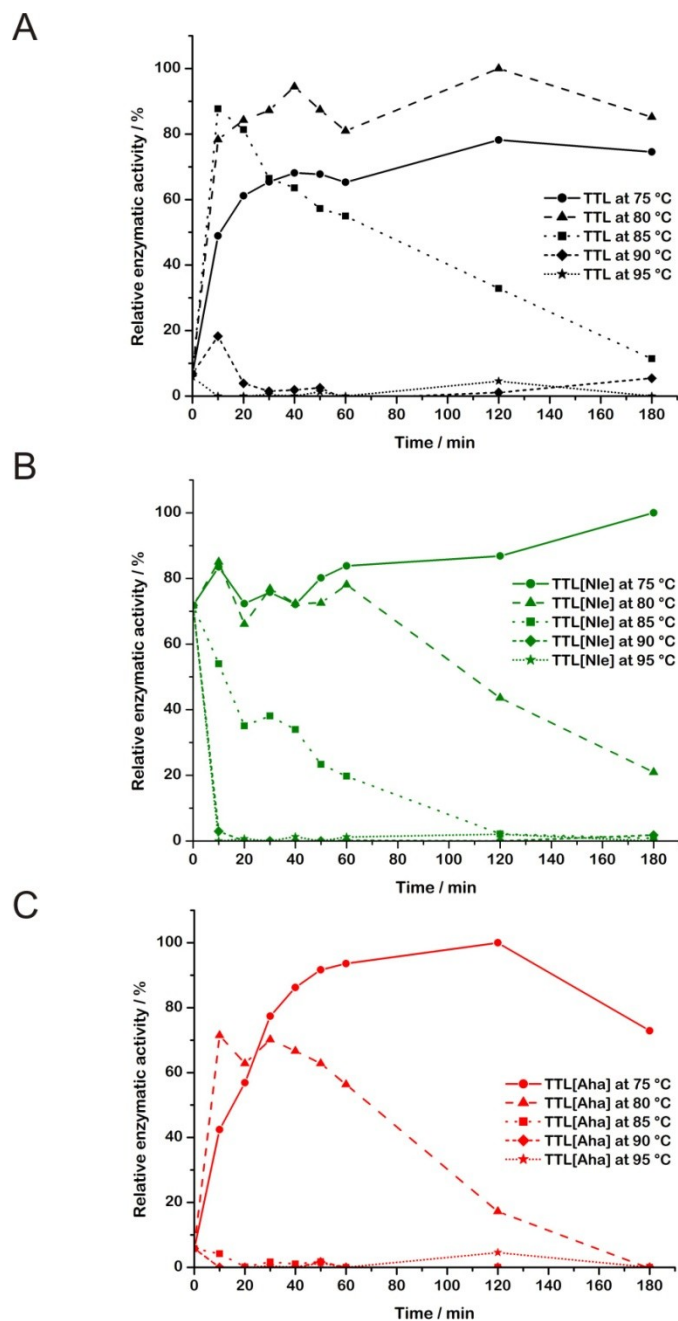


Figure 20. Thermal stability of lipase congeners. A) TTL, B) TTL[Nle], and C) TTL[Aha] were incubated at different temperatures for 10, 20, 30, 40, 50, 60, 120, and 180 minutes. Residual lipase activity of each sample was measured in triplicate for 10 min at T_{opt} and pH 8 using pNPP as substrate.

Native TTL is the most thermostable enzyme up to 3 hr at 80 °C (**Figure 20A**), followed by TTL[Nle] (**Figure 20B**) at the same time but incubated at 75 °C, and finally TTL[Aha] for up to 2 hr at 75 °C (**Figure 20C**). At 85 °C, native TTL displayed residual activity for three hours, while TTL[Nle] had residual activity for two hours but TTL[Aha] was almost inactive (**Figure 20**). However, the thermostability of the TTL congeners decreased with time when incubated at 90 °C, with only the native protein showing residual activity after 10 min; none of the enzymes was active at 95 °C (**Figure 20**). The most important finding, however, was that native and TTL[Aha] need thermal activation to be active whereas the TTL[Nle] showed as high as 70% lipase activity at the onset of incubation (**Figure 20**).

3.1.6 Thermal activation

The curves in **Figure 20** indicate that the requirement for thermal activation is restricted to native TTL and TTL[Aha], given that their activities sharply increased within the first 10 to 20 min after incubation at different temperatures. As mentioned previously, however, the most prominent feature among the lipase congeners is a several-fold higher activity of TTL[Nle] in the absence of thermal activation ($T = 0$ min, **Figure 20B**). Based on these observations, the TTL congeners were re-incubated at their T_{opt} for 10 or 60 min, or at their maximal thermal activation. Maximal thermal activation is defined as the temperature and time period where the lipase exhibited its maximum activity, i.e. native TTL (80 °C for 120 min), TTL[Nle] (75 °C for 10 min) and TTL[Aha] (75 °C for 120 min) (see **Figure 20** for details). In this way, the activity of all lipases was measured after different kinds of thermal activation (**Figure 21**).

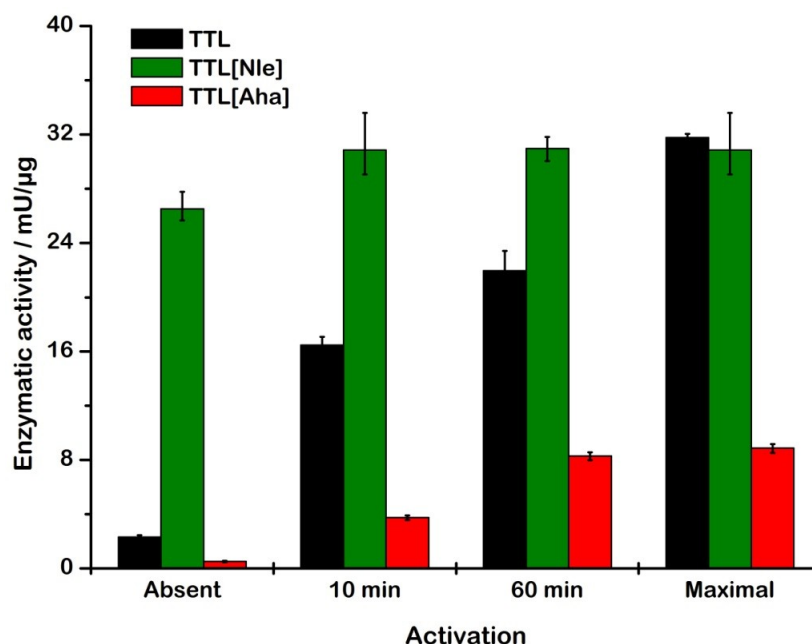


Figure 21. Thermal activation of lipase congeners. The activities of the TTL congeners were measured after activation for 10 and 60 min at their optimal temperature, which is 70 °C for native and TTL[Nle] and 65 °C for TTL[Aha]. For maximal activation, native TTL was incubated at 80 °C for 120 min, TTL[Nle] at 75 °C for 10 min and TTL[Aha] at 75 °C for 120 min. The values are averaged from three independent measurements using pNPP as substrate.

The most interesting finding is that the activity of TTL[Nle] did not significantly change after any kind of maximal thermal activation (Figure 23). In contrast, native and Aha-containing lipases showed a several-fold increase in activity following different setups of thermal activation (Figure 23). This result is rather interesting, since it is expected that the Met residues will enhance the hydrophilic properties of these lipases in contrast to the much more hydrophobic residues of TTL[Nle]. Nevertheless, it is important to note the activity differences between native and TTL[Aha]. Following maximal thermal activation, native TTL reaches an enzymatic activity only little higher than TTL[Nle], while TTL[Aha] loses 75% of the activity of TTL (Figure 23). Normally, lipases are not active in aqueous phase without either interfacial or thermal activation. In native TTL and TTL[Aha], the lid domain could be opened upon thermal activation to allow substrate contact; TTL[Nle], however, is always active in the absence of thermal activation, i.e. the enzyme is fully accessible to the substrate in the aqueous

phase. In this congener, the lid-loop must be flipped out to expose the lipid-binding cavity. The structural basis for this aqueous phase activation of TTL[Nle] can be understood in the context of the Met residues distribution across the lipase. To this end, advanced protein modeling techniques (see 6.2.5.1 for details) allowed the generation of a 3D structure homology model for TTL (**Figure 22**).

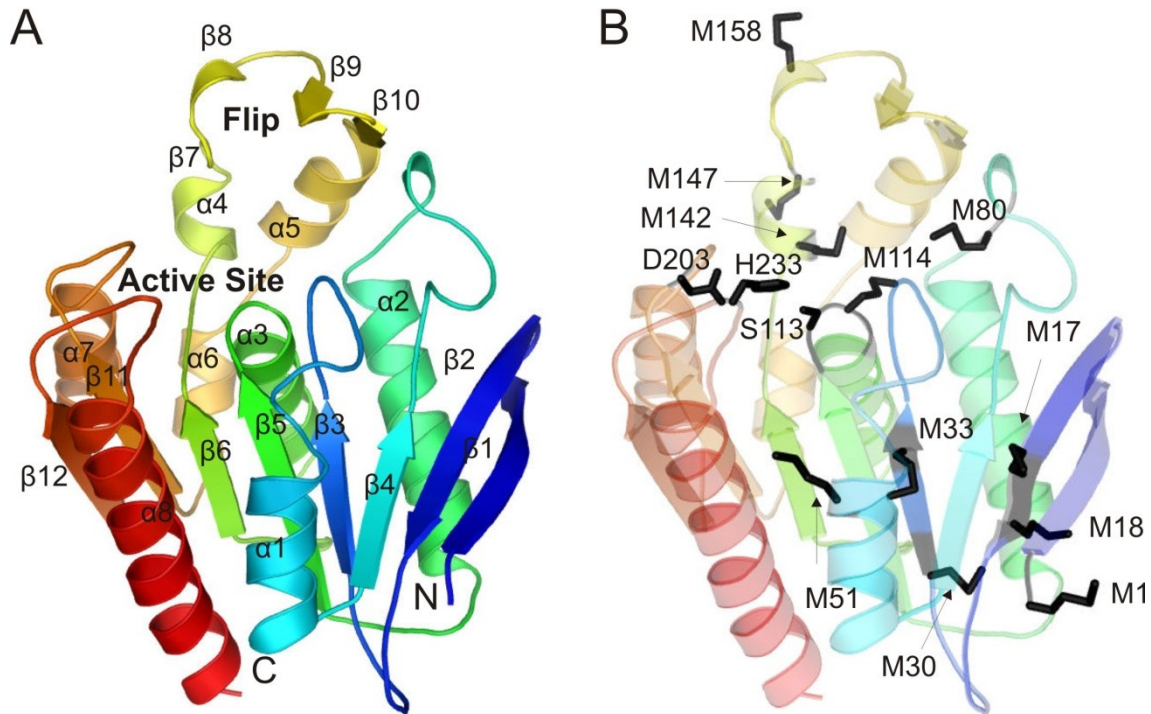


Figure 22. 3D structure homology model for TTL. A) The lipase displays a canonical α/β hydrolase fold (secondary structure elements are shown in black) and the lid. B) The active site of the lipase is composed of the catalytic residues Ser113, Asp203, and His233 (black). The Met residues (labeled black) are located within the hydrolase fold (M1, M17, M18, M30, M33, M51, and M80), close to the active site (M114) or in the lid domain (M142, M147, M158). N = N-terminus; C = C-terminus

Out of a total of 11 Met residues, three are positioned in the lid region; of these, Met147 and Met158 are surface exposed whereas Met142 is buried (**Figure 22B**). Met is a moderately hydrophobic amino acid whereas Nle is extremely hydrophobic (**Figure 6**), and its presence in the lid region should mimic hydrophobicity as delivered by lipid aggregates. As expected, the hydrophobic side of the lid is usually exposed to the lipid phase, enhancing the hydrophobic interactions between the enzyme and the lipid

surface.¹⁰³⁻¹⁰⁵ Consequently, the global Met → Nle replacement would result in a hydrophilicity/hydrophobicity balance alteration where the “closed lid” of the native TTL could be converted permanently into a lipase congener having an “open lid”. The open lid congener could be tested against TTL[Aha], which is expected to be more hydrophilic, and in which this “permanently activated” state would not be observable.

Additionally, it is well known that presence or absence of the lipase lid over the active site is not the sole determinant of its activity. Dimerisation is a basic prerequisite for activity in many lipases¹⁰⁶, and the presence of hydrophobic residues in the dimerisation interface could further enhance lipase structural and functional integrity. Of the Met residues, Met1 is part of this interface, while Met17, Met18, and Met30 are in the vicinity (**Figure 22B**). Finally, the replacement of the residues Met80 and M114, which are close to the active center of the enzyme, could have a great impact on the overall lipase activity. In summary, the replacement of Met with more hydrophobic Nle residues across the TTL molecule may act as a coupled network to beneficially promote catalysis.¹⁰⁷

For all these reasons, the global Met → Nle substitution could be an elegant way to design a stable lipase allowing the substrate to be accessed in the aqueous phase without thermal activation. This feature could be a great advantage in detergent applications where washing-powder lipases are used. In fact, the lid is usually removed in commercial lipases via classical genetic engineering to achieve constant substrate accessibility.¹⁰⁸ The lid region, however, certainly plays an important role in the overall structural integrity of the lipase and its removal might have detrimental effects on the structural and functional integrity of the enzyme.¹⁰⁸ Unfortunately, due to the lack of high-resolution structural data it is difficult to speculate on how the global substitution of Met residues with Nle results in the enormous changes in activation by thermal activation. Nonetheless, all samples were submitted to CD spectroscopy to see whether the secondary structure was affected (**Figure 23**; see 6.2.4.6 for details).

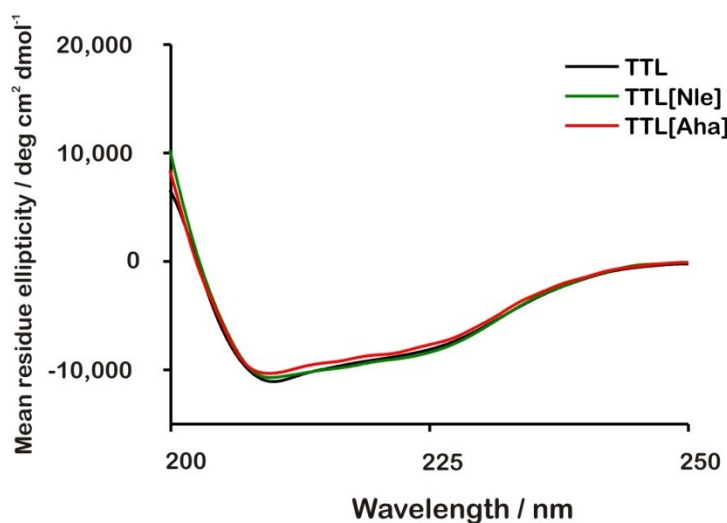


Figure 23. Secondary structure of lipase congeners. The far-UV CD spectra from 200–250 nm was recorded at T_{opt} of 70 °C for native TTL and TTL[Nle], and at 65 °C for TTL[Aha].

The CD spectrum of the two lipase congeners revealed only negligible deviations from that of the native TTL (Figure 23). These findings indicate that the lipase secondary structure is not altered, thus suggesting that the lipase activity of the generated congeners may be retained. In support of this, however, NMR or X-ray crystallographic studies are necessary although other proteins have revealed that the incorporation of Nle did not perturb their 3D structures.⁴⁸

3.1.7 Substrate specificity

Lipases hydrolyze triacylglycerols into fatty acids and glycerol, and esterify fatty acids and alcohols. The synthesis of specific compounds depends on the nature of the substrate binding site formed by a hydrophobic tunnel near the catalytic residues. In addition, the fatty acid chain-length of the corresponding substrate depends on the shape of the tunnel and its amino acid composition.¹⁰⁹ It is therefore reasonable to think that the substrate specificity of the lipase congeners could be affected upon incorporation of Nle and Aha in place of Met, since the residues M114 and M142 are located near the active site (Figure 22). To determine the substrate specificity of all TTL lipases, two types of substrates were used (Figure 24).

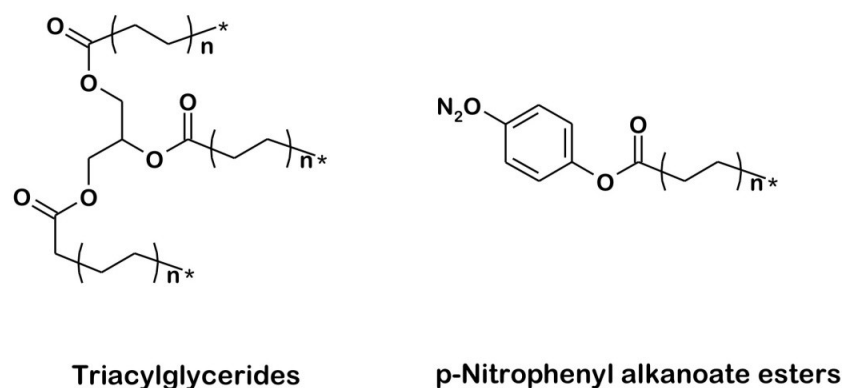


Figure 24. Two types of lipase substrates. Triacylglycerides or p-nitrophenyl alkananoate esters of varying acyl or alkyl side-chain lengths were used to determine substrate preferences of the lipase congeners. n = variable number of substituent; * = CH_3

Lipase activity of all TTL congeners was measured using triacylglycerides of varying acyl side-chain lengths (Figure 25; see 6.2.4.5.2 for details).

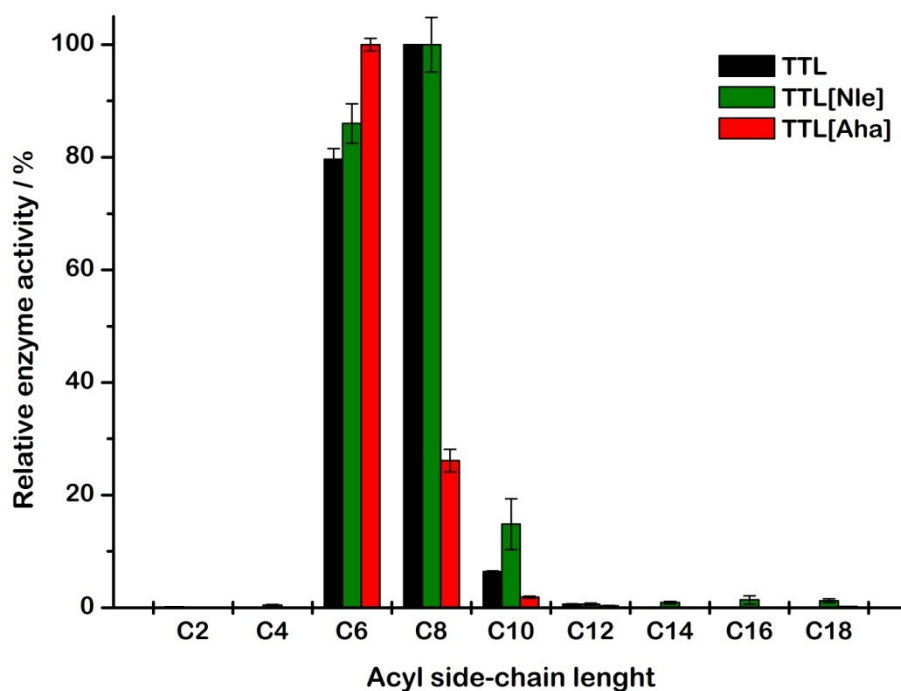


Figure 25. Lipases substrate specificity for triacylglycerols. The substrates triacetin (C2:0), tributirin (C4:0), tricaproin (C6:0), tricaprylin (C8:0), tricaprin (C10:0), trilaurin (C12:0), trimyristin (C14:0), tripalmitin (C16:0), and tristearin (C18:0) were incubated with all TTLs at T_{opt} , pH 8 for 18 h.

TTL normally shows high activity in the hydrolysis of triacylglycerols: C8:0 > C6:0 > C10:0, but low activity with shorter or longer acyl side-chains.¹⁰⁰ Importantly, the same behavior was detected for TTL but some differences were found for Nle- and TTL[Aha] (Figure 25). TTL[Nle] shows a similar pattern as parent TTL, except for a two-fold enhanced activity in tricaprins hydrolysis (C10:0), whereas the more hydrophilic TTL[Aha] accommodates short- over long-chain length acyls better: C6:0 > C8:0 > C10:0 (Figure 25).

The enzymatic activity of the other lipases was also determined using varying alkyl side-chain lengths derived from *p*-nitrophenyl alkananoate esters (Figure 26; see 6.2.4.4.3 for details).

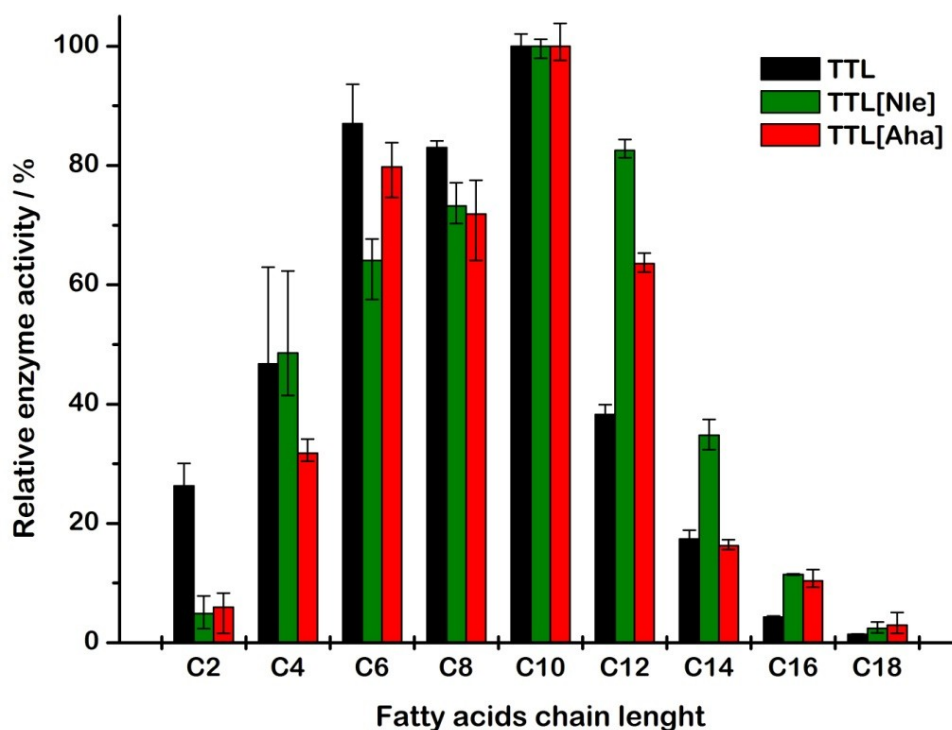


Figure 26. Lipases substrate specificity for *p*-nitrophenyl alkananoate esters. The *p*NP-derived substrates acetate (C2:0), butyrate (C4:0), caproate (C6:0), caprylate (C8:0), caprate (C10:0), laurate (C12:0), myristate (C14:0), palmitate (C16:0), and stearate (C18:0) were incubated with all TTLs at T_{opt} , pH 8 for 10 min.

In this case, the accessibility of the single fatty acid side-chain substrate seems to be less limited than in the side-chains of the triacylglycerides. When hydrolyzing *p*-nitrophenyl alkanoate esters, TTL displays broad substrate specificity: C10:0 > C6:0 > C8:0 > C4:0 > C12:0 > C2:0 (**Figure 26**). TTL[Nle] displayed a different preference when compared to native TTL: C10:0 > C12:0 > C8:0 > C6:0 > C4:0 > C14:0 (**Figure 26**). TTL[Aha] shares more similarities with native than TTL[Nle]: C10:0 > C6:0 > C8:0 > C12:0 > C4:0 > C14:0 (**Figure 26**). It is noteworthy to mention that TTL[Nle] hydrolyzes trilaurin (C:12), trimyristin (C14:0), and tripalmitin (C16:0) twice as better as compared with the native TTL. The substitution of M114 and M142 by Nle could alter the composition of the lipase tunnel, allowing the lipase to achieve more accessibility to substrates with longer side-chains.

3.1.8 Influence of additives on lipase activity

To study the effects of several substances on lipase activity, the purified TTL congeners were pre-incubated with different concentrations of organic solvents, metal ions, surfactants, and inhibitors at RT for 1 hr without substrate (see 6.2.4.4.1 for details); subsequently, the residual lipase activity was measured. It is important to mention that in all the assays for evaluating the effect of different additives on lipase activity, no thermal activation was performed because of practical reasons. Consequently, the comparison of the activities between the different lipases could be considered for both an 'open' conformation congener, TTL[Nle], and a 'closed' congener, as the case is for TTL and TTL[Aha]. It is noteworthy to mention that absolute effect of the substances is related to the basal lipase activity (BLA) for each congener, i.e. negative values indicate a negative effect on the previously active enzyme.

3.1.8.1 Organic solutions

The nature of the organic solvent is crucial in maintaining the water content required for catalytic activity. More hydrophobic solvents preserve the catalytic activity, leaving

a water layer that adheres to the enzyme surface acting as a protective shell. On the other hand, hydrophilic solvents tend to strip essential water molecules from the enzyme surface, thereby altering its catalytic conformation. To determine the extent of influence of different organic solvents on lipase activity, the TTL congeners were exposed to 90% solutions of the substances of interest. Residual enzyme activities of each lipase were measured thrice and normalized against water (Figure 27).

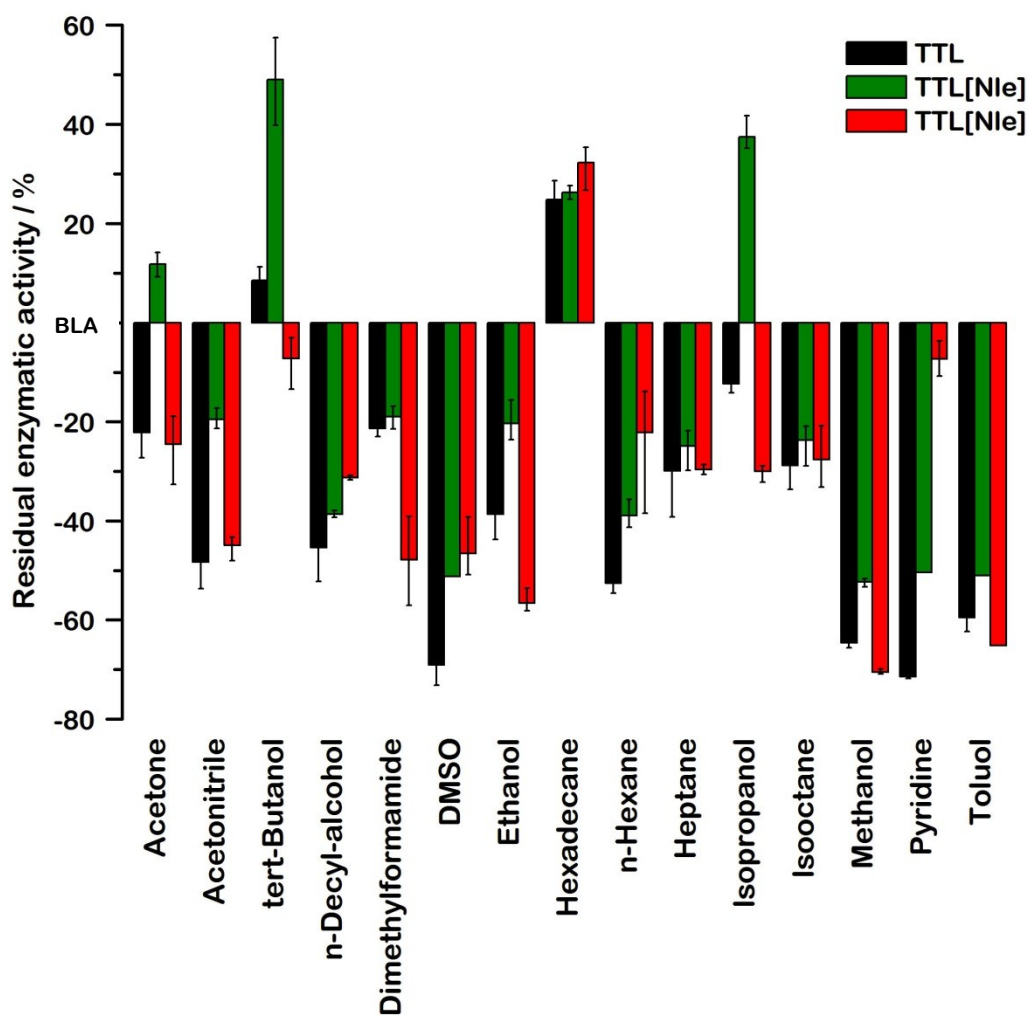


Figure 27. Influence of solvents on lipase activity. The TTL congeners were exposed to 90% of different organic solutions for 60 min and the residual lipase activity was measured in triplicates at T_{opt} and pH 8 with pNPP as substrate. All enzymes were active after treatment except TTL[Nle] in pyridine, DMSO, methanol, and toluol; and TTL[Aha] in methanol and toluol. Data is normalized to the basal lipase activity (BLA) of the corresponding congener in the presence of water, and without thermal activation. DMSO = Dimethyl sulfoxide.

Hexadecane was the only solvent that enhanced lipase activity of all congeners, with TTL[Aha] having the highest activity. This finding is very interesting, since this lipase is known to be the least active lipase with or without thermal activation (Figure 21). While the incubation with acetone, *tert*-butanol, and isopropanol enhanced the basal lipase activity of TTL[Nle] in 10%, 50%, and 40%, respectively; the activities of native TTL (except for *tert*-butanol) and TTL[Aha] are strongly diminished (Figure 27). The rationale behind these differences could be due to the intrinsic hydrophobicity of these substances, allowing the more hydrophobic Nle-containing congener to be more active. This may translate not only into economical savings but also advantages in particular chemical reactions. For instance, it has been suggested that isopropanol favors an open conformation in *Candida rugosa* lipase, allowing a better resolution of 2-(4-chlorophenoxy)-propanoic acid, whose (*R*)-enantiomer lowers cholesterol levels and prevents platelet aggregation.¹¹⁰ The hydrophobic TTL[Nle] with an 'open' conformation would allow more efficient catalysis to take place in isopropanol.

On exposure to acetonitrile, *N*-decyl-alcohol, dimethylformamide, DMSO, ethanol, methanol, heptane, hexadecane, *n*-hexane, isooctane, pyridine, and toluol the activity of all lipases was strongly affected in different degrees. Nevertheless, after pyridine treatment, TTL[Aha] residual activity was less-detectable when compared to parent and TTL[Nle] (Figure 27). Interestingly, there is a great interest in lipase-catalyzed transesterifications between sugars and esters for the synthesis of biodegradable polymers¹¹¹; however, this reaction is relatively inefficient, since the solubility of sugars in inorganic solvents is very low. Pyridine is a solvent widely used for the solubilization of huge amounts of sugar; therefore, the potential of using TTL[Aha] in these reactions should not be underestimated. Overall, these results suggest that in contrast to native TTL, the Nle and Aha congeners could be used in specific esterification reactions that otherwise would not be optimal without incorporating noncanonical amino acids.

3.1.8.2 Metal ions

As previously indicated, lipases are frequently used in the production of enantiomers. However, the lack of enantioselectivity of some lipases still remains a major problem for many organic chemists. To solve this drawback, different strategies have been proposed, including the optimization of the solvent, water content, modifications in the lipase, protein engineering, and additive effects.¹¹² Of these, the most attractive alternative is the addition of metal ions due to its simplicity and its potential. A lipase-catalyzed enantioselectivity reaction, for example, is increased hundred-fold by adding a small amount of LiCl.¹¹³ Moreover, when the temperature of the reaction decreased, an almost perfect enantioselective reaction took place. This illustrates the importance of using metal ions in lipase-catalyzed reactions. Accordingly, the effect of metal ions on lipase activity was investigated using various salt solutions (Figure 28).

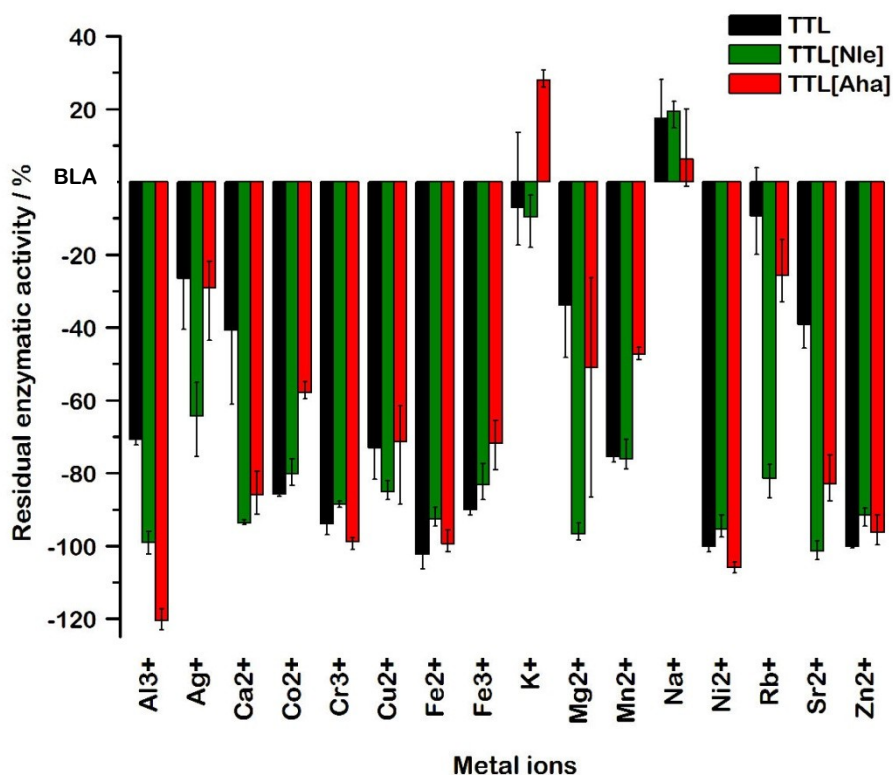


Figure 28. Influence of metal ions on lipase activity. The TTL congeners were exposed to 10 mM of different salt solutions for 60 min and the residual lipase activity was measured at T_{opt} and pH 8 with pNPP as substrate. All enzymes were active after treatment except TTL (Fe^{2+} , Ni^{2+} , and Zn^{2+}), TTL[Ni²⁺] (Al^{3+} and Sr^{2+}) and TTL[Aha] (Al^{3+} , Cr^{3+} , Fe^{2+} , Ni^{2+} and Zn^{2+}). The data is normalized with respect to the basal lipase activity (BLA) of the corresponding congener in presence of water, and without activation.

The only case where the enzyme activity of all lipases was stimulated over their basal values was observed in the presence of Na^+ (**Figure 28**). The only congener whose activity was enhanced after K^+ treatment was TTL[Aha], while 10% of native and TTL[Nle] activity was lost (**Figure 28**). Except for Ag^+ , these results suggest that the monovalent cations did not alter significantly lipase activity. On the other hand, after Rb^+ treatment, TTL was also slightly inhibited (10%), with TTL[Aha] being inhibited to a larger extent (30%), but TTL[Nle] was strongly affected (close to 80%; **Figure 28**). Other metal ions resulted in inhibitory effects on at least 25% of the activities of all lipases (**Figure 28**). The inhibitory effect of calcium ions on lipase activity is well documented.¹¹⁴ Finally, Cr^{3+} , Fe^{2+} , Ni^{2+} , and Zn^{2+} had the same strong inhibitory effect on all lipases (**Figure 28**). After Mg^{2+} and Rb^{2+} treatment, both native and TTL[Aha] were much less inhibited than the more hydrophobic TTL[Nle]. The overall inhibition differences could be due to strong interactions between divalent metal ions and the appended C-terminal His-Tag.

3.1.8.3 Surfactants

Lipases are active at the oil-water interface of emulsified substrates. However, emulsions are inherently unstable, with their degree of stability being influenced by the nature and concentration of surfactant used. A surfactant consists of both hydrophobic and hydrophilic groups, allowing it to be marginally soluble in both, polar and non-polar substances. Emulsifiers or surfactants help lowering the interfacial tension between phases or surrounding the emulsion droplet with a thin, charged film. Hence, lipase activity at the oil-water interface could be altered by the presence of these substances. Moreover, there is an overwhelming interest in screening lipases for use in the cosmetic and perfume industry because of their activity in surfactants and their use in aroma production.¹¹⁵ To further characterize the effect of surfactants, the lipase congeners were incubated with different detergents and other agents (**Figure 29**).

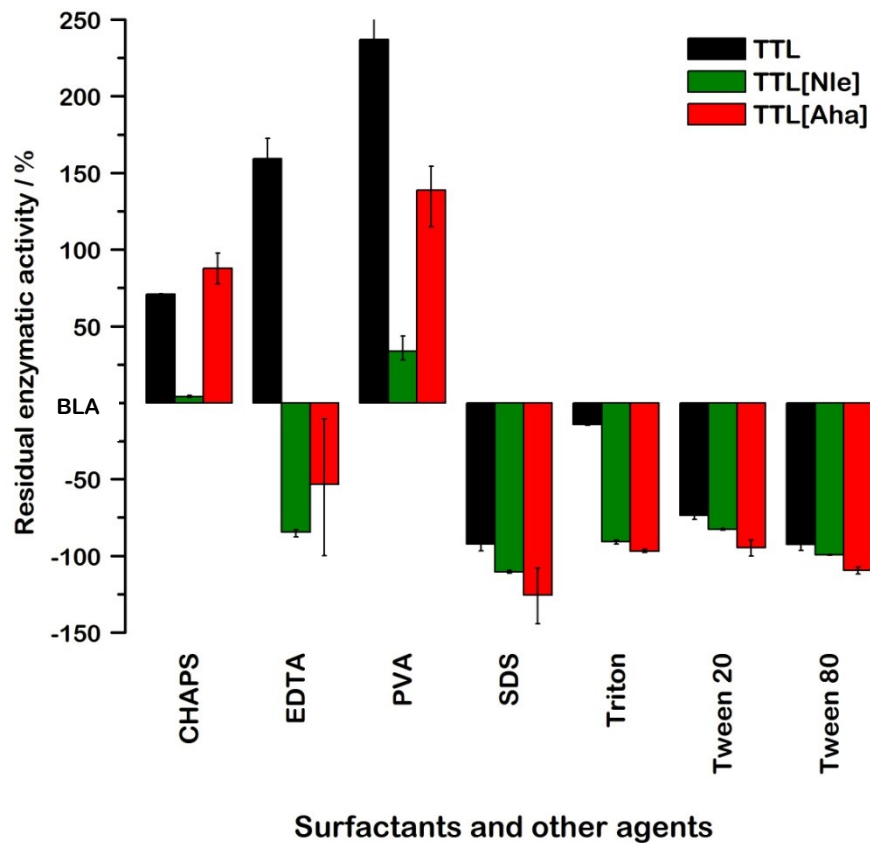


Figure 29. Influence of surfactants in lipase activity. The TTL congeners were exposed to 10% solutions for 60 min and the residual lipase activity was measured thrice at T_{opt} and pH 8 with pNPP as substrate. Data is normalized against the basal lipase activity (BLA) of the corresponding congener in water, and without activation. CHAPS = 3-[(3-Cholamidopropyl)dimethylammonio]-1-propanesulfonate; EDTA = Ethylenediaminetetraacetate; PVA = Polyvinylalcohol; SDS = Sodium dodecyl sulfate; Triton = Triton X-100 or polyethylene glycol p-(1,1,3,3-tetramethylbutyl)-phenyl ether; Tween 20 = Polyoxyethylene (20) sorbitan monolaurate; Tween 80 = Polyoxyethylen (20) sorbitan monooleat

CHAPS had a positive influence on lipase activity of native TTL (70%) and TTL[Aha] (80%), but this improvement is not mirrored in TTL[Nle] (5%; **Figure 29**). A similar but more marked pattern was found in the presence of PVA, where the activity of native lipase increased by more than 230%, TTL[Aha] by 140%, and TTL[Nle] by only 30% when compared to their basal activities (**Figure 29**). The alterations observed are probably attributable to the chemical nature of these substances. CHAPS is a detergent containing hydrophobic regions whereas PVA is a water-soluble synthetic polymer; however, both contain many polar hydroxyl groups. Hence, these

substances could preferentially interact with the exposed hydrophilic Met and Aha residues of native and TTL[Aha], respectively, but not with those hydrophobic Nle residues of the TTL[Nle]. Enhancement of lipase activity upon treatment with CHAPS has been previously reported in the literature.¹¹⁶⁻¹¹⁸ Since EDTA can chelate most metal ions, it is used to treat water, and also as an additive in detergents, chemical, paper, food, medical and cosmetic industries. It also has applications in the inactivation of metal-dependent enzymes. While the activity of TTL increased by more than 150% in presence of EDTA, the opposite effect was induced in TTL[Nle] and TTL[Aha] with almost 80% and 50% inhibition, respectively (**Figure 29**). This suggests that the presence of metal ions has more influence on the activity of the generated congeners than parent TTL. These inhibitory effects of EDTA on other lipases have also been previously reported.¹¹⁴

A general decrease of all lipase activities was noticed after incubation with SDS, Triton, Tween 20, or Tween 80, where Triton was the only surfactant having a less negative effect on native TTL (10%; **Figure 29**). Triton X-100 is nonionic and contains both hydrophilic and hydrophobic regions, but no net charges. The hydrophilic part is composed of a polyethylene oxide group of 9.5 ethylene oxide units on average. Tween 20 is a polyoxyethylene derivative of sorbitan monolaurate (C12:0). Tween80 is a nonionic surfactant and emulsifier derived from polyethoxylated sorbitan and oleic acid which is very soluble in water and often used in food industry. SDS is one of the most widely used anionic surfactants in cleaning and products for general hygiene including toothpastes, shampoos, and shaving foams. The effects on the lipase activities could only be understood by more in-depth studies of the interactions between the surfactants, the substrate, and the lipases.

3.1.8.4 Inhibitors

The effect of inhibitors on lipases is important because it provides information on its catalytic mechanism. The effect of enzyme can be reversible or irreversible; reversible inhibitors for lipase inhibit its activity by changing the conformation or

interfacial properties, but do not act directly on the active site. Irreversible inhibitors, on the other hand, act directly on the active site. To further characterize the lipase congeners, the irreversible inhibitors Pefabloc and PMSF, as well as denaturing agents were used (Figure 30).

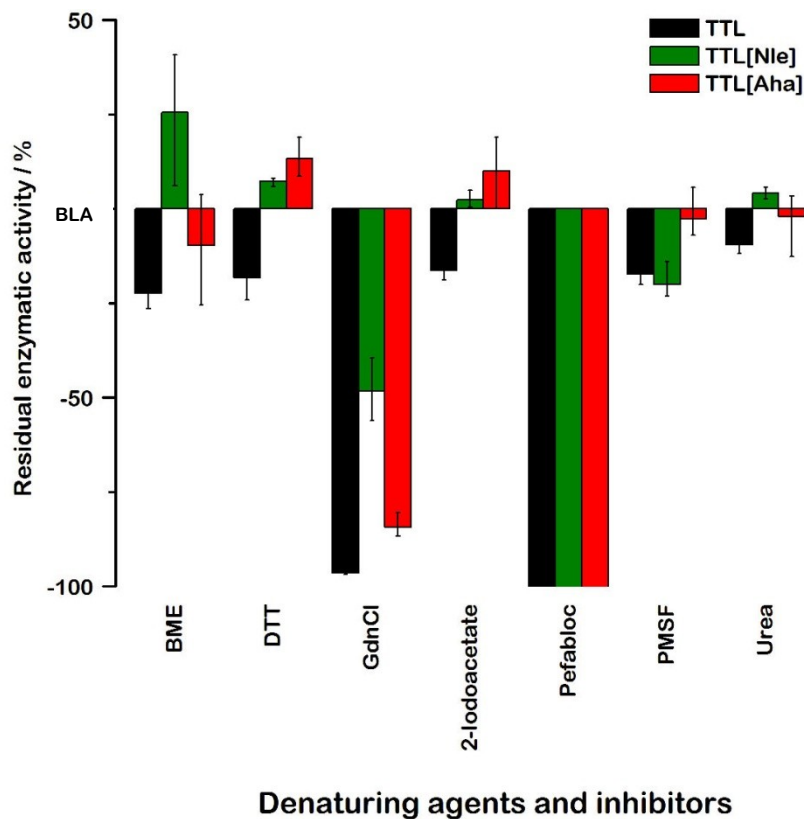


Figure 30. Influence of inhibitors in lipase activity. The TTL congeners were exposed to 1 mM of different inhibitors (500 mM guanidinium chloride and 2M urea) for 60 min and the residual lipase activity was measured three times at T_{opt} and pH 8 with *p*NPP as substrate. Data is normalized against the basal lipase activity (BLA) of the corresponding congener in presence of water, and without activation. BME = β -Mercaptoethanol; DTT = dithiotreitol; GdnCl = Guanidine hydrochloride; Pefabloc = 4-(2-aminoethyl)-benzenesulfonyl fluoride hydrochloride; PMSF = phenylmethylsulfonyl fluoride

The lipase activity of all congeners was strongly affected after treatment with GdnCl, one of the strongest denaturants used in physiochemical studies, and irreversibly inhibited by the water soluble, serine-specific inhibitor Pefabloc (Figure 30). The total inactivation of all lipases by Pefabloc is caused by the modification of the essential serine residue that plays a key role in the catalytic mechanism of all known lipases.¹¹⁹

Although TTL activity was completely lost when it was preincubated at 30 °C for 90 min with 1 mM PMSF,¹⁰⁰ the same amount of PMSF for 60 min did not affect that much the activity of TTL[Aha] activity, but inhibited as much as 25% the activity of parent TTL and TTL[Nle] (**Figure 30**). These differences could be explained by the length exposure time.

Most lipases do not contain neither free –SH or S–S bridges that play an important role in catalytic activity. Consequently, it is expected that the reducing agents β -mercaptoethanol (BME), DTT, and 2-iodoacetate will have no effect on lipase activity. However, all these agents affected the activity of parent TTL but showed an opposite effect on the activities of TTL[Nle] and TTL[Aha] (except for BME that also diminished lipase activity; **Figure 30**). Interestingly, similar patterns in different intensities were found in lipase activities when BME or urea was used (**Figure 30**). Surprisingly, the parent TTL is the most vulnerable congener to harsh denaturing and reducing agents, while TTL[Aha] is more resistant, followed by TTL [Nle]. The rationale behind these results, however, should be carefully done, since the differences in lipase activities are small among the congeners.

In summary, the global substitution of Met residues with the related isosteric analog Nle and the surrogate Aha yielded lipase congeners with both elevated and lowered optimal temperature and pH, thermostability, substrate access and specificity, as well as resistance toward organic solutions, metal ions, surfactants and inhibitors. However, it is difficult to say whether the emergent features of the TTL congeners are due to synergistic effects of multiple (all-or-none) replacements or mostly due to individual effects of key Met residues in the enzyme structure. To this end, the development of a method that allows the site-specific incorporation of Met analogs is necessary.

3.2 Making up the faces of Janus

Currently, no method for the site-specific incorporation of Met analogs into proteins has been developed, probably because the AUG codon has an unambiguous meaning: Methionine. Nevertheless, using AUG sense codons with ambivalent meanings for the site-specific incorporation of Met analogs may allow us to further engineer biocatalysts of industrial interest. This possibility can only be realized by introducing an orthogonal pair, which is composed of an aminoacyl-tRNA synthetase and its cognate tRNA, which does not cross-react with the endogenous components from the host. Several orthogonal pairs from *S. cerevisiae* (Phe), *M. jannaschii* (Tyr), *M. maize* (Pyr), and *M. barkeri* (Pyr) have already been imported into *E. coli*.⁸ Most of these, however, rely on stop codon suppression-based methods applicable only to aromatic analogs (Tyr or Phe) or long aliphatic Lys analogs such as Pyr. Nevertheless, the fact that Tirrell and coworkers were able to reassign two degenerate sense codons with two different Phe analogs through a yeast orthogonal pair¹²⁰ suggests that in principle, it is feasible to apply the same concept to the AUG sense codon that actually participates both in translation initiation and elongation.

3.2.1 Searching for an orthogonal pair of methionine

The evolution of an orthogonal pair may not be a serendipitous finding¹²¹, considering that an AARS and its cognate tRNA from an organism belonging to a life domain (e.g. bacteria, archaea, or eukarya) usually do not cross-react with counterparts from other evolutionary distinct organisms.¹²² For instance, *EcMetRS* exhibits low affinity for eukaryotic cytoplasmic elongator tRNAs^{Met 123-125}, but has a high affinity for initiator tRNAs from other bacteria, as well as mitochondrial and chloroplastic tRNAs from eukaryotes.¹²⁴⁻¹²⁶ Similarly, *MetRSs* from mitochondria and chloroplasts efficiently aminoacylate tRNA^{Met} from *E. coli*, whereas eukaryotic cytoplasmic *MetRSs* aminoacylate mitochondrial, chloroplastic and *E. coli* tRNAs^{Met} with low efficiency.¹²⁷⁻¹²⁹ Finally, mammalian cytoplasmic *MetRSs* aminoacylate yeast cytoplasmic tRNA^{Met}.¹³⁰ Taken together, these cross-aminoacylation experiments suggest that

there are two types of pairs in the Met system (Figure 31).¹³¹

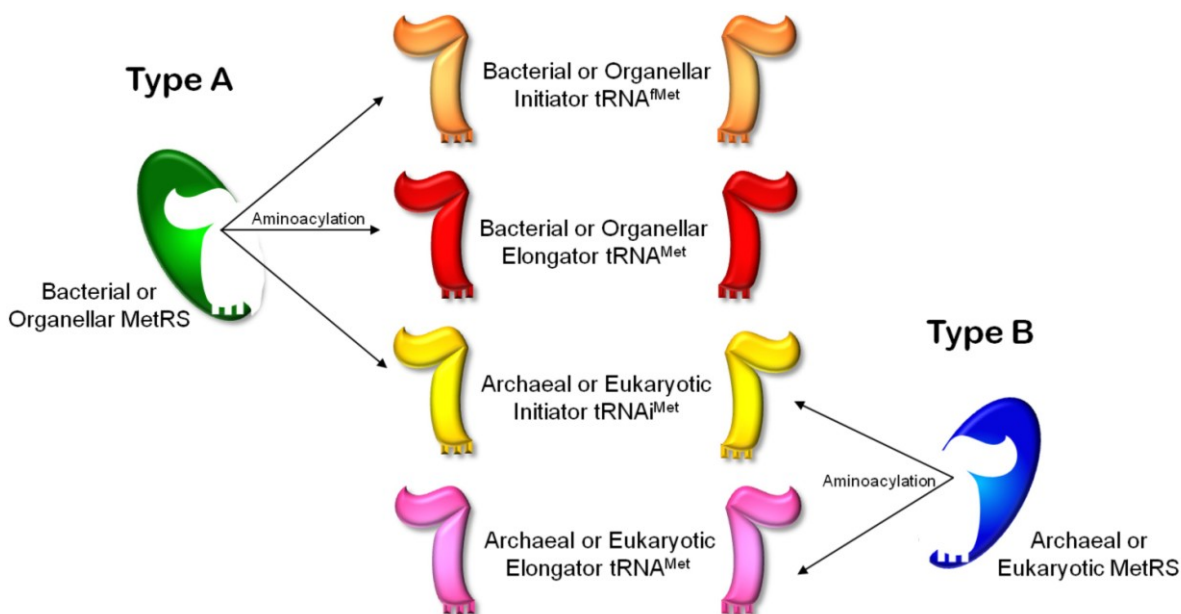


Figure 31. Two types of MetRS:tRNA^{Met} pairs. Type A includes the MetRS from eubacteria and eukaryotic organelles, which are able to preferentially aminoacylate their initiator (tRNA^{fMet}) and elongator (tRNA^{Met}) counterparts, as well as archaeal or eukaryotic cytoplasmic initiator tRNA^{iMet} (tRNA^{iMet}). Type B includes archaeal or eukaryotic cytoplasmic MetRS, which exclusively aminoacylate their cognate elongator tRNAs^{Met} (tRNA^{Met}) and their tRNA^{iMet} (tRNA^{iMet}).

Consequently, it should be feasible to use a type B MetRS:tRNA^{Met} pair that incorporates a Met analog at AUG codons exclusively or at least preferentially during elongation in *E. coli*, since exogenous MetRS would not be able to aminoacylate either the bacterial initiator tRNA^{fMet} or elongator tRNA^{Met}. The overexpression of the orthogonal elongator tRNA^{Met} charged with a Met analog should theoretically be able to efficiently compete with the presumably less abundant, misaminoacylated bacterial elongator tRNA^{Met}. Exogenous tRNA^{Met} should not be aminoacylated by any of the 20 *E. coli* AARSs, including the endogenous MetRS. The type B tRNA^{Met} should also behave as a normal substrate of the bacterial ribosomal machinery. Finally, the Met analog should not be recognized as a substrate of endogenous MetRS nor any other AARS. In summary, the participating molecules have to be orthogonal.¹³²

Given this, finding an orthogonal MetRS can be realized by identifying as many enzymes of archaeal or eukaryotic origin as possible. First, the available coding sequences of all MetRSs were obtained from the American National Center for Biotechnology Information (NCBI) databases. Next, the bacterial or archaeal genomic DNA or eukaryotic cDNA of many organisms were acquired from different sources, so that their respective genes amplify by PCR (see 6.2.1.1 for details). Based on these, the MetRS from bacteria (*Aquifex aeolicus*, *E. coli*), archaea (*Aeropyrum pernix*, *Methanocaldococcus jannaschii*, *Natronomonas pharaonis*, *Pyrobaculum aerophilum*, *Pyrococcus abyssi*, *Sulfolobus acidocaldarius*, and *Thermoplasma acidophilum*), and eukarya (*Arabidopsis thaliana*, *Danio rerio*, *Drosophila melanogaster*, *Homo sapiens*, and *Saccharomyces cerevisiae*) were cloned into suitable expression vectors (see 6.1.8.2 for details). Finally, thirteen 'orthogonal candidate' MetRSs, excluding EcMetRS, which is intended as a positive control, were generated. Each MetRS is referred to on the basis of the organism where it comes from, e.g. MetRS from *A. pernix* = ApMetRS, etc.

3.2.1.1 Expression and solubility in *E. coli*

Vectors containing the different MetRS were transformed into suitable *E. coli* strains and protein expression was induced by adding IPTG (see 6.2.2.3 for details). A solubility test was subsequently performed to check if the MetRS was expressed in either in the soluble fraction or as inclusion bodies (see 6.2.2.6 for details). Insoluble exogenous MetRS would be disadvantageous, and are discarded. In all cases, the same amount of non-induced (NI) or IPTG-induced (I) cells, as well as their soluble fraction (SF) and insoluble fraction (IF) was analyzed by SDS-PAGE using a 12% gel (Figure 32).

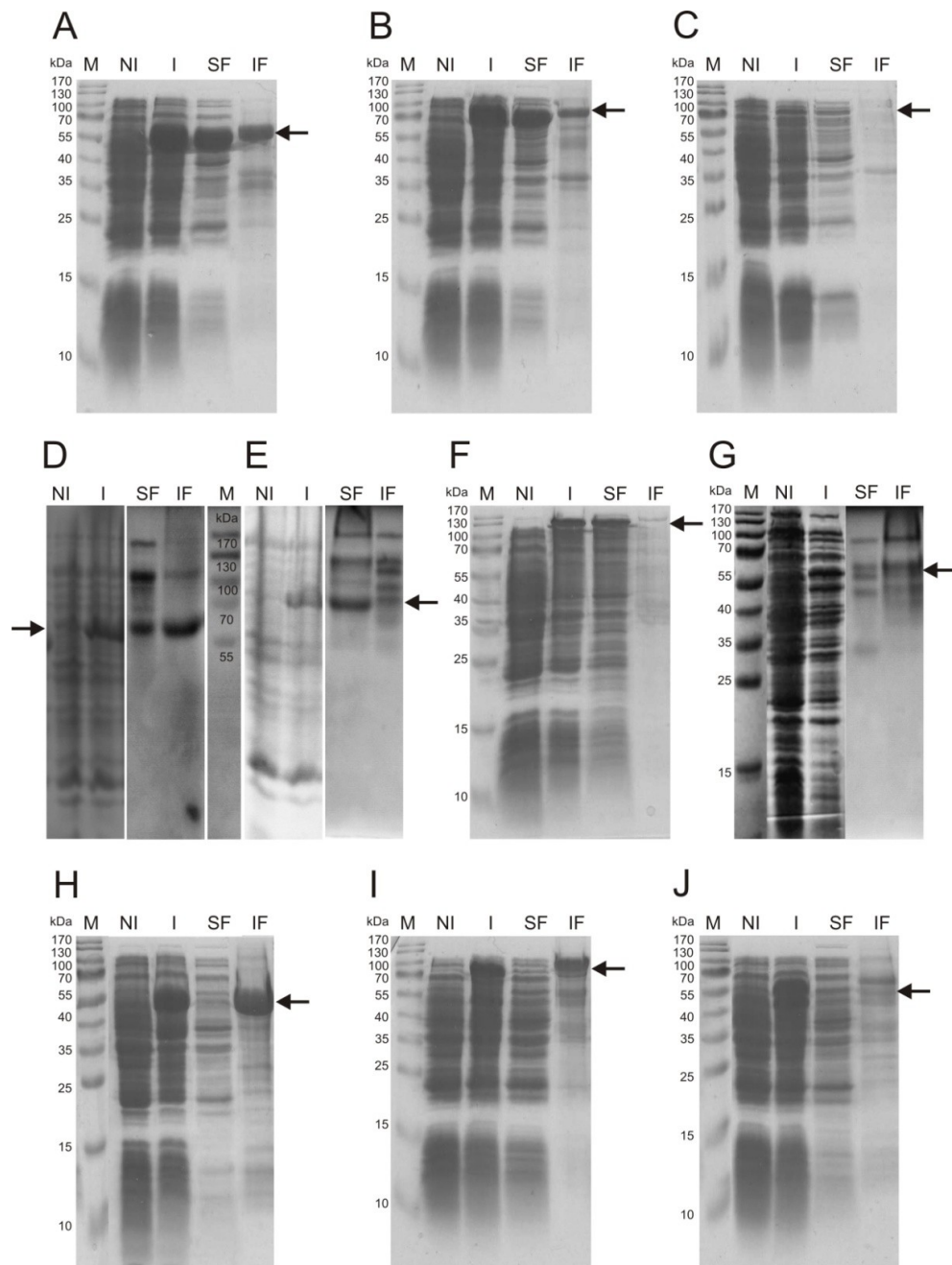


Figure 32. Expression and solubility of different MetRSs in *E. coli*. The MetRSs are indicated with an arrow, with their corresponding theoretical masses in brackets. A) *Aa*MetRS WT (61093.5 Da); B) *Ec*MetRS WT (80398.5 Da); C) *Mj*MetRS WT (77337.9 Da); D) *Ap*MetRS WT (70624.7 Da); E) *Pa*MetRS WT (69896.7 Da); F) *Np*MetRS WT (79924.7 Da); G) *Sa*MetRS WT (70222.9 Da); H) *Ta*MetRS WT (64681.1 Da); I) *Sc*MetRS WT (87400 Da); and J) *Sc*MetRS TF (6-185Δ; 66825.7 Da). M = MW protein marker; NI = Non-induced cells I = induced cells; SF = Soluble Fraction; IF = Insoluble Fraction

As expected, the bacterial MetRS from *A. aeolicus* and *E. coli* were relatively high concentrations in the soluble form (Figure 32A/B). Archaeal MetRS from *A. pernix*, *P. aerophilum*, and *S. acidocaldarius* are similarly well-expressed and soluble (Figure 32D/E/G). This is very important, since archaeal MetRSs are type B enzymes. The only question that remains is whether they are active at 37 °C, since all used archaea are hyperthermophilic (optimum grow temperature is from 80 to 100 °C). Archaeal MetRS from *M. jannaschii* was poorly expressed (Figure 32C), while MetRS from *N. pharaonis* had an unexpected size (Figure 32F). MetRS from *T. acidophilum* was completely insoluble (Figure 32H). These patterns might have been caused by the extreme environments in which these organisms normally thrive. For example, *M. jannaschii* is a thermophilic, and has an optimal temperature of 85 °C. *N. pharaonis*, on the other hand, lives optimally in 3.5 M NaCl and at a pH of 8.5; and *T. acidophilum* grows optimally at 56 °C and pH 1.8. Finally, most of the eukaryotic MetRSs could not be expressed in *E. coli* (data not shown, except for the baker's yeast MetRS or ScMetRS in both WT and truncated forms (6-185Δ), since they were very well expressed, though insoluble; Figure 32I/J). The finding that most eukaryotic MetRSs are not even expressed in *E. coli* could be due to the presence of an N-terminal extension. Eukaryotic MetRSs usually contain an N-terminal extension absent in bacterial or archaeal MetRSs (see Appendix 9.4 for more details). This appended region is believed to improve tRNA binding efficiency.¹³³ Finally, the problem of codon usage can be partly disregarded, since the strains contained plasmids to supplement *E. coli* with rare tRNAs.

3.2.1.2 Purification and analytical characterization

Large-scale LB cultures were used to express soluble MetRSs (see 6.2.2.6 for details). Proteins were subsequently purified to a level approximately between 80 to 95% using Ni-NTA affinity chromatography (see 6.2.2.7 for details). The degree of purity was dependent on the enzyme stability and the yield was in the order of milligrams of protein per liter of culture. As expected, *EcMetRS* WT was the best-expressed enzyme. The yields for *EcMetRS* mutants are lower; more mutated

enzymes exhibited both lower stability and a faster precipitation at 4 °C (data not shown). The different *E. coli* mutants were generated because it has been reported that these have a preferential activation toward certain Met analogs. For example, the group of Tirrell demonstrated that mutant *EcMetRS* L13G is able to activate and efficiently charge azidonorleucine (Anl).¹³⁴⁻¹³⁶ Similarly, although 6,6,6-trifluoronorleucine (Tfn) does not support significant protein synthesis *in vivo*¹³⁷ and *in vitro*^{138,139}, the same group was able to evolve a triple-mutated *EcMetRS* that activates Tfn at modest levels.¹⁴⁰ Hence, the single-mutant L13S, double-mutant L13S/Y260L and triple-mutant L13S/Y260L/H301L of *EcMetRS* were generated and included in the collection to confirm the preferential activities of those Met analogs. The same scheme was followed for the MetRS of *M. jannaschii*, where the mutations from the *E. coli* enzymes were transferred according to primary structure alignment (see Appendix 9.4 for details). Lower yields were obtained from the archaeal MetRSs whose expression was only achieved using *E. coli* strains supplemented with rare tRNAs. Finally, although *ScMetRS* TF was mainly insoluble, proteins in the order of milligrams could be purified in soluble form. The purification of the enzymes is indicated by the presence of bands with MW of 60 to 80 kDa after 12% SDS-PAGE (Figure 33).

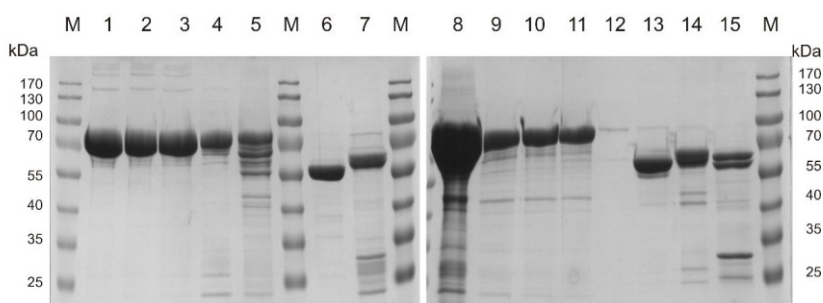


Figure 33. Purification of soluble MetRSs in *E. coli*. Purified MetRSs and their calculated masses: 1. *EcMetRS* WT (80399.5 Da); 2. *EcMetRS* L13G (80343.4 Da); 3. *EcMetRS* L13S (80373.5 Da); 4. *EcMetRS* L13S/Y260L (80323.5 Da); 5. *EcMetRS* L13S/Y260L/H301L (80299.5 Da); 6. *AaMetRS* WT (61094.6 Da); 7. *ScMetRS* TF (6-185 Δ) (66826.7 Da); 8. *MjMetRS* WT (77338.9 Da); 9. *MjMetRS* L9G (77282.8 Da); 10. *MjMetRS* L9S (77312.9 Da); 11. *MjMetRS* L9S/H254L (77262.8 Da); 12. *MjMetRS* L9S/H254L/H288L (77238.9 Da); 13. *ApMetRS* WT (70625.7 Da); 14. *PaMetRS* WT (69897.7 Da); 15. *SaMetRS* WT (70223.9 Da). In all cases a defined protein amount was loaded in a 12% SDS-polyacrylamide gel. M = MW protein marker.

After purification, samples were further characterized using ESI-MS (Figure 34).

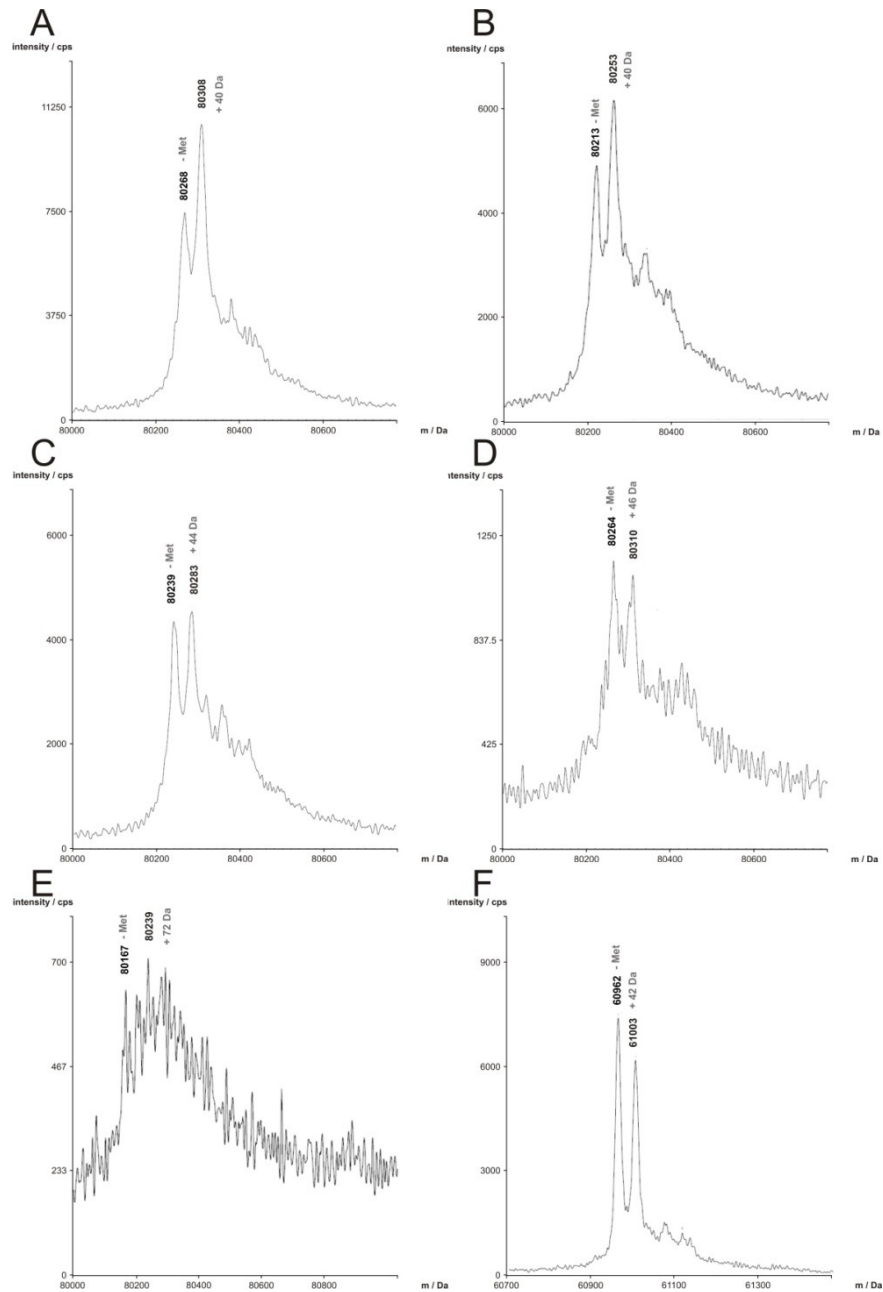


Figure 34. ESI-MS spectra of purified MetRSs. Each MetRS peak is labeled with the determined masses; theoretically calculated masses minus the Met excision are underlined, and indicated parenthetically: A) *EcMetRS* WT (80399.5 – 131.1 = 80268.3 Da); B) *EcMetRS* L13G (80343.4 – 131.1 = 80212.2 Da); C). *EcMetRS* L13S (80373.5 – 131.1 = 80242.3 Da); D) *EcMetRS* L13S / Y260L (80323.5 – 131.1 = 80192.3 Da); E). *EcMetRS* L13S / Y260L / H301L (80299.5 – 131.1 = 80168.3 Da); F). *AaMetRS* WT (61094.6 – 131.1 = 60963.5 Da).

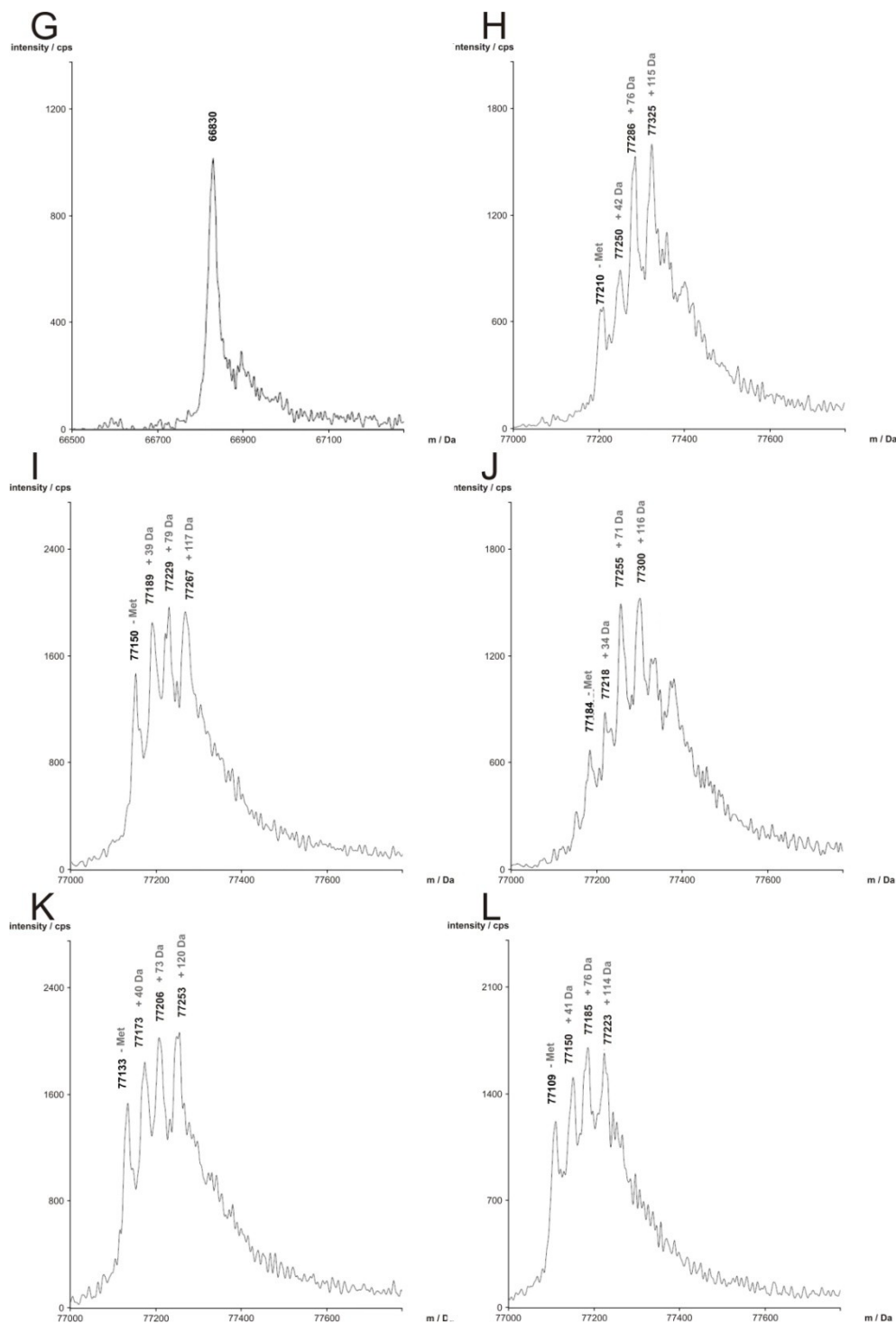


Figure 34. ESI-MS spectra of purified MetRSs (continuation). G) ScMetRS TF (1-185 Δ /736-751 Δ) (66826.7 Da, no Met excision); H) *Mj*MetRS WT (77338.9 – 131.1 = 77207.7 Da); I) *Mj*MetRS L9G (77282.8 – 131.1 = 77151.6 Da); J) *Mj*MetRS L9S (77312.9 – 131.1 = 77181.7 Da); K) *Mj*MetRS L9S / H254L (77262.8 – 131.1 = 77131.6 Da); L) *Mj*MetRS L9S / H254 L / H288L (77238.9 – 131.1 = 77107.7 Da).

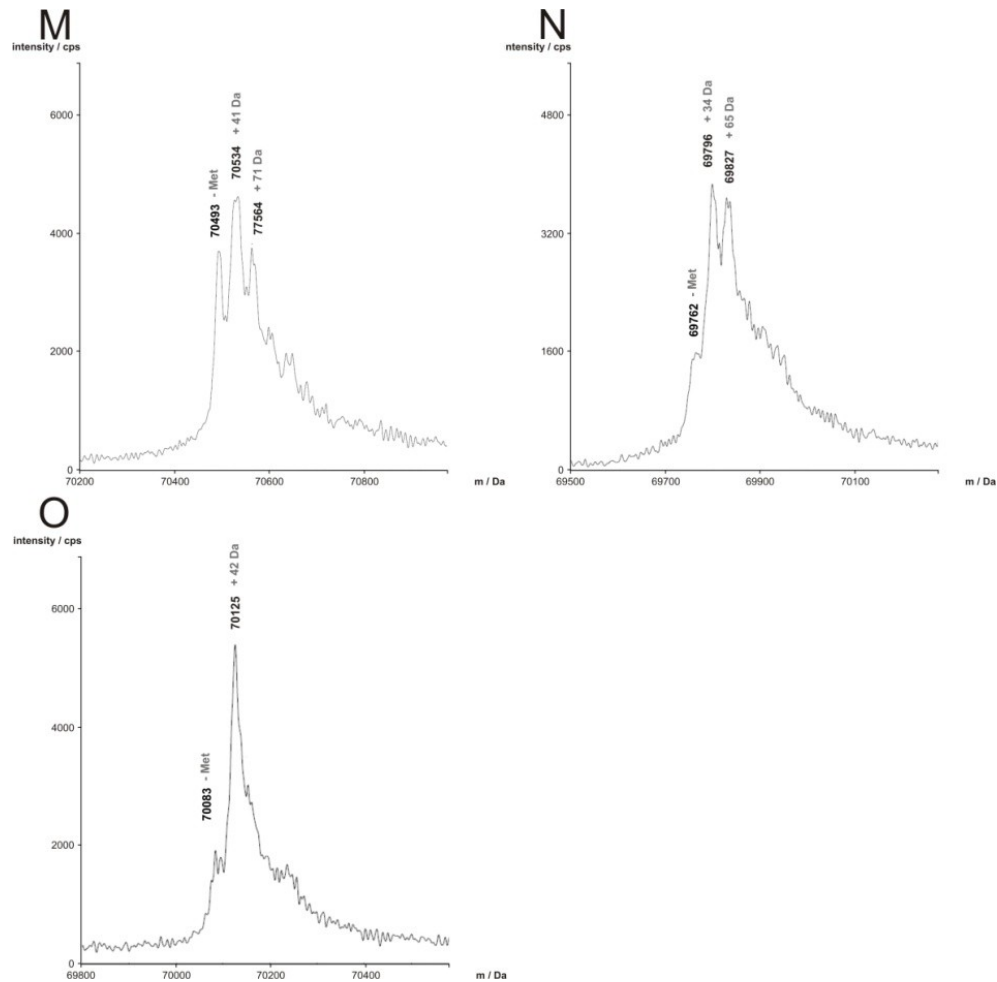


Figure 34. ESI-MS spectra of purified MetRSs (continuation). M) *Ap*MetRS WT (70625.7 – 131.1 = 70494.5 Da); N) *Pa*MetRS WT (69897.7 – 131.1 = 69766.5 Da); O) *Sa*MetRS WT (70223.9 – 131.1 = 70092.7 Da).

In all cases the *N*-terminal Met was excised according to the *N*-terminal rules¹⁴¹, except for *Sc*MetRS TF whose second residue is not a bulky amino acid. Thus, 131.1 Daltons (the equivalent of one Met forming a peptide bond) were subtracted to the theoretical calculated mass. The determined masses for all the MetRSs nearly corresponded with the theoretical ones, i.e. in addition to the most prominent expected peak, all preparations revealed another peak of similar size, with an additional 34-46 Da; these are protein adducts of unknown nature (Figure 34). More mutated enzymes were less stable, as indicated by the low yield, intensity, and suboptimal spectra display of *Ec*MetRS (Figure 34D/E) and *Mj*MetRS (Figure 34K/L).

The preparations from *M. jannaschii* had several peaks with ca. 71 and 120 Da protein adducts of similarly unknown nature (Figure 34H/I/J). In contrast, the rest of the archaeal MetRSs showed spectra with better quality (Figure 34M/N/O).

3.2.1.3 *In vitro* cross-aminoacylation experiments

On MetRSs purification and characterization, their activities were measured by using radioactive Met and commercially available *E. coli* initiator tRNA^{fMet} and elongator tRNA^{Met} (present in bulk tRNA; see 6.2.3.1 for details). The methionylation extent for both tRNA preparations by all enzymes is shown in Figure 35.

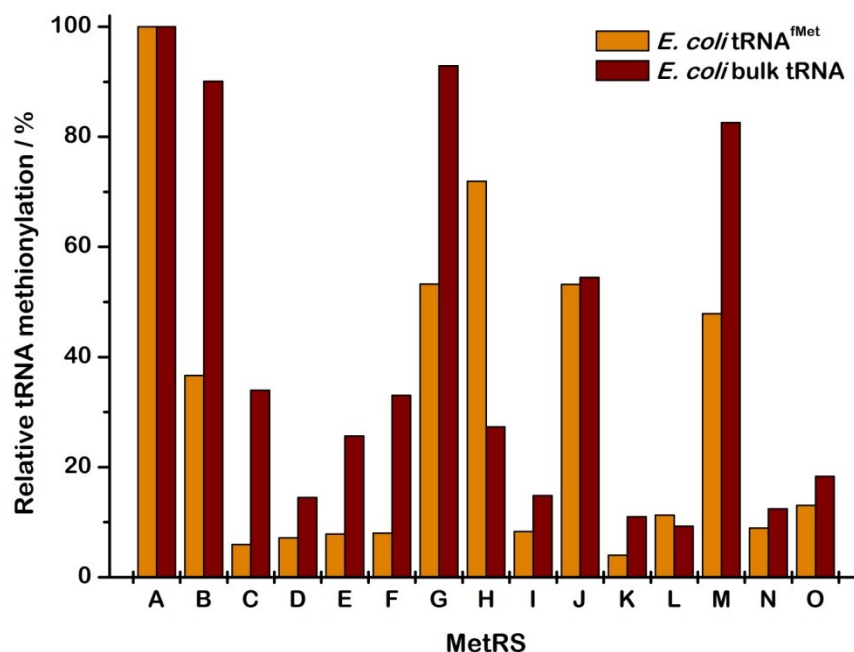


Figure 35. Cross-aminoacylation experiments. The charging efficiency for ³⁵S-Met onto initiator tRNA^{fMet} and bulk tRNA was measured at 37 °C after 20 min using the same concentration of A) *EcMetRS* WT; B) *EcMetRS* L13G; C) *EcMetRS* L13S; D) *EcMetRS* L13S/Y260L; E) *EcMetRS* L13S/Y260L/H301L; F) *AaMetRS* WT; G) *ScMetRS* TF (6-185Δ); H) *MjMetRS* WT; I) *MjMetRS* L9G; J) *MjMetRS* L9S; K) *MjMetRS* L9S/H254L; L) *MjMetRS* L9S/H254L/H288L; M) *ApMetRS* WT; N) *PaMetRS* WT; O) *SaMetRS* WT.

The most active enzyme toward both tRNA preparations was expectedly *EcMetRS* WT (**Figure 35A**). These values were used as a reference to determine the degree of methionylation for both the different mutants and the different enzymes, which could also yield clues as to its orthogonality in *E. coli*. The *EcMetRS* mutants displayed less activity toward initiator tRNA^{fMet} than elongator tRNA^{Met} but these activities diminished when the number of mutations increased (**Figure 35B-E**). This findings support the idea that mutations in the MetRS binding pocket may increase the specificity for other Met analogs, but compromise tRNA recognition as a tradeoff. These mutations could be therefore more detrimental than beneficial for MetRS optimal activity. The other bacterial enzyme whose affinity for both tRNA preparations was not significant at 37°C was *AaMetRS* (**Figure 35F**); however, more than 75% activity for bulk *E. coli* tRNA was detected at 70 °C (data not shown). Thus it could be confirmed that *AaMetRS* is thermophilic and cross-reacts with *E. coli* tRNAs under suitable conditions. Likewise, other enzymes cross-reacted to some extent with both tRNA preparations, particularly *ScMetRS* TF (**Figure 35G**), *MjMetRS* WT (**Figure 35H**), *MjMetRS* L9S (**Figure 35J**), and *ApMetRS* WT (**Figure 35M**). Unexpectedly, *MjMetRS* WT and L3S still showed some activity despite the use of noncognate tRNAs (**Figure 35H/J**), but the double- and triple-mutated enzymes were not as active as the single-mutated or wt (**Figure 35I/K/L**). These results indicate that the eukaryotic MetRS from yeast, as well as the two archaeal MetRS from *M. jannaschii* and *A. pernix* are not suitable for use in *E. coli*. This was not expected since these MetRS are considered as type B. Nonetheless, the less active enzymes with respect to both tRNA^{Met} isoacceptors were the type B MetRS from *P. aerophilum* (**Figure 35N**) and *S. acidocaldarius* (**Figure 35O**). These two archaeal enzymes could be considered as candidate orthogonal MetRSs, since they did not aminoacylate at all *E. coli* tRNAs. The only prerequisite would be that they are as active as *EcMetRS* at 37 °C.

3.2.1.4 *In vitro* activation of methionine analogs

Since it would obviously be preferred by both the host and all other MetRSs, Met must be depleted from the system to so that Met analogs will be preferentially

incorporated by each MetRS. It is imperative though, that there are differential preferences in terms of charging two different Met analogs, as well as in the subsequent transfer of the aminoacylated parts onto the respective initiator or elongator tRNAs, by both the host and orthogonal MetRS. For this, the different Met analogs were either purchased or synthesized (Figure 36; see 6.1.3 for details).

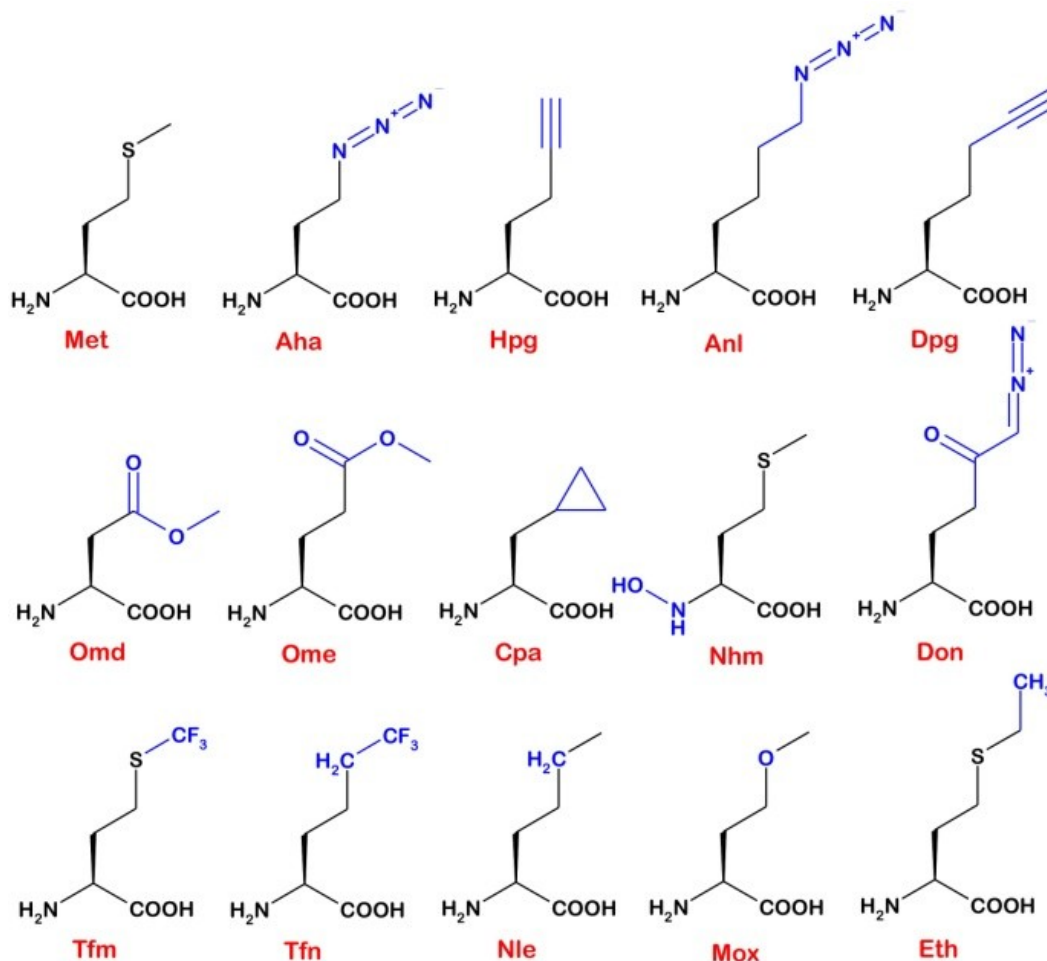


Figure 36. Met analogs. The synthetic amino acids contain chemical groups with single atom substitutions and large side-chains (blue). Met, Methionine; Aha, Azidohomoalanine; Hpg, Homopropargylglycine; Anl, Azidonorleucine; Dpg, Dihomopropargylglycine; Omd, aspartic acid β-methyl ester; Ome, glutamic acid γ-methyl ester; Cpa, β-cyclopropyl-alanine; Nhm, N-hydroxy-methionine; Don, 6-diazo-5-oxo-norleucine; Tfm, 5,5,5-trifluoromethionine; Tfn, 6,6,6,-trifluoronorleucine; Nle, norleucine; Mox, methoxinine; and Eth, ethionine.

The substrate specificities of *EcMetRS*, *PaMetRS* and *SaMetRS* for the different Met analogs were subsequently determined using the isotopic ATP:PPi exchange assay (Figure 37; see 6.2.3.2 for details).¹⁴²

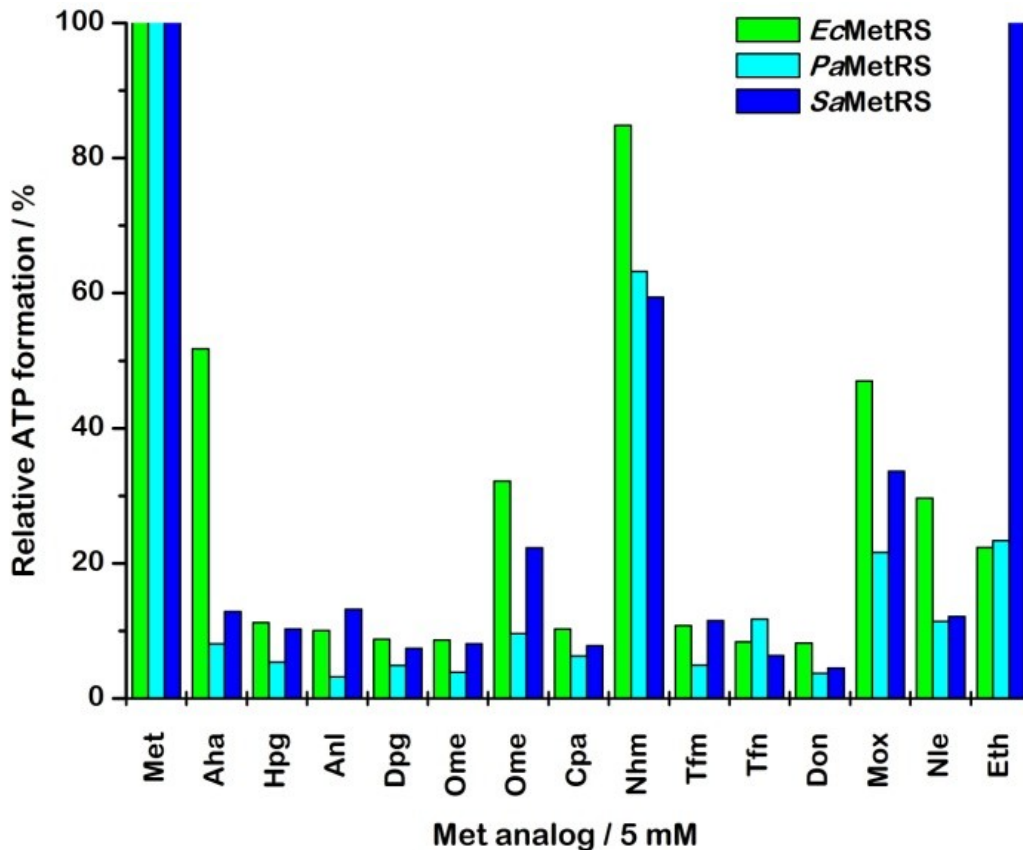


Figure 37. Activation of Met and its analogs by host and ‘orthogonal’ MetRSs. The activation efficiency of *EcMetRS*, *PaMetRS* and *SaMetRS* for several Met analogs was measured at physiological condition.

Importantly, the only case of differential activation of two different Met analogs by the host *EcMetRS* and *SaMetRS* was found for Aha and Eth (Figure 37). Here, *EcMetRS* preferred Aha over Eth, while *SaMetRS* preferred Eth over Aha. Otherwise, no differential activation for the rest of the Met analogs by both MetRSs was found (Figure 37). To rule out any experimental artifact, the activation profiles for Aha and Eth by *EcMetRS* and *SaMetRS* were reevaluated at 37 °C (Figure 38).

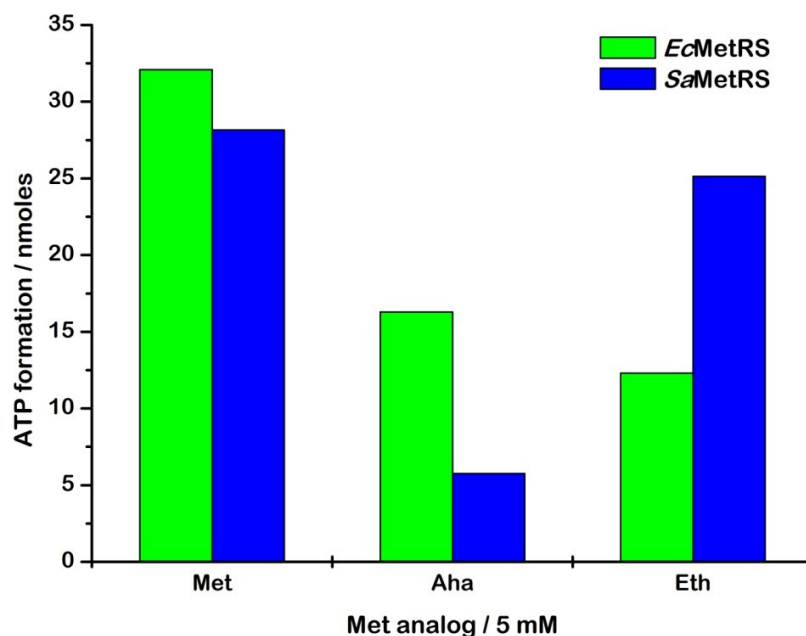


Figure 38. Differential activation of Met analogs by host and ‘orthogonal’ MetRS. The activation efficiency by *EcMetRS* and *SaMetRS* towards Met, Aha, and Eth was measured at 37 °C after 20 min. The bars are depicted without normalization. *EcMetRS* displayed for Aha 16.3 nmoles and for Eth 12.3 so the ratio of preference for Aha over Eth is $16.3 / 12.3 = 1.3$ whereas *SaMetRS* prefers Eth over Aha for about $25.13 / 5.75 = 4.4$.

Strikingly, the *SaMetRS* showed 4.4 times more enhanced substrate specificity for Eth than Aha, whereas *EcMetRS* exhibited a 1.3 fold better activation of Aha than Eth (**Figure 38**). Additionally, *SaMetRS* has very similar activation efficiency for both Met and Eth. This is not surprising for *S. acidocaldarius*, since this extremely thermophilic archaea found in geothermal habitats is a sulfur-metabolizing organism with strains that can even growth in the presence of Eth.¹⁴³ On the other hand, Eth is a very toxic amino acid because it inhibits growth in many microorganisms including *E. coli*.¹⁴⁴ In any case, the finding that Aha and Eth are differentially recognized by both the host *EcMetRS* and the orthogonal *SaMetRS* is very important since this is a prerequisite for the differential reassignment of AUG codons. These findings are significant but were found *in vitro*. It was thus important to study the *in vivo* preferences of *E. coli* for both Aha and Eth. To this end, a model protein containing both 1 and 2 AUG codons located at appropriate sites was used.

3.2.2 Incorporation of Aha and Eth into barstar 1M

Barstar is an intracellular single-domain inhibitor of the extracellular ribonuclease barnase from *Bacillus amyloliquefaciens*, a protein normally secreted to the environment to degrade foreign RNA as a defense mechanism. The structure of barstar is characterized by a β - α - β motif, typical for a nucleic acid binding proteins. It is widely used in folding studies as a small recombinant protein of 90 amino acids.¹⁴⁵ The barstar mutant P28A/C41A/C83A (ψ -b* from the *Greek* is abbreviated as b*1M for clarity reasons; see Appendix 9.2 for sequence details) was used to estimate the natural preference for Aha and Eth at the N-terminus *in vivo* (Figure 39).

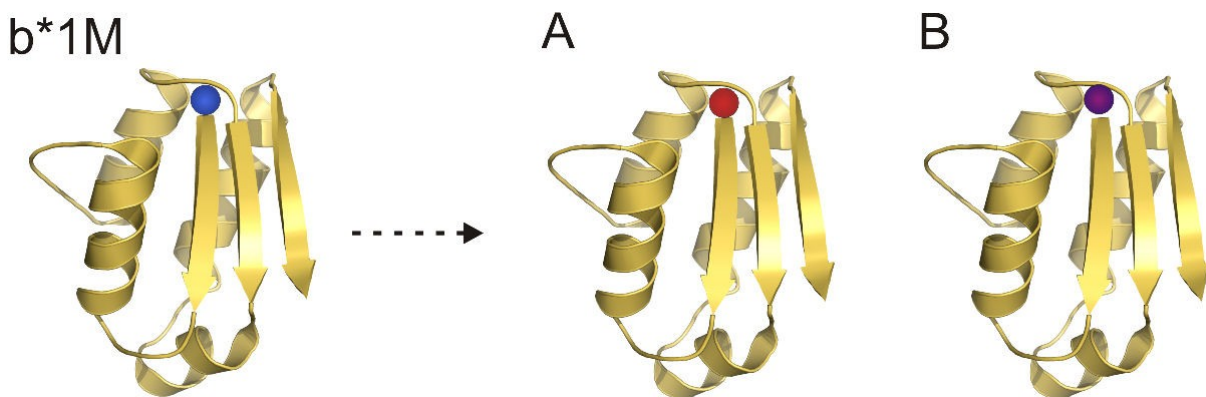


Figure 39. Tandem incorporation of Aha and Eth into barstar 1M. The N-terminal Met (blue) was replaced by Aha (red) or Eth (purple) to generate two congeners: (A) b*1M[Aha] and (B) b*1M[Eth].

This barstar mutant lacks complications arising from oxidation of cysteines or re-folding, which occur in the WT.¹⁴⁶

E. coli Met auxotrophic strains were transformed with the barstar gene containing only one AUG codon at the starting position and supplemented with a limiting amount of Met. After Met depletion, the cells were transferred to NMM containing different amounts of Aha and Eth (see 6.2.2.8 for details). Before expression, six different conditions were established, i.e. Met, Aha, and Eth (as positive controls), and

different ratios of Aha:Eth (3:1, 1:1, 1:3) to assess if the incorporation of the Met analogs is concentration dependent. Under these conditions, three different b* congeners containing one Met, one Aha, and one Eth were produced in single incorporation experiments, while two congeners in different amounts containing either Aha or Eth at the N-terminus were generated in the tandem incorporations. The expression and purification of b* congeners was indicated by a corresponding band with an average mass of approx. 10 kDa (**Figure 40**).

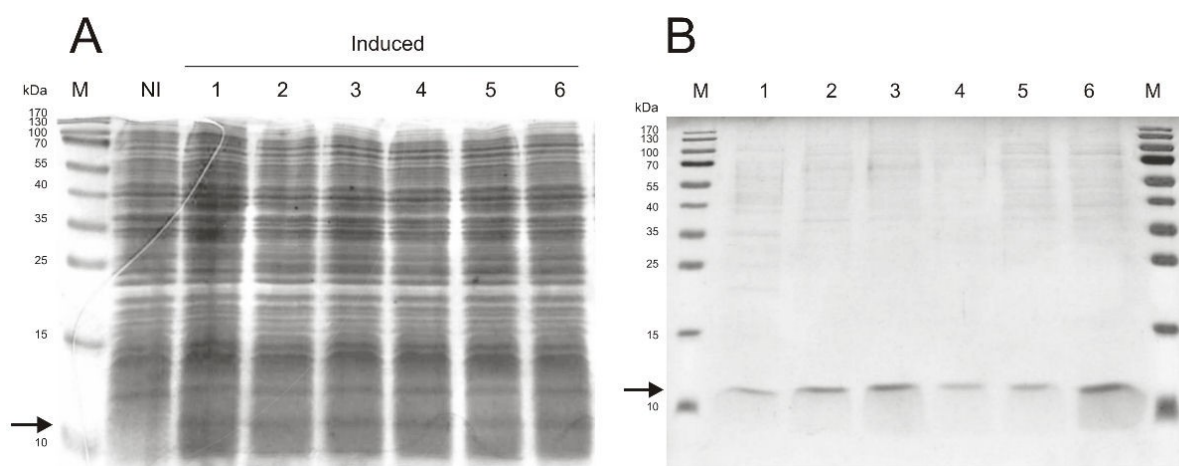


Figure 40. Barstar 1M alloproteins. The b*1M variants were produced through the use of medium supplementats containing 1) Met; 2) Aha; 3) Aha>Eth (3:1); 4) Aha=Eth (1:1); 5) Aha<Eth (1:3); and 6) Eth. These are indicated by arrows in profiles obtained after expression (A) and purification (B) using 17% SDS-polyacrylamide gels and Coomassie staining. M = Standard MW bands; NI = Non-induced culture.

After expression and purification, all b*1M alloproteins were analyzed by ESI-MS and N-terminal sequencing to determine its mass and the amount of Aha or Eth at the N-terminus (**Figure 41**).

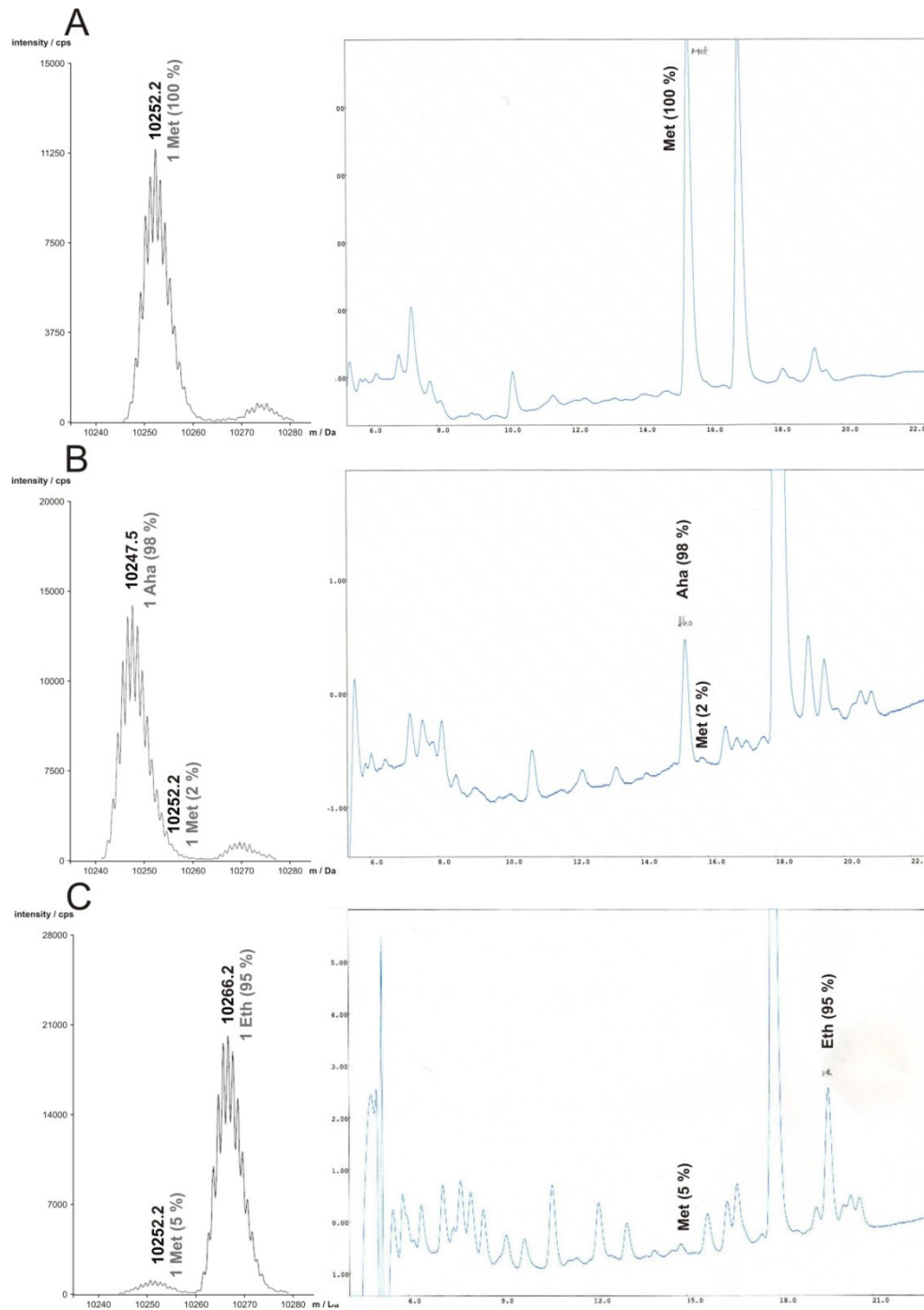


Figure 41. Analytical characterization of barstar 1M congeners. The mass and the N-terminal-sequencing spectra for b*1M supplemented with A) Met; B) Aha; C) Eth are shown in the left and right columns, respectively. In both cases, the combined intensities of the corresponding peaks sum up to 100%, from which each species percentage was calculated and annotated. For ESI-MS, the calculated mass for b* with 1 Met is 10252.6 Da; with 1 Aha is 10247.6 Da; and with 1 Eth is 10266.8 Da. For N-terminal sequencing, Aha and Eth showed retention times at 15 and 19 units, respectively.

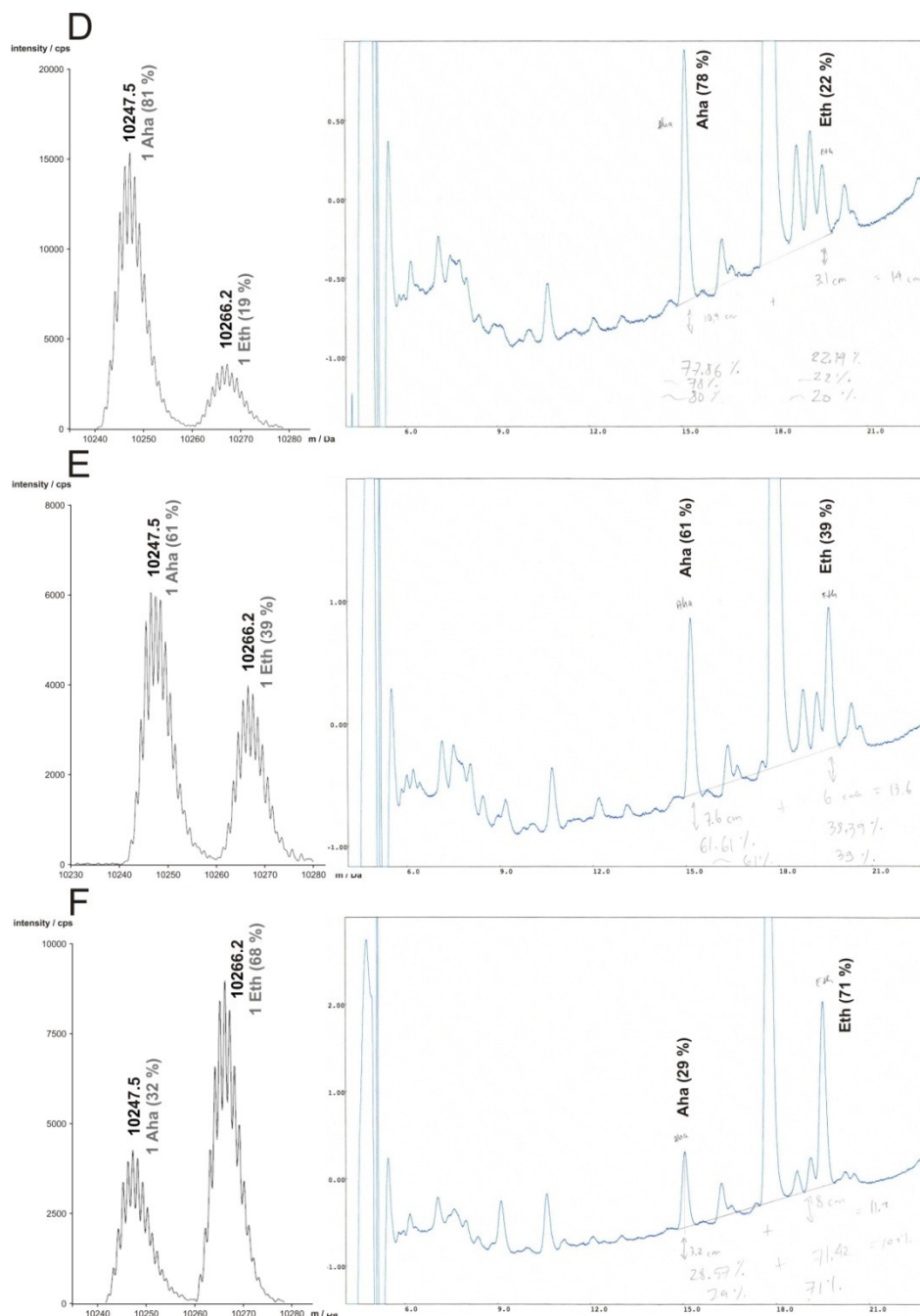


Figure 41. Analytical characterization of barstar 1M congeners (continuation). The mass and the N-terminal-sequencing spectra for b*1M supplemented with D) Aha > Eth (3:1); E) Aha = Eth (1:1); and F) Aha < Eth (1:3) are shown in the left and right columns, respectively. In both cases, the combined intensities of the corresponding peaks sum up to 100%, from which each species percentage was calculated and annotated. For ESI-MS, the calculated mass for barstar with 1 Met is 10252.6 Da; with 1 Aha is 10247.6 Da; and with 1 Eth is 10266.8 Da. For N-terminal sequencing, Aha and Eth show retention times at 15 and 19, respectively.

The congeners that only contained Met, Aha, or Eth at the N-terminus displayed a prominent peak at the expected mass (**Figure 41A/B/C**; left panel). Importantly, the N-terminal sequencing results are tightly correlated with the ESI-MS results (**Figure 41A/B/C**; right panel). When the medium was supplemented with different amounts of Aha and Eth, two peaks of different intensities, corresponding to each of the congeners, were found (**Figure 41D/E/F**; left panel). The calculated proportions of the peaks from the ESI-MS spectra were also very similar to those from N-terminal sequencing (**Figure 41D/E/F**; right panel). One can say that both ESI-MS and N-terminal sequencing methods are reliable for accurately determining the incorporation of Aha and Eth into barstar. Furthermore, the summary of the results obtained from both methods in **Table 3** provides an easy way for comparing the natural preferences in terms of ratios of Aha and Eth for the N-terminus of the different b*1M variants.

Table 3. Natural preference of Aha and Eth at the N-terminus of barstar 1M alloproteins.

Amino acids supplemented	Method	N-terminus (%)		Ratio
		Aha	Eth	
Aha / Eth (0.75 / 0.25)	ESI-MS	81	19	81 / 19 = 4.0 for Aha
	N-terminal sequencing	78	22	78 / 22 = 3.5 for Aha
Aha / Eth (0.50 / 0.50)	ESI-MS	61	39	61 / 39 = 1.5 for Aha
	N-terminal sequencing	61	39	61 / 39 = 1.5 for Aha
Aha / Eth (0.25 / 0.75)	ESI-MS	32	68	68 / 32 = 2.0 for Eth
	N-terminal sequencing	29	71	71 / 29 = 2.5 for Eth

Interestingly, it was found Aha was found to be incorporated fourfold higher at the N-terminus compared to Eth when it is four times more abundant in the medium than (**Table 3**). On the other hand, when there was four times more Eth in the medium than Aha to the medium, Eth incorporation at the N-terminus was only twice as more than Aha (**Table 3**). This indicates that the extent of incorporation of Aha or Eth at the N-terminus of b*1M could be fine-tuned by changing the concentration of the analogs in the media. Moreover, if one considers the experiment with both analogs present in

equal amounts (Table 3), it is plausible to suggest that the *EcMetRS* exhibited *in vivo* a 1.5 fold Aha-tRNA^{fMet} to Eth-tRNA^{fMet} charging preference *in vivo*. This finding is consistent with previous *in vitro* data where *EcMetRS* showed a 1.3 fold increase in activation of Aha as compared to Eth (Figure 38).

These findings suggest that the activation data of an aminoacyl-tRNA synthetase for a given amino acid not only reflects the charging value with respect to its cognate tRNA, but also its incorporation efficiency into proteins, a very common observation described in the literature.³⁶ Additionally, it is assumed that the noncanonical amino acids are efficiently up taken by the cells and accumulated several-fold inside them; this factor has also been well documented even for Met analogs in *E. coli*.¹⁴⁷ What would be interesting now would be to assess if there is a preference for Aha or Eth at start or internal AUG codons.

3.2.3 Incorporation of Aha and Eth into barstar 2M

To estimate the natural incorporation preference for Aha and Eth of *E. coli in vivo*, the model protein barstar containing one AUG codon at the start position and at position 47 was used (P28A/C41A/E47M/C83A; b*2M; see Appendix 9.3 for sequence details). Prior to protein expression, the same six different conditions as in b*1M were used (see 6.2.2.8 for details), i.e. Met; Aha; and Eth (as positive controls), and different ratios of Aha:Eth (3:1, 1:1, 1:3) to assess if the incorporation of the Met analogs is concentration-dependent. Under these conditions, three different b*2M congeners containing two Met, two Aha, and two Eth were expressed in single incorporation experiments and four congeners containing either Aha or Eth at the N-terminus or internal positions in different amounts were produced in the following tandem incorporations: 1) b*2M containing two Aha residues (Figure 42A); 2) b*2M containing one Aha at the N-terminus and one Eth at the internal position (Figure 42B); 3) b*2M containing one Eth at the N-terminus and 1 Aha at the internal position (Figure 42C); and 4) b*2M containing two Eth residues (Figure 42D).

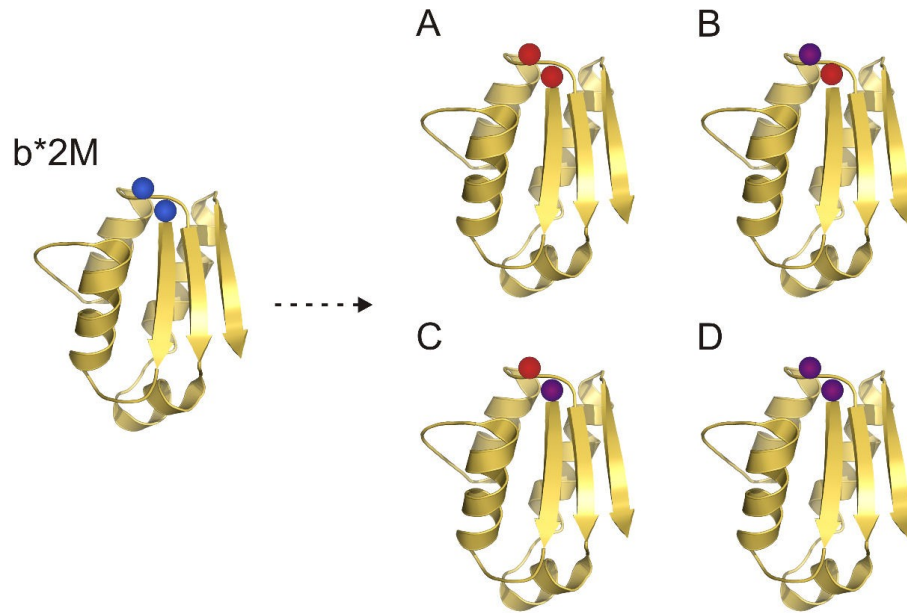


Figure 42. Tandem incorporation of Aha and Eth into barstar 2M. The N-terminal and internal Met (blue) at position 46 from b*2M was replaced by Aha (red) and/or Eth (purple) yielding four different congeners: A) b*2M[Aha1/Aha47]; B) b*2M[Aha1/Eth47]; C) b*2M[Eth1/Aha47]; or D) b*2M[Eth1/Eth47].

The expression and successful purification of b*2M congeners was indicated by a corresponding band with an average mass of 10 kDa (Figure 43). Thereafter, all b*2M alloproteins were analyzed by ESI-MS and N-terminal sequencing (Figure 44).

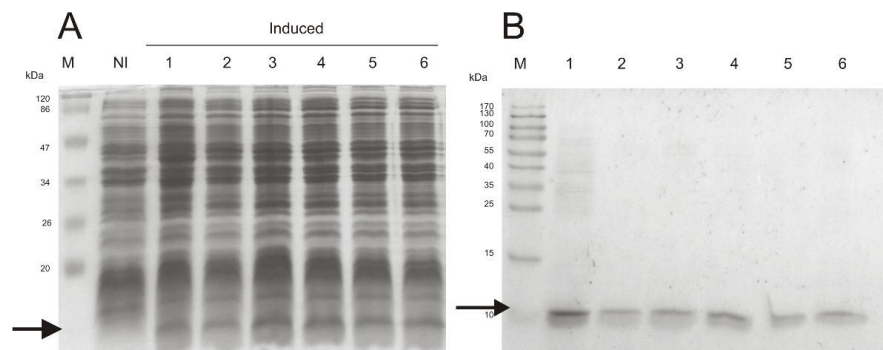


Figure 43. Barstar 2M alloproteins. The b*2M congeners produced in six different conditions (supplemented with: 1) Met; 2) Aha; 3) Aha>Eth; 4) Aha=Eth; 5) Aha<Eth; and 6) Eth) are shown with an arrow after expression (A) and purification (B) using a 17% SDS-polyacrylamide gel and Coomassie staining. M = Standard MW bands; NI = Non-induced culture.

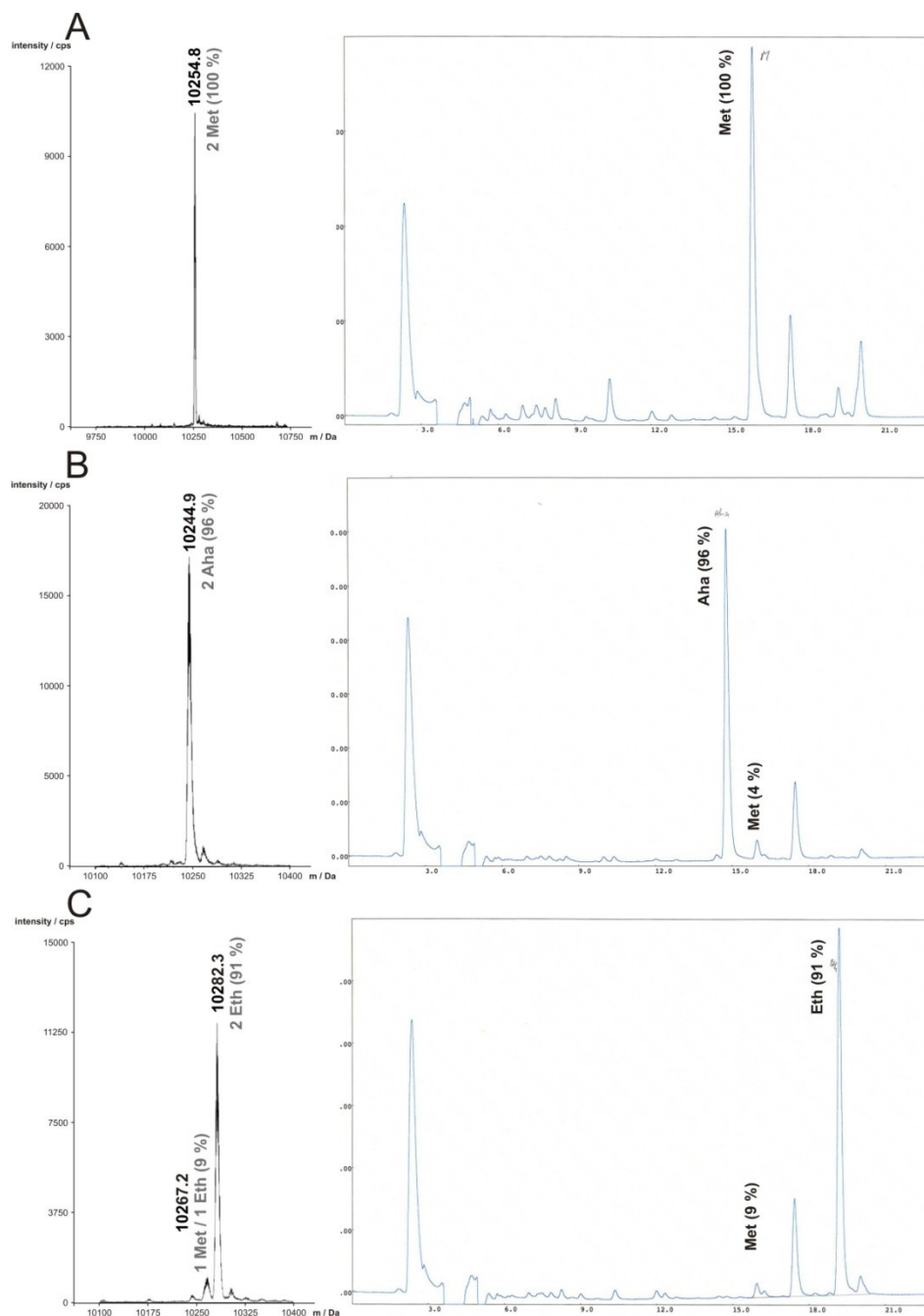


Figure 44. Analytical characterization of barstar 2M congeners. The mass and the N-terminal-sequencing spectra for b*2M supplemented with A) Met; B) Aha; and C) Eth are shown in the left and right columns, respectively. In both cases, the combined intensities of the corresponding peaks sum up to 100%, from which each species percentage was calculated and annotated. For ESI-MS, the theoretical calculated mass for barstar with two Met residues is 10254.5 Da; with 2 Aha residues is 10244.5 Da; and with two Eth residues is 10282.9 Da. For N-terminal sequencing, Aha and Eth show distinctive retention times at 15 and 19, respectively.

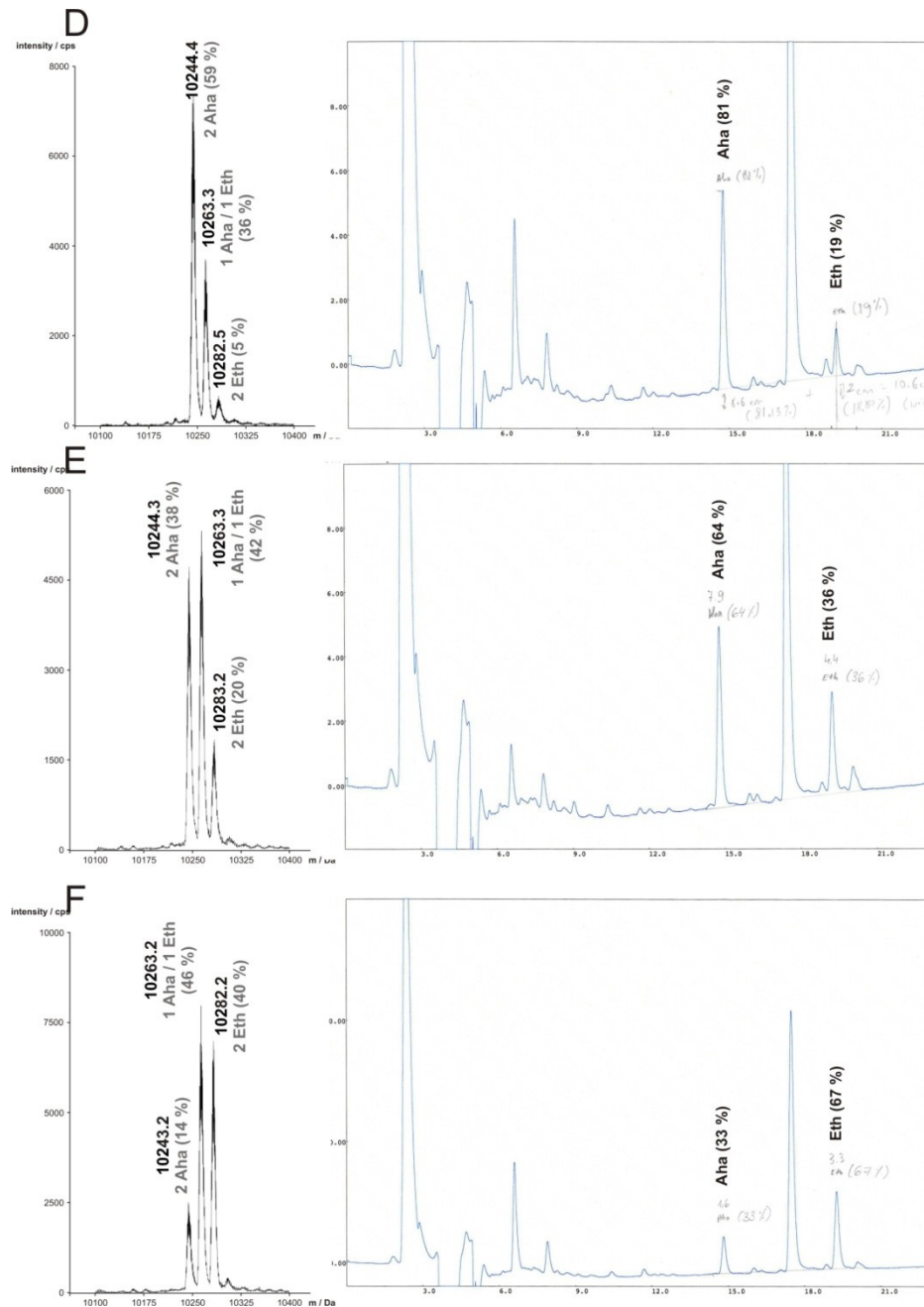


Figure 44. Analytical characterization of barstar 2M congeners (continuation). The mass and the N-terminal-sequencing spectra for b*2M supplemented with D) Aha > Eth (3:1); E) Aha = Eth (1:1); and F) Aha < Eth (1:3) are shown in the left and right columns, respectively. In both cases, the combined intensities of the corresponding peaks sum up to 100%, from which each species percentage was calculated and annotated. For ESI-MS, the theoretical calculated mass for barstar with two Aha residues is 10244.5 Da; with one Aha and one Eth is 10263.7 Da; and with two Eth residues is 10282.9 Da. For N-terminal sequencing, Aha and Eth show distinctive retention times at 15 and 19, respectively.

The congeners with Met, Aha, or Eth at both the N-terminus and internal position displayed a prominent peak where it is expected (**Figure 44A/B/C**; left panel). N-terminal sequencing results are similar to those obtained from ESI-MS in terms of peaks and intensities (**Figure 44A/B/C**; right panel) and could be considered reliable. However, when different concentrations of Aha and Eth were used to supplement the medium, three peaks of different intensities corresponding to the four variants were found (**Figure 44D/E/F**; left panel). The first and third peaks correspond to the Aha and Eth double-substituted b*2M congeners, respectively, while the second peak corresponds to two congeners – one with Aha at the N-terminus and Eth at the internal position and the other exhibiting the opposite distribution. To determine the exact amount of Aha and Eth in each of these variants, N-terminal sequencing was necessary (**Figure 44D/E/F**; right panel). **Table 4** provides an easy way for comparing natural preferences in terms of ratios of both Aha and Eth in the N-terminus and internal position of the different b*2M congeners.

Table 4. Natural preference for Aha and/or Eth at the N-terminus and/or position 47 of barstar 2M.

<i>Amino acids supplemented</i>	<i>Distribution of Aha and Eth (%)*</i>				<i>Ratio**</i>	
	<i>A</i>	<i>B</i>	<i>C</i>	<i>D</i>	<i>N-terminus</i>	<i>Internal</i>
	<i>1Aha 47Aha</i>	<i>1Aha 47Eth</i>	<i>1Eth 47Aha</i>	<i>1Eth 47Eth</i>		
Aha / Eth (0.75 / 0.25)	59	22	14	5	4 for Aha	2.7 for Aha
Aha / Eth (0.50 / 0.50)	38	26	16	20	1.8 for Aha	1.2 for Aha
Aha / Eth (0.25 / 0.75)	14	19	27	40	2 for Eth	1.4 for Eth

*The percentage of b*2M containing two Aha residues (A) or two Eth residues (D) was determined by ESI-MS. To calculate the distribution of Aha at the N-terminus/Eth at the internal position (B) and Eth at the N-terminus/Aha at the internal position (C), the percentage obtained from N-terminal sequencing results (N) was subtracted from the ESI-MS percentage, e.g. when Aha / Eth (0.50 / 0.50), N is 64% for Aha and 36% for Eth, so $64 - 38 = 26\%$ and $36 - 20 = 16\%$

**The ratio of preference for the N-terminus was determined with the formula $N = A + B / C + D$, e.g. $38 + 26 / 16 + 20 = 1.8$ when Aha / Eth (0.50 / 0.50); and that for the Internal 47 position with $I = A + C / B + D$, e.g. $38 + 16 / 26 + 20 = 1.2$ when Aha / Eth (0.50 / 0.50).

When there was four times more Aha than Eth in the medium, it was found that Aha occurs at the N-terminus and the internal position 4 and 2.7 times more, respectively (Table 4). On the other hand, when there was four times more Eth in the medium than Aha, the preference for Eth at the N-terminus was two times more, while for the internal position, it was 1.3 more (Table 4). Since the values for Aha over Eth are almost two-fold different, it is possible to see not only an overall preference for Aha than Eth, but also a particular preference for Aha at the N-terminus over the internal position. Moreover, when both analogs were present in equal amounts, Aha was preferred both at the N-terminus and internal position 47 but differently, i.e. for each Eth, there were 1.8 and 1.2 Aha residues at the N-terminus and internal position, respectively (Table 4).

As previously suggested for b*1M, if one assumes that the Met analogs are efficiently taken up by the cells and accumulated several-fold inside them¹⁴⁸, it can be said that the *EcMetRS* could have a preference to charge both the initiator tRNA^{fMet} and elongator tRNA^{Met} with Aha rather than Eth. Of course, the extent of formylation from both Aha- and Eth-tRNA^{fMet} and their subsequent recognition during translation initiation will certainly play a role, although it is known that the ethionyl-tRNA^{fMet} is recognized and formylated to the same extent as methionyl-tRNA^{fMet}¹⁴⁹, and the same is applicable to azidohomoalanyl-tRNA^{fMet}¹⁵⁰. The elongation factors could likewise differentially accept both Aha- and Eth-tRNA^{Met}, but this should be carefully addressed. In the best case, it is desirable that *EcMetRS* could produce as much as initiator Aha-tRNA^{fMet} as possible, and as less initiator Eth-tRNA^{fMet}, elongator Aha-tRNA^{Met} or Eth-tRNA^{Met} as possible, if the goal is to separate AUG-dependent translation. To this end, an efficient *in vivo* expression of the type B MetRS:tRNA^{Met} pair derived from *S. acidocaldarius* that incorporates Eth at AUG codons exclusively, or at least preferentially in translation elongation in *E. coli* is required.

3.2.4 Cloning of orthogonal pair and SaMetRS expression

The construction of an appropriate expression system that allows the expression of the orthogonal MetRS and tRNA^{Met} in *E. coli* was developed (plasmids for Tandem expression in *E. coli* or pTEc system). pTEc plasmids are derived from pRARE, a plasmid containing six rare *E. coli* tRNA genes under their natural promoters, which are incorporated to enhance the expression of exogenous proteins in *E. coli* e.g. the orthogonal SaMetRS. These vectors are resistant to chloramphenicol and contain the *p15A* origin of replication that allows the orthogonal pair in a mid- to low-copy plasmid number.¹⁵¹ This system is compatible with the pQE or pET systems because they contain the origins of replication *colE1* or *pBR22*, respectively, and are either resistant to ampicillin or kanamycin. In addition, these plasmids allow an efficient expression of the target gene under the control of either the T5 or T7 inducible promoters. Accordingly, the vector pTEc0 was generated to allow the cloning of the orthogonal pair (see Appendix 9.5 for sequence details). pTEc1 was subsequently developed by cloning the SaMetRS under the control of the constitutive EM7 promoter and by substituting the elongator tRNA^{Met} already present with an elongator tRNA from *S. acidocaldarius* (Figure 45).

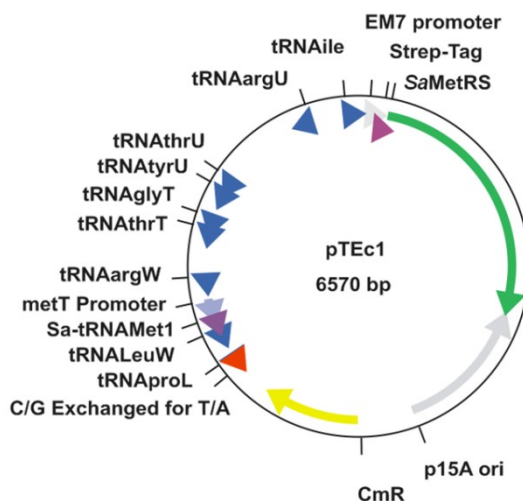


Figure 45. pTEc1. The vector for the tandem expression of the orthogonal pair SaMetRS:Sa-tRNA^{Met} in *E. coli* has a bacterial EM7 synthetic constitutive promoter (light gray), followed by the exogenous SaMetRS (green) containing an N-terminal Strep-tag (light purple). The p15A origin of replication is depicted in light gray. The chloramphenicol marker CmR confers resistance (yellow). The rare tRNA genes are indicated in dark blue and the exogenous Sa-tRNA^{Met} in purple under the natural promoter from the *E. coli* elongator tRNA^{Met} (light blue).

S. acidocaldarius contains three putative Met tRNA isoacceptors coded in the genes *tRNA8*, *tRNA16*, and *tRNA43*.¹⁵² As deduced from its similarities with the initiator tRNA^{fMet} from *E. coli*, the gene *tRNA43* would correspond to the initiator tRNA^{iMet} from *S. acidocaldarius* (Figure 46; see Table 1 for details). Thus, the elongator tRNA^{Met} isoacceptors should be coded by the genes *tRNA8* and *tRNA16* (Figure 47).

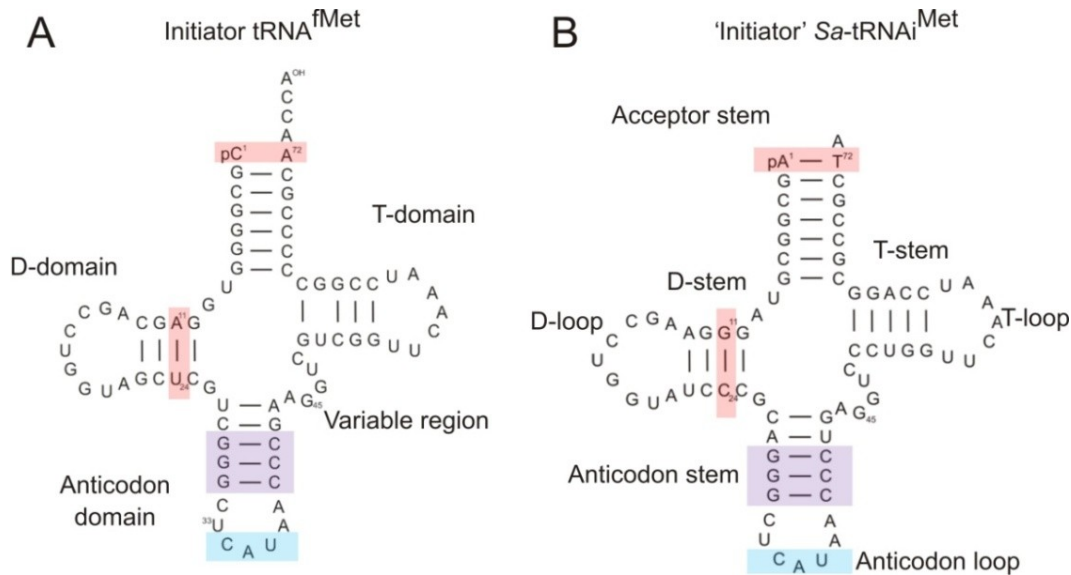


Figure 46. Initiator tRNAs. Secondary structure of the initiator tRNA from A) *E. coli*⁷² and B) *S. acidocaldarius* (derived from the gene *tRNA43*).¹⁵² The dihydrouridine (D), thymidine (T), and anticodon domains, as well as the acceptor arm are labeled. Each domain contains a stem and loop region. A variable arm occurs between the anticodon and T domains. The required identity elements for formylation (red), initiation (purple), and aminoacylation (blue) are highlighted for comparison.

Since the rare *E. coli* elongator tRNA^{Met} (Figure 10B) was previously present in the pRARE, it was substituted for the *S. acidocaldarius* 'elongator 1' tRNA^{Met} (Sa-tRNA^{Met}; Figure 47A). The 'elongator 1' tRNA^{Met} was chosen because its D-loop is larger (10 bases; Figure 47A) compared to that of the 'elongator 2' tRNA^{Met} (9 bases; Figure 47B). This slight difference in the D-loop could resemble the one-base substitution in the anticodon loop that serves as the determinant for specific aminoacylation of type B elongator tRNA^{Met} by type B MetRS but not type A MetRS.¹³¹

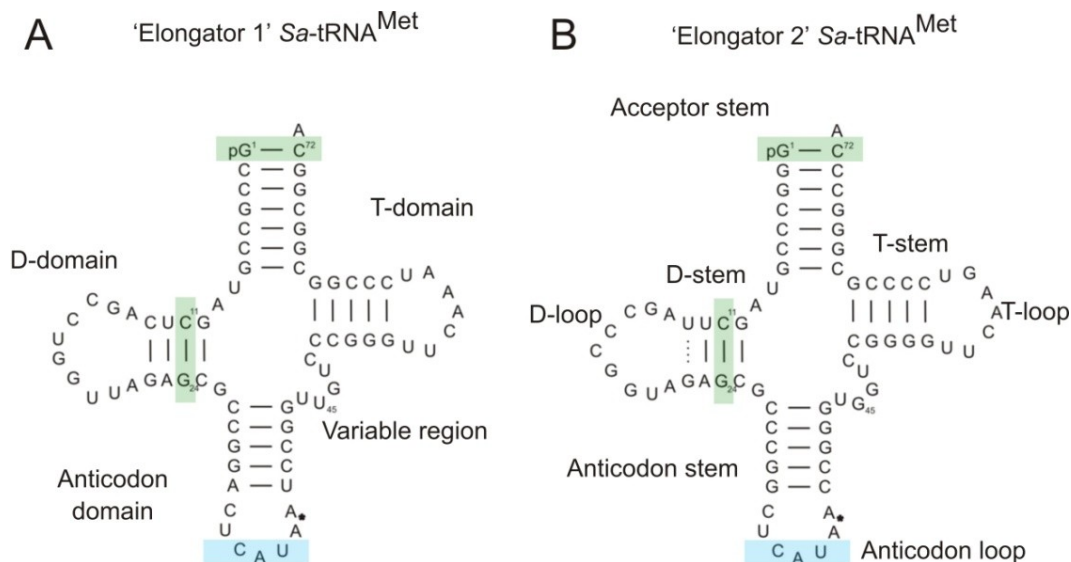


Figure 47. Elongator tRNAs from *S. acidocaldarius*. Secondary structure of the *S. acidocaldarius* elongator tRNA A) No. 1; gene tRNA16 (*Possible intron: 40-59 removed) and B) No. 2; gene tRNA8 (*Possible intron: 39-56 removed).¹⁵² The dihydrouridine (D), thymidine (T), and anticodon domains, as well as the acceptor arm are labeled. The required identity elements for elongation (green) and aminoacylation (blue) are shown. The dotted line indicates that a base modification is required for hydrogen bonding.

A Strep·Tag II was appended to the N-terminus of SaMetRS so that its expression can be assessed by immunoblotting. The Strep·Tag II is an eight-residue minimal peptide sequence (WSHPQFEK) that exhibits intrinsic affinity towards streptavidin. The advantages of using Strep·Tag II are its short size, stability against proteases, and lack of interference with protein folding.¹⁵³ To discard the factor of genetic background as a problem for expressing SaMetRS, two different *E. coli* Met auxotrophic strains were transformed with pTEc1. Their protein extracts were subsequently blotted onto nitrocellulose membrane and probed with a mouse anti-Strep·Tag II antibody (see 6.2.1.4 for details). However, no expression of the SaMetRS could be detected after 60 min of exposure time (**Figure 48**).

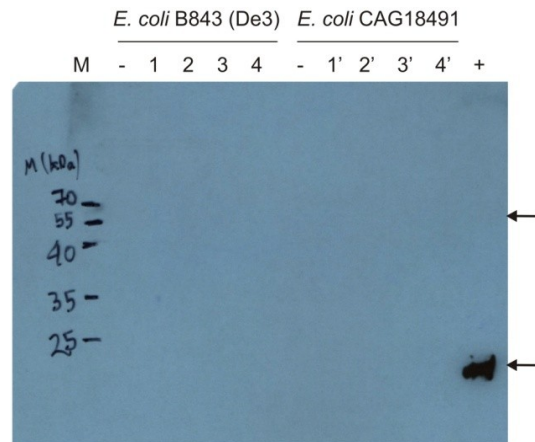


Figure 48. Intracellular expression of SaMetRS in *E. coli* transformed with pTEc1. No expression of SaMetRS (calculated mass of 67.5 kDa, see upper arrow) was detected for any of the four clones from *E. coli* B834 (DE3) (1, 2, 3, 4) or CAG18491 (1', 2', 3', 4'). The negative control (-) corresponds to *E. coli* cells transformed with pTEc0 instead of pTEc1. The positive control (+) is the 17 kDa protein hSOD1 (A2K) containing an N-terminal Strep-Tag II, indicated with an arrow. M = Standard MW.

Since the sequence of pTEc1 was verified (see Appendix 9.6 for details), the lack of expression of SaMetRS could be only attributed to either codon usage or a relatively weak expression of the constitute promoter EM7. To rule out the first possibility, an *in silico* codon optimization analysis for the expression of SaMetRS in *E. coli* was performed with the aid of the OptimumGene Codon Optimization Analysis software from GeneScript (Figure 49).¹⁵⁴

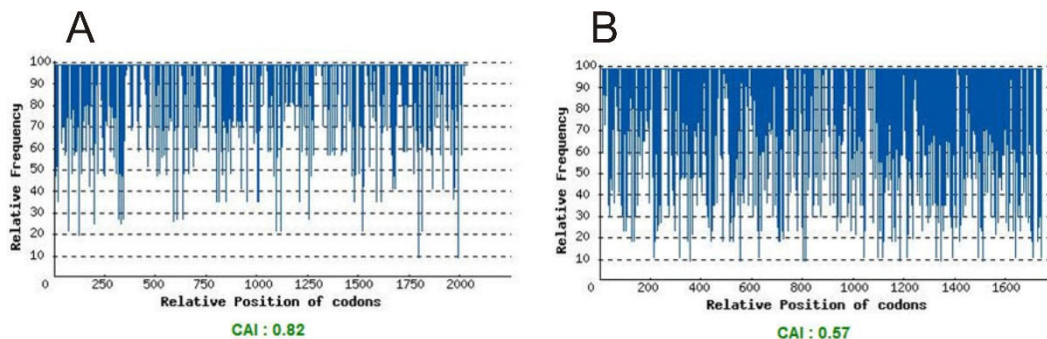


Figure 49. *In silico* expression of EcMetRS and SaMetRS in *E. coli*. The distribution of codon usage frequency for EcMetRS (left panel) and SaMetRS (right panel) confers a codon adaptation index (CAI) of 0.82 and 0.57, respectively. The closer the CAI is to 1.0, the bigger the possibility that the gene can be expressed in *E. coli*.

Codon usage is defined as the specific use of the tRNA population, which is in direct correlation with the codon composition of total mRNA, by each living cell.¹⁵⁵ The fact that the archaeal SaMetRS gene is not expressed in the bacterium *E. coli* could be due to the lack of specific tRNAs to decode it. To approach this “codon usage” problem, a detailed analysis of the rare *E. coli* tRNAs whose codons are present in gene sequence of SaMetRS was performed (Figure 50).

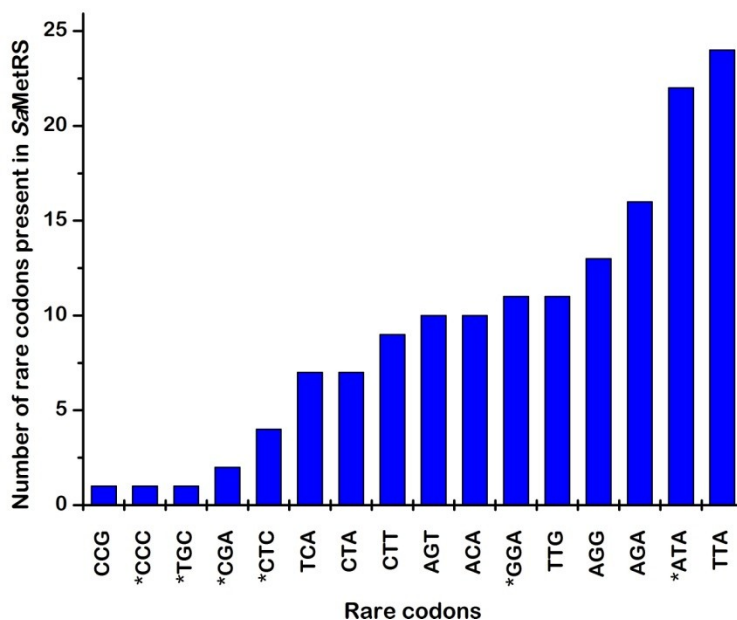


Figure 50. Distribution of codons present in SaMetRS whose tRNAs are the rarest in *E. coli*. The ‘rarest’ tRNA is tRNA^{Leu}, which decodes the TTA codon and is present 24 times along the sequence of the orthogonal MetRS. * are codons that are decoded by rare tRNAs already supplemented by pTEc1.

In order to improve the expression of heterologous proteins in *E. coli*, there are mainly two strategies: 1) supplementation of rare tRNAs or 2) *de novo* synthesis of the target gene.¹⁵⁶ Both methods are considered equally efficient, but supplying tRNA is the most economical approach; therefore, the gene *leuZ* corresponding to the rarest tRNA (tRNA^{Leu} with the anticodon UAA) whose codon is the most frequent along the gene sequence of SaMetRS was cloned into pTEc1. The promoter EM7 was also substituted with the strong constitutive promoter *glnS*’ along with the terminator *rho T* (see 6.1.8.4 for details). The *glnS*’ promoter is derived from the original glutamine tRNA-synthetase promoter with several mutations is considered one of the strongest

promoters in *E. coli*¹⁵⁷, while *rho T* is a very common naturally occurring release factor that binds nascent RNA molecules in *E. coli*.¹⁵⁸ With these, an optimized vector for SaMetRS expression, pTEc1.1.G-R/L, containing new tRNA, promoter, and terminator sequences, was produced (Figure 51; see Appendix 9.7 for sequence details).

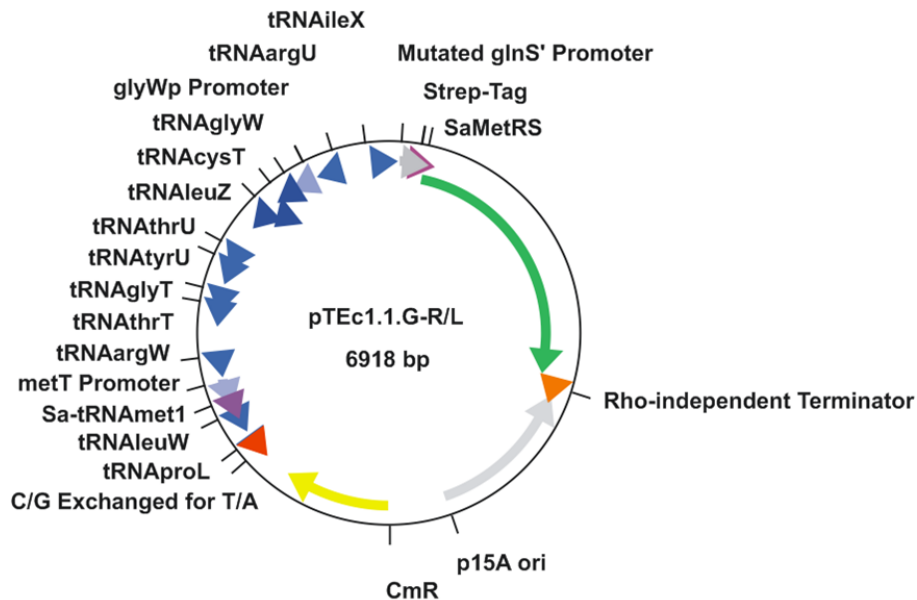


Figure 51. pTEc1.1G-R/L. The vector for the expression of the orthogonal pair SaMetRS:Sa-tRNA^{Met} in *E. coli* harbors the strong constitutive promoter *glnS'* (dark gray), followed by the exogenous SaMetRS (green) containing an N-terminal Strep-Tag II (light purple) and flanked by the *rho T* terminator (orange). The p15A origin of replication is depicted in light gray. The chloramphenicol marker CmR confers resistance (yellow). The rare tRNA genes are indicated in dark blue and the exogenous Sa-tRNA^{Met} in purple under the natural promoter from the *E. coli* elongator tRNA^{Met} (light blue).

To check for the expression of SaMetRS, an immunoblot assay was carried out (see 6.1.5.4 for details). However, even with the cloning of the rarest tRNA and the use of a stronger promoter, no SaMetRS could be detected (Figure 52).

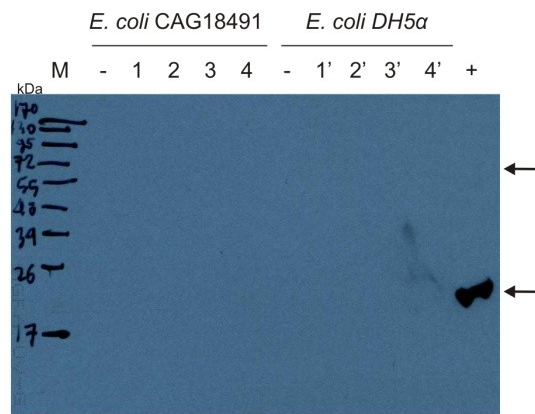


Figure 52. Expression of SaMetRS in *E. coli* transformed with pTEc1.1G-R/L. No expression of SaMetRS (calculated mass of 67 kDa, shown with the upper arrow) is detected for any of the four clones from *E. coli* strains CAG18491 (1, 2, 3, 4) or DH5 α (1', 2', 3', 4'). The negative control (-) corresponds to *E. coli* cells transformed with pTEc0 instead of pTEc1.1G-R/L. The positive control (+) corresponds to the 17 kDa protein hSOD1 (A2K) containing a C-terminal-Strep-Tag II, indicated with the lower arrow. M = Standard MW.

To rule out the lack of expression due to low activity, the last experiment was repeated but with an aliquot corresponding to 10 OD₆₀₀ enriched by Strep-Tag II mini-columns. As in the previous cases, no SaMetRS could be detected (Figure 53).

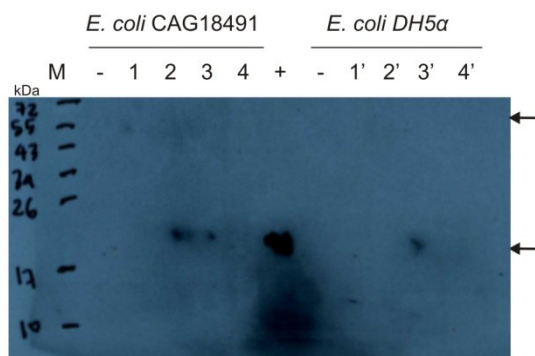


Figure 53. Expression of SaMetRS in *E. coli* transformed with pTEc1.1G-R/L after enrichment. No expression of SaMetRS (calculated mass of 67.5 kDa shown with the upper arrow) is detected in the 1) soluble purified fraction, 2) bound sample after washing, 3) sample after loading, or 4) insoluble fractions for any of the two *E. coli* strains. The negative control (-) corresponds to *E. coli* cells transformed with pTEc0 instead of pTEc1.1G-R/L. The positive control (+) corresponds to the 17 kDa protein hSOD1 (A2K) containing a C-terminal-Strep-Tag II, indicated with the lower arrow. M = Standard MW.

To completely rule out the problem of codon usage, the rare codons present in the gene sequence of SaMetRS were optimized for expressing this gene in *E. coli*. After *de novo* gene synthesis, SaMetRS was cloned into pTEc1.1.G-R/L to yield the plasmid pTEc2, which was thereafter transformed into *E. coli*; however, no expression of the orthogonal SaMetRS could be detected (data not shown), not even after a 10x enrichment of 1 OD₆₀₀ using Strep-Tag II columns, as previously done (Figure 54).

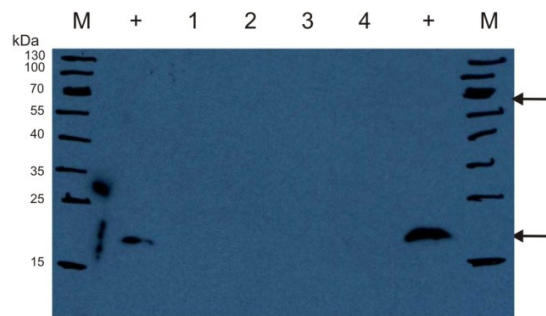


Figure 54. Expression of SaMetRS in *E. coli* transformed with pTEc2 after enrichment. No expression of SaMetRS (calculated mass of 67.5 kDa, shown with the upper arrow) is detected in the 1) sample before loading, 2) sample after loading, 3) bound sample after washing, or the 4) soluble purified fraction from *E. coli* strain CAG18491. The positive control (+) corresponds to the 17 kDa protein hSOD1 (A2K) containing a C-terminal-Strep-Tag II, indicated with the lower arrow. M = Standard MW.

The absence of SaMetRS expression is most likely due to the promoter used. It was recently shown that the *glnS'* promoter is not as efficient as previously described, i.e. the constitutive expression of the AARS alone may not be sufficient to aminoacylate its cognate tRNA.¹⁵⁹ This is very important in the development of a technique for the efficient expression of an orthogonal pair in *E. coli* using an inducible arabinose promoter together with the *glnS'* one for optimal AARS expression. Here, it would make more sense to use an inducible promoter that would allow an efficient expression of SaMetRS and subsequent aminoacylation of the Sa-tRNA^{Met} with Eth. The development of such an expression system is underway. Importantly, a preferential incorporation of the bioorthogonal chemical reporter Aha by EcMetRS and Eth by the SaMetRS at the N-terminal and internal positions, respectively, would allow us to specifically modify the N-termini and retain or even improve the activity of

proteins. In fact, attempts to recode the N-terminus of proteins with noncanonical amino acids for controlled N-terminal protein processing have only been started in started *in vitro*.¹⁶⁰⁻¹⁶⁷ Thus, this system represents the first step towards the *in vivo* control of N-terminal post-translational modifications, as well as the site-specific recoding of a single sense codon by an orthogonal AARS:tRNA pair (Figure 55).

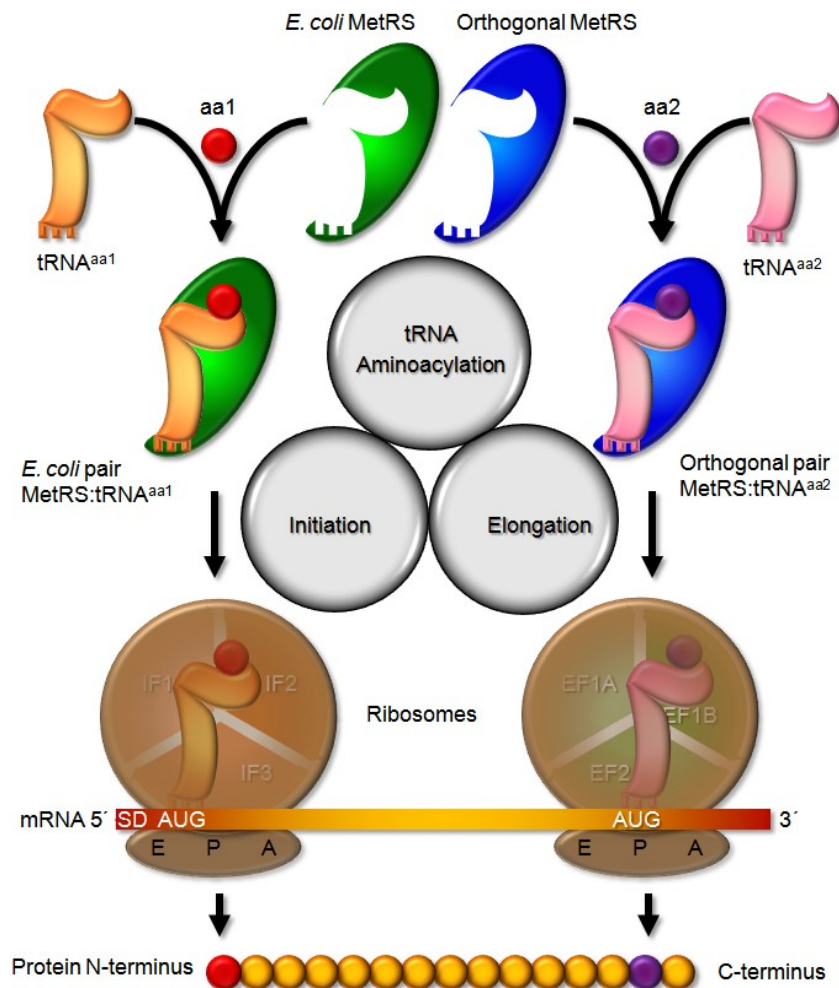


Figure 55. Making up the faces of Janus. Due to its substrate promiscuity, the *E. coli* MetRS can charge a Met analog (aa1; red) onto tRNA^{fMet} (represented as tRNA^{aa1}). By combining the SPI and SCS methods, a new functional orthogonal MetRS (blue) would specifically aminoacylate its cognate elongator tRNA^{aa2} (pink) with a Met analog (aa2; purple). Intracellular accumulation of the orthogonal elongator tRNA^{aa2} results in preferential incorporation of aa2 at internal AUG codons. The exogenous MetRS should not cross-react with endogenous MetRS:tRNA^{aa1} pair. Finally, the tRNAs should be accurately discriminated by the initiation and elongation factors. SD = Shine-Dalgarno sequence

4 Conclusions

This work presents the potentials of genetic code engineering in synthetic biotechnology. Specifically, it demonstrates that it is possible to design lipase congeners with physicochemical properties fully reflected by the global incorporation of the Met analogs Nle and Aha. Instead of causing global perturbations in the protein structure, these noncanonical amino acids were responsible for bringing about striking differences in optimal temperature and pH, thermal stability, substrate access and specificity, as well as resistance toward organic solutions, metal ions, surfactants and inhibitors in the functional congeners. The finding that TTL[Nle] most probably has an open substrate access might pave the way for generating stable lipases with improved characteristics for industrial processes without necessitating the energy and material expenditure required in classical genetic engineering. Furthermore, the generated chemical diversity by globally incorporating noncanonical amino acids can also increase the tolerance of the lipase congeners toward different additives. Doubtless, such chemical diversity is the main cause for the unique and emergent properties observed exclusively in the lipase congeners.

Nevertheless, the SPI method alone is not sufficient to determine if key lipase residues are exclusively responsible for the observed differences. Thus, the development of a new method that allows the simultaneous use of more than one Met analog will definitely enhance the potentials of engineering the genetic code. In this context, the first efforts toward the site-specific incorporation of Met analogs into proteins were presented too. The fact that *E. coli* MetRS prefers activating Aha over Eth and *S. acidocaldarius* MetRS Eth over Aha, could serve as a starting point for further developing their substrate specificity. Additionally, combined together with the fact that the single AUG codon is decoded by two different tRNAs, the importance of using new MetRS:tRNA^{Met} pairs from evolutionary distinct organisms should help developing the required technology for the position-specific AUG recoding. In this thesis, the first steps toward this goal are described.

5 Outlook

Lipases contain one of the most common natural protein folds, the so-called α/β hydrolase fold, which is usually present in most hydrolytic enzymes. In fact, the ESTHER database¹⁶⁸ includes hundreds of proteins that belong to this family, including carboxyl esterases, thioesterases, lipases, peptidases, aminoester hydrolases, deacetylases, or acyl transferases. The fact that the lipase from *T. thermohydrosulfuricus* (TTL) tolerated a relative high number of Met replacements very well indicates that the incorporation of Nle into proteins with the same α/β hydrolase fold could be also beneficial in engineering other biocatalysts of industrial interest. Of course, it would be necessary to obtain 3D structural data of these alloproteins with noncanonical amino acids to be able to correlate its structural and functional properties, and this work is being pursued in this direction. Likewise, the recently successful incorporation of three different noncanonical amino acids using the SPI method with polyauxotrophic *E. coli* strains¹⁶⁹ will permit the generation and characterization of beneficial and emergent properties provided by three or even more chemistries to lipases or other biocatalysts. Currently, we are combining many noncanonical amino acids into TTL (double, triple, quadruple, and quintuple incorporations) to search for lipases with *de novo* properties with interesting applications in white biotechnology.

The nature of scientific research has become increasingly interdisciplinary. In this context, the field of genetic code engineering is not only limited to fundamental academic questions. As a subfield of synthetic biology, it is geared towards new and useful applications in biotechnology. This makes the cross-talk between basic and applied research fundamental: it drives toward innovation. The finding that Nle-TTL's lid is 'open' raises the question: which Met residues play key roles in this conversion? The answer can be obtained by combining different efforts in protein engineering and synthetic biology. Currently, no method that allows the site-specific incorporation of Met analogs exists, but in this work, the first efforts in this direction are presented by combining the SPI and SCS methods. From the results, it is clear that the presented

orthogonal pair has to be optimally cloned and its expression and functionality has to be properly assessed *in vivo*. Such proof-of-principle will bring the next step, namely the insertion of the orthogonal molecules into the host genome. The group of Link recently showed that it is possible to introduce a mutated MetRS with substrate specificity for AnI into the genome of a Met auxotrophic *E. coli* strain without perturbing cell growth while enabling high levels of expression of recombinant proteins containing the Met analog.¹⁷⁰ In our case, the mechanisms governing the translation initiation and AUG-dependent elongation will not only depend on the extent of incorporating an orthogonal MetRS into the host genome, but also on how it would affect the host physiology. The potential pitfalls, however, might be in the form of some difficulties in the regulation of transcription during the expression of the orthogonal pair, given that AARSs complexes have multiple tasks.¹⁷¹ For this, it would be necessary to engineer metabolic pathways. Furthermore, this step might lead towards the next fundamental problem that needs to be solved: would it be possible to evolve heritable changes in the genetic code interpretation?

The major drawback of all existing genetic code engineering techniques is that the coding units, i.e., sense or stop codons are only transiently reassigned. Permanent reassignment of existing coding units inevitably leads to detrimental effects. On one hand, auxotrophic cells cannot grow using just the noncanonical analogs. On the other, a permanent read through of stop codons is lethal for the cells.¹⁷² Thus, for stable and inheritable recoding, new coding units have to be introduced into the genome of the target organism. From the current point of view, the only way to introduce *de novo* coding units is the *de novo* chemical synthesis of a whole genome in which rare codons are exchanged for more frequent ones with the same meaning, which serves as an alternative to the generation of artificial DNA pairs.¹⁷³ Thus, rare codons disappear from the genetic code and can subsequently be specifically reintroduced with a new meaning into suitable target genes. However, this approach is still hampered by the rather inefficient and prohibitively expensive chemical DNA synthesis and is currently a perspective for the distant future.

6 Experimental section

6.1 Materials

6.1.1 Equipment

- Autoclave: Varioklav Dampfsterilisator Typ 500 E (H+P Labortechnik GmbH, Oberschleißheim, Germany).
- Balances: TE1502S, BP211D (Sartorius, Göttingen, Germany); GB2002, PC4400 Delta Range (Mettler-Toledo GmbH, Giessen, Germany).
- Blotting apparatus: Trockenblot 250/180, 05/04 (MPI of Biochemistry, Munich, Germany).
- CD spectropolarimeter: Jasco J-715, temperature control by Peltier FDCD attachment PFD-350S/350L (JASCO International Co., Ltd., Tokyo, Japan).
- Centrifuges: Avanti J-25; Avanti J-20 XP (Beckmann, Munich, Germany); Centrifuge 5415 C/D; Zentrifuge 3200 (Eppendorf, Hamburg, Germany); Universal 32R (Hettich Zentrifugen, Tuttlingen, Germany).
- Centrifuge rotors: JA 25.50, JLA 8.1000, JLA 10.500, (Beckmann, Munich, Germany).
- Cuvettes: Hellma 104.002-QS, Hellma 104.002F-QS, Hellma 110-QS, (Hellma, Müllheim, Germany).
- Electroporator: Electroporator 1000 (Stratagene, La Jolla, CA, USA).
- FPLC: Äktaexplorer, Äktabasic (GE Healthcare, Munich, Germany)
- Gel documentation: Eagle Eye II (Stratagene, La Jolla CA, USA), High Performance CCD Camera (COHU, Inc., San Diego CA, USA).
- Incubators: Thermomixer comfort, Thermomixer compact (Eppendorf, Hamburg, Germany), Incubator 3033 (GFL, Burgwedel, Germany).
- Magnetic stirrer: MR 3001 (Heidolph, Kehlheim, Germany).
- Mass spectrometer: MicrOTOF ESI-MS (Bruker Daltonics, Bremen, Germany)
- N-terminal sequencer: Gas-phase sequenator precise cLC (Applied Biosystems, Darmstadt, Germany).

- PCR cycler: Robocycler gradient 96 (Stratagene, La Jolla CA, USA).
- PH meter: MP 220, (Mettler-Toledo GmbH, Giessen, Germany).
- Photometer: UV/VIS Spectrometer Lambda 19 (PerkinElmer Life Sciences, Boston MA, USA); Ultrospec 6300 pro (GE Healthcare, München, Germany); ND 1000 (NanoDrop, Wilmington DE, USA).
- Sonifier: Sonifier 450 Macrotip (Branson, St. Louis, MO, USA).
- Sterile bench: Lamin Air HA244GS (Heraeus, Hanau, Germany).
- Vortex: Vortex Genie 2 (Bender & Hobein AG, Zurich, Switzerland).
- Ultra-Turrax Emulsifier (IKA Werke GmbH & Co. KG, Staufen, Germany)

6.1.2 Extendable materials

- Blotting membrane: Protran 0.1 μm (Whatman International Ltd, Maidstone Kent, UK).
- Centrifugal concentrators: Vivaspin 30 kDa (Sartorius Stedim Biotech, Aubagne, France).
- Columns: HiTrap Chelating HP and HiTrap Q Sepharose (GE Healthcare, Munich, Germany). Waters RP C4 column (Waters GmbH, Eschborn, Germany)
- Dialysis membranes: Spectra/por molecularporous membrane MW cutoff: 3,500 (Spectrum Laboratories, Rancho Dominguez CA, USA).
- Electroporation cuvettes: GenePulser/Micropulser cuvettes, 1 mm gap width (Biorad, Hercules CA, USA).
- Filter paper: Whatman 3MM (Whatman International Ltd, Maidstone Kent, UK).
- X-ray film paper: Curix Ultra UV-G (AGFA, Cologne, Germany).
- Sterile Filters: Millex-HA Filter Unit 0.45 μm /0.22 μm and Steritop GP (Millipore, Billerica MA, USA).

6.1.3 Chemicals

All standard chemicals were purchased from Sigma (Steinheim, Germany) or Merck KGaA (Darmstadt, Germany) unless otherwise specified. L-isomers of all amino acids

were used. Aha and Hpg were synthesized as previously described.^{37,174} Anl, Dpg and Nhm were kindly provided by Dr. Shouliang Dong (Lanzhou University, China). Omd, Ome, Cpa, and Don were purchased from Bachem (Weil am Rhein, Germany) and Tfn from Fluorochem (Derbyshire, UK). Tfm, Nle and Eth were obtained from Sigma and Mox from CBL Patras (Patras, Greece). *E. coli* initiator tRNA^{fMet} was purchased from Sigma and total tRNA from *E. coli* MR600 from Roche Diagnostics (Mannheim, Germany).

6.1.4 Commercial reagents

6.1.4.1 Kits and markers

- PCR purification: QIAquick PCR Purification Kit or Gel Extraction Kit (Qiagen GmbH, Hilden, Germany).
- Plasmid preparation: QIAprep Spin Miniprep Kit and Qiagen Plasmid Midi Kit (Qiagen GmbH, Hilden, Germany).
- Chemiluminescence reagent: Supersignal West Pico Chemiluminescence Substrate (Perbio Science Deutschland GmbH, Bonn, Germany).
- Bradford reagent: Biorad Protein Assay (Biorad, Hercules CA, USA).
- DNA MW marker: GeneRuler 1kb Ladder from Fermentas (St. Leon-Rot, Germany).
- Protein MW marker: PageRulerTM Prestained Protein Ladder from Fermentas (St. Leon-Rot, Germany).

6.1.4.2 Enzymes and antibodies

- Protein purification: Lysozyme, DNase I, and RNase A were from Sigma.
- PCR: Takara ExTaq polymerase from TakaraBio (Mountain View, CA, USA).
- Cloning: T4 DNA ligase and all restriction enzymes were obtained from New England Biolabs (Frankfurt am Main, Germany).
- Primary antibody: Monoclonal mouse antibody anti-Streptag II (ZNP, LMU,

Martinsried, Germany).

- Secondary antibody: Goat anti-mouse IgG coupled to alkaline phosphatase (Dianova, Hamburg, Germany).

6.1.5 Buffers and solutions

All aqueous buffers and solutions were prepared using autoclaved, sterile filtered or bi-distilled water when required.

6.1.5.1 DNA electrophoresis

- TAE buffer: Stock solution 50x (2 M Tris·HCl, 1 M glacial acetic acid, 100 mM EDTA, pH 8.5) and working concentration 1x TAE buffer (40 mM Tris·HCl, 20 mM glacial acetic acid, 2 mM EDTA, pH 8.5).
- 6x DNA sample buffer: 0.25% bromophenol blue, 0.25% xylencyanole, 30% glycerol.

6.1.5.2 Protein purification

- Ni-NTA lysis buffer: 50 mM NaH₂PO₄, 300 mM NaCl and 10 mM imidazole, pH 8.
- Ni-NTA high-salt washing buffer: 50 mM NaH₂PO₄, 2 M NaCl and 20 mM imidazole, pH 8.
- Ni-NTA low-salt washing buffer: 50 mM NaH₂PO₄, 300 mM NaCl and 20 mM imidazole, pH 8.
- Ni-NTA elution buffer: 50 mM NaH₂PO₄, 300 mM NaCl/250 mM imidazole, pH 8.
- Ion Exchange (IE) resuspension buffer: 50 mM Tris·HCl, 7.5 M urea, pH 8.
- Ion Exchange washing buffer: 50 mM Tris·HCl, 100 mM NaCl, pH 8.
- Ion Exchange elution buffer: 50 mM Tris·HCl, 1 M NaCl, pH 8.

6.1.5.3 Protein electrophoresis (SDS-PAGE)

- 12% resolving gel: 375 mM Tris·HCl, pH 8, 12% of Acrylamide:Bis-acrylamide [30:0.8%(w/v)], 0.1% SDS, 0.1% APS, 0.1% TEMED.
- 17% resolving gel: 375 mM Tris·HCl, pH 8, 17% of Acrylamide:Bis-acrylamide [30:0.8%(w/v)], 0.1% SDS, 0.1% APS, 0.1% TEMED.
- Stacking gel: 195 mM Tris·HCl, pH 6.8, 5% of Acrylamide:Bis-acrylamide [30:0.8%(w/v)], 0.1% SDS, 0.1% APS, 0.1% TEMED.
- Running buffer: 190 mM glycine, 25 mM Tris·HCl, 3.5 mM SDS.
- 5x SDS-PAGE sample buffer: 450 mM Tris·HCl, pH 6.8; 3.6% SDS, 0.2% bromophenol blue; 30% glycerol; 45% β -mercaptoethanol.
- Coomassie staining solution: 0.1% Coomassie Brilliant Blue R 250; 25% ethanol; 8% acetic acid.
- Coomassie destaining solution: 25% ethanol; 8% acetic acid
- Fixing solution: 5% glycerol; 10% ethanol

6.1.5.4 Western Blot (Protein immunoblotting)

- Transfer buffer: 25 mM Tris·HCl, 192 mM glycine, 20% methanol, 0.1% SDS, pH 8.
- TBS buffer: 50 mM Tris·HCl, 150 mM NaCl, 0.1% Tween20, pH 8.
- Ponceau S staining solution: 0.5% (w/v) Ponceau S in 1% (v/v) acetic acid.

6.1.5.5 Protein storage

- MetRS buffer: 20 mM Tris·HCl, 150 mM KCl, 15 mM $MgCl_2$ and 5 mM β -Mercaptoethanol, pH 8.
- Barstar buffer: 50 mM Tris·HCl and 100 mM NaCl, pH 8.
- Lipase buffer: 50 mM Tris·HCl pH 8.

6.1.6 Media and supplements

For bacterial growth, fermentation, and protein expression, LB medium and New Minimal Medium (NMM) were used. The components of LB medium were purchased

from BD Biosciences (San José, CA, USA). LB liquid medium was autoclaved for 20 min at 121 °C and 1.5 bars; for agar plates, 1.5% agar was added prior to autoclaving. Antibiotics were filter sterilized before addition to the media.

6.1.6.1 Media

- LB medium: 10 g Bacto™, Tryptone, 5 g Bacto™ Yeast Extract, and 10 g NaCl were dissolved in 1 L H₂O and autoclaved before use.
- NMM: 7.5 mM (NH₄)₂SO₄, 8.5 mM NaCl, 22.5 mM KH₂PO₄, 50 mM K₂HPO₄, 20 mM Glucose, 50 mg of all amino acids, except the amino acid to be replaced, 1 mM MgSO₄, 1 mg Ca²⁺, 1 mg Fe²⁺, 10 mg trace elements (Cu²⁺, Zn²⁺, Mn²⁺, MoO₄²⁺), 10 mg thiamine, 10 mg biotin. Adjust to 1 L with H₂O.

6.1.6.2 Supplements

- Ampicillin: Stock concentration 100 mg/mL in H₂O and final working concentration 100 µg/mL.
- Chloramphenicol: Stock concentration 34 mg/mL in EtOH and final working concentration of 50 µg/mL.
- Kanamycin: Stock concentration 30 mg/mL in H₂O and final working concentration of 15 and 30 µg/ml for cells with a chromosomal and plasmid-containing Kan^RLgene, respectively.
- Streptomycin: Stock concentration 50 mg/mL in H₂O and final working concentration 50 µg/ml.
- Tetracycline: Stock concentration 5 mg/mL in H₂O and final working concentration 12.5 µg/mL.
- IPTG: Stock 1 M IPTG in H₂O and final concentration of 1 mM.

6.1.7 Bacterial strains

For plasmid amplification, the DH5α and OmniMax strains were used; for MetRS

protein expression, the BL21(DE3) and strains were used. The Rosetta-gammi 2 strain alleviates codon bias and enhances disulfide bond formation in the cytoplasm when heterologous proteins are expressed in *E. coli*. This strain also carries the chloramphenicol-resistant pRARE2 plasmid, which supplies seven rare tRNAs (Novagen; Merck Chemicals Ltd., Nottingham, UK). For the incorporation of Aha and Nle into lipase and Aha and Eth into barstar, the *E. coli* Met auxotrophic strain CAG18491 (CGSC *E. coli* Genetic Resources at Yale, CGSC# 7464) was used.

6.1.7.1 Plasmid amplification

- DH5 α : F⁻ endA1 glnV44 thi-1 recA1 relA1 gyrA96 deoR nupG Φ 80d/lacZ Δ M15 Δ (lacZYA-argF)U169, hsdR17(r_K⁻ m_K⁺), λ -.
- OmniMax: F' [proAB+ lacIq lacZ Δ M15 Tn10(TetR) Δ (ccdAB)] mcrA Δ (mrr-hsdRMS-mcrBC) ϕ 80(lacZ) Δ M15 Δ (lacZYA-argF) U169 endA1 recA1 supE44 thi-1 gyrA96 relA1 tonA panD.

6.1.7.2 Protein expression

- BL21(DE3): F⁻ ompT gal dcm lon hsdS_B (r_B⁻ m_B⁻) λ (DE3 [lacI lacUV5-T7 gene 1 ind1 sam7 nin5]).
- Rosetta-gami 2: Δ (ara-leu)7697 Δ lacX74 Δ phoA PvuII phoR araD139 ahpC galE galK rpsL (DE3) F'[lac⁺ lacI^q pro] gor522::Tn10 trxB pLysSRARE2 (Cam^R, Str^R, Tet^R).

6.1.7.3 Congener expression

- B834 (DE3): F⁻ ompT hsdS_B (r_B⁻ m_B⁻) gal dcm met.
- CAG18491: LAM- rph-1 metEo-3079::Tn10.

6.1.8 Plasmids

The pET (Novagen) and pQE (Qiagen, Hildesheim, Germany) systems allow the efficient expression of recombinant proteins. In these systems, the *trans*-acting *lac*-repressor blocks protein expression by binding to the *cis*-regulatory *lac*-operator upstream of the promoter sequence. Protein expression is then induced by the addition of the artificial inducer IPTG, which binds to the *lac* repressor protein and inactivates it. In addition, these systems allow fast, efficient production and purification of N- or C-terminally 6xHis-Tagged proteins. The pET and pQE transcription–translation systems are based on the phage-derived T7 and T5 promoters, respectively. The T7 expression vectors require lysogenic *E. coli* strains for λ -DE3, which can provide the T7 RNA polymerase. The T5 promoter is recognized by any host *E. coli* RNA polymerase. In this work, the lipase was cloned into pQE80L. To generate the MetRS constructs, the pET15b, pET22b, pET28a or pQE80L vectors were used. The site-directed mutagenesis QuikChangeMult Kit (Stratagene, La Jolla, CA, USA) was used for the generation of MetRS mutants. All MetRS and barstar constructs were kindly provided by Petra Birle and Tatjana Krywcun (MPI of Biochemistry, Martinsried, Germany). The pRARE1-derived construct for the orthogonal pair cloning was given by Dr. Yuri Cheburkin (MPI of Biochemistry, Martinsried, Germany). All plasmid sequences were verified (DNA sequencing service at the MPI of Biochemistry, Martinsried, Germany). All primers were synthesized by Metabion International AG (Martinsried, Germany).

6.1.8.1 Lipase construct

pQE80L-TTL: The sequence encoding the lipase from *T. thermohydrosulfuricus* was PCR amplified with the following primers: 5'-tatactatatacgaattcattaagaggagaaattaagcatgcaaaaggctgttgaaattacataaac-3' / 5'-cgtgccggcggctgcagttatcagtgatggtgatggtgatggatcctcccttaacaattccttttgaaaaact-3' and cloned into the previously double-digested *EcoRI* and *PstI* cleavage sites (underlined) of pQE80L. A hexahistidine tag was attached to the C-terminus of TTL with an intervening short spacer (Gly-Ser). Additional random nucleotides at the 5'-end were added for efficient restriction.

6.1.8.2 MetRS constructs

The MetRS available coding sequences from different organisms were extracted from NCBI databases, PCR-amplified and cloned into suitable expression vectors. Some *EcMetRS* mutants have enhanced substrate specificities for Met analogs (see 3.2.1.2 for details).

- pET15b-*AaMetRS*-WT: The gene encoding *A. aeolicus* MetRS WT (497 residues) was cloned by PCR from genomic DNA using the following primers: 5'-gccatatgacacttatgaagaagttctacg-3' / 5'-gcggatcctcaaccttccctttgggaaatag-3' between the *NdeI* and *BamHI* sites (underlined) of the pET-15b plasmid. Additional random nucleotides at the 5'-end were added for efficient restriction. This plasmid is ampicillin resistant (Amp^R) and contains an N-terminal His-Tag.
- pET28a-*EcMetRS*-WT: The gene encoding *E. coli* MetRS WT (676 residues) was cloned by PCR from genomic DNA using the following primers: 5'-agctagctgaattcattgaaggccgtactcaagtcgcaagaaa-3' / 5'-agctagctgaattctcattatttcac-ctgatgacccggttt-3' between the *EcoRI* sites (underlined) of the pET-28a plasmid. This plasmid is kanamycin resistant (Kan^R). Additional random nucleotides at the 5'-end were added for efficient restriction. An Fxa cleavage site (IEGR) was added between the N-terminal His-Tag and the MetRS coding region.
- pET28a-*EcMetRS*-SM(L13G): pET28a-*EcMetRS*-WT-derived.
- pET28a-*EcMetRS*-DM(L13G/Y260L): pET28a-*EcMetRS*-SM-derived.
- pET28a-*EcMetRS*-TM(L13G/Y260L/H301L): pET28a-*EcMetRS*-DM-derived.
- pET28a-*ApMetRS*-WT: The gene encoding *A. pernix* MetRS WT (572 residues) was cloned by PCR from genomic DNA using the following primers: 5'-ccgccgccggaattcatcgaggggaagggttaagtagtagtaacctccgcgtg-3' / 5'-catgcatgcat-

gaagcttcactagtccctgaggagagggggcctct-3' between the *EcoRI* and *HindIII* sites (underlined) of the Kan^R pET-28a plasmid. Additional random nucleotides at the 5'-end were added for efficient restriction. An Fxa cleavage site (IEGR) was added between the N-terminal His-Tag and the MetRS coding region.

- pET15b-*Mj*MetRS-WT: The gene encoding *M. jannaschii* MetRS WT (648 residues) was cloned by PCR from genomic DNA using the following primers: 5'-atgacatatgagatatctaataacaactgcc-3' / 5'-gcggtacctcaactacgtctttatccttatc-3' between the *NdeI* and *BamHI* sites (underlined) of the Amp^R pET-15b plasmid. Additional random nucleotides at the 5'-end were added for efficient restriction. The plasmid contains an N-terminal His-Tag.
- pET15b-*Mj*MetRS SM (L9G): pET15b-*Mj*MetRS-WT-derived.
- pET15b-*Mj*MetRS DM (L13G/Y260L): pET15b-*Mj*MetRS-SM-derived.
- pET15b-*Mj*MetRS TM (L13G/Y260L/H301L): pET15b-*Mj*MetRS-DM-derived.
- pET15b-*Np*MetRS-WT: The gene encoding *N. pharaonis* MetRS WT (698 residues) was cloned by PCR from genomic DNA using the following primers: 5'-gccatatgccagaggagttccgacc-3' / 5'-gcggtaccctactgaaccttcggtcccgg-3' between the *NdeI* and *BamHI* sites (underlined) of the Amp^R pET-15b plasmid. This plasmid contains an N-terminal His-Tag.
- pET28a-*Pa*MetRS-WT: The gene encoding *P. aerophilum* MetRS WT (570 residues) was cloned by PCR from genomic DNA using the following primers: 5'-ccgccgcccggaattcatcagaggaagggcgaaatacgtaataggctcggcg-3' / 5'-catgcatgcatgaagcttccattatatcactacctgttcccacgggta-3' between the *EcoRI* and *HindIII* sites (underlined) of the Kan^R pET-28a plasmid. Additional random nucleotides at the 5'-end were added for efficient restriction. An Fxa cleavage site (IEGR) was added between the N-terminal His-Tag and the MetRS coding region.

- pET15b-*Pab*MetRS-WT: This Amp^R plasmid containing the MetRS WT sequence from *P. abyssi* was kindly provided by Dr. Mechulam.¹³³
- pET28a-*Sa*MetRS-WT: The gene encoding *S. acidocaldarius* MetRS WT (570 residues) was cloned by PCR from genomic DNA using the following primers: 5'-ccgccgccgccggaattcatcgaggggaaggaaggttttagtaacatctgcatggcct-3' / 5'-catgcatgcatg-gcg-gccgctcattacctaagatcaggtcttctttcc-3' between the *EcoRI* and *NotI* sites (underlined) of the Kan^R pET-28a plasmid. Additional random nucleotides at the 5'-end were added for efficient restriction. An Fxa cleavage site (IEGR) was added between the N-terminal His-Tag and the MetRS coding region.
- pET22b-*Ta*MetRS-WT: The gene encoding *T. acidophilum* MetRS WT (698 residues) was cloned by PCR from genomic DNA using the following primers: 5'-tacacatatggtggttcagatcaagataactg-3' / 5'-tacagtcgacagataaccagggttcaaggtc-3' between the *NdeI* and *Sall* sites (underlined) of the Amp^R pET-22b plasmid. Additional random nucleotides at the 5'-end were added for efficient restriction. The plasmid contains a C-terminal His-Tag.
- pET28a-*At*MetRS-WT: The gene encoding *A. thaliana* MetRS WT (797 residues) was cloned by PCR from cDNA using the following primers: 5'-cgccgccgccgcatccatcgaggggaaggaagacgacggcaagagcagccccaag-3' / 5'-catgcatgcatgctcgagtcattaccggatcgtgccattgctgatg-3' between the *BamHI* and *XhoI* sites (underlined) of the Kan^R pET-28a plasmid. Additional random nucleotides at the 5'-end were added for efficient restriction. An Fxa cleavage site (IEGR) was added between the N-terminal His-Tag and the MetRS coding region.
- pET28a-*Dr*MetRS-WT: The gene encoding *D. rerio* MetRS WT (922 residues) was cloned by PCR from cDNA using the following primers: 5'-ccgccgccgccggaattcatcgaggggaaggaagctgtttatcggtgagggaaa-3' / 5'-catgcatgcatg-aagcttcattattcttcttggtttttg-cg-cgg-3' between the *EcoRI* and *HindIII* sites (underlined) of the Kan^R pET-28a plasmid. Additional random nucleotides at the 5'-

end were added for efficient restriction. An Fxa cleavage site (IEGR) was added between the N-terminal His·Tag and the MetRS coding region.

- pET28a-*Dm*MetRS-WT: The gene encoding *D. melanogaster* MetRS WT (1022 residues) was cloned by PCR from cDNA using the following primers: 5'-ccgccgcccgcggaattcatcgaggggaaggataatctacacgaatgatggcaaccc-3' / 5'-catgcatgcatgctcgagtcactacttcttctttgccccttgcctgt-3' between the *EcoRI* and *XhoI* sites (underlined) of the Kan^R pET-28a plasmid. Additional random nucleotides at the 5'-end were added for efficient restriction. An Fxa cleavage site (IEGR) was added between the N-terminal His·Tag and the MetRS coding region.
- pET28a-*Hs*MetRS-WT: The gene encoding *H. sapiens* MetRS WT (900 residues) was cloned by PCR from cDNA using the following primers: 5'-ccgccgcccgcggaattcatcgaggggaaggagactgttcgtgagtgatggcgtc-3' / 5'-catgcatgcatg-aagctttcattacttttcttcttgcctttagggg-3' between the *EcoRI* and *HindIII* sites (underlined) of the Kan^R pET-28a plasmid. Additional random nucleotides at the 5'-end were added for efficient restriction. An Fxa cleavage site (IEGR) was added between the N-terminal His·Tag and the MetRS coding region.
- pQE80L-*Sc*MetRS-WT: The gene encoding *S. cerevisiae* MetRS WT (751 residues) was cloned by PCR from genomic DNA using the following primers: 5'-agctagctagctggatccattgaaggccgttcttctcatttctttgataaatc -3' / 5'- agctagct-agctggatcctcattacacttgttgaccacatattg- 3' between the *BamHI* sites (underlined) of the Amp^R pQE80L plasmid. This plasmid contains an N-terminal His·Tag.
- pQE80L-*Sc*MetRS-TF (6-185Δ): The coding region from the residue 1 to 5 and 185 to 751 of *S. cerevisiae* MetRS was cloned by PCR from genomic DNA using the following primers: 5'- cgccgccgcccgcggatccatgtcttctcattgattcagaaatttgcctaagc-caaac-3'; 5'- agctagctagctggatcctcattacacttgttgaccacatattg -3' between the *BamHI* sites (underlined) of the Amp^R pQE-80L plasmid. This plasmid contains an N-terminal His·Tag.

6.1.8.3 Barstar constructs

- pQE80L-b*1M: The gene encoding *B. amyloliquefaciens* barstar WT (90 residues) was originally cloned by PCR from genomic DNA between the *EcoRI* and *HindIII* sites of the pKK223-3 (Pharmacia) plasmid. Barstar was subsequently cloned into the same restriction sites of pQE80L, eliminating the N-terminal His-Tag. The barstar WT was then subjected to site-directed mutagenesis to generate barstar P28A (b*) under the control of the inducible T5 promoter. This plasmid is Amp^R.
- pQE80L-b*2M: Derived from pQE80L-b*1M, this plasmid contains barstar P28A/E47M with two AUG codons for Met reassignment.

6.1.8.4 Orthogonal pair constructs

Several strategies were followed to set up a system for the efficient expression of the orthogonal MetRS and tRNA.

- pTEc0: The fragment of plasmid pPICZB (Invitrogen, Carlsbad, CA, USA) containing the EM7 constitutive promoter and the zeocine resistance gene was initially PCR-amplified using the primers: 5'-ggactagtgtgacaattaatcatcggc-3' / 5'-ggaattcgtgaatgtaagcgtgacataac-3' and cloned between the previously double-digested *SpeI* and *EcoRI* sites (underlined) of the pBluescript II SK plasmid (Stratagene, La Jolla, CA, USA). A Multiple Cloning Site (MCS) was then attached next to the EM7 promoter using a three-step PCR procedure: i) Amplification of *SpeI*-EM7 and the first part of the MCS using the 5'-cgacggccagtgagcgcgc-3' / 5'-cctcatatggggccccgatcgtgatcaatgcatggttagttcctc-acctgtcg-3' primers to generate the first template, ii) Amplification of first template *SpeI*-EM7 and second part of the MCS using the 5'-cgacggccagtgagcgcgc-3' / 5'-ggctcgaggctgacagatctcacgtggatcaggcctcatatggggccccgatc-3' primers to generate the third template, and iii) the amplification of second template *SpeI*-EM7 and the third part of the MCS-*SacI* using the 5'-cgacggccagtgagcgcgc-3' / 5'-ggtaccgagctcgggcccttaattaacccgggctcg-

aggtcgacagatctc-3' primers. Finally, the EM7-MCS PCR product was subcloned between the previously double-digested *SpeI* and *SacI* sites of the pRARE vector (Novagen Merck Chemicals Ltd., Nottingham, UK). The plasmid pTEc0 contains a chloramphenicol resistance marker, a relatively mid-copy number origin of replication p15A, rare *E. coli* tRNA genes under their natural promoters that enhance the expression of exogenous proteins in *E. coli*, the constitutive promoter EM7 for the expression of orthogonal MetRS, and a MCS for cloning it. See Appendix 9.5 for sequence details.

- pTEc1: Derived from pTEc0, this vector no longer contains the elongator tRNA^{Met} from *E. coli* since it was substituted by the orthogonal tRNA in a two-step PCR procedure: i) Amplification of a region partially containing the *ScaI*-Cam^R and the first part of the orthogonal tRNA^{Met} using the 5'-gcttaatgaattacaacagtactgcg-3' / 5'-agcgccggactcataatccggtgtccgggggtcaaatccccgcgggcggcaccatctttttgcgggag-3' primers to generate the first template, and ii) the amplification of first template partially containing the *ScaI*-Cam^R and the second part of the orthogonal tRNA^{Met}-*NruI* using the 5'-gcttaatgaattacaacagtactgcg-3' / 5'-tatatatatatatcgcgaaaaaaaaagatgccgccgtagctcagcctggtagagcgccggactcataatc-3' primers. Additional random nucleotides at the 5'-end were added for efficient restriction. The Cam^R-tRNA^{Met} product was subcloned between the *ScaI* and *NruI* of previously double-digested pTEc0. The orthogonal MetRS was PCR amplified and cloned between previously double-digested *NdeI* and *Sall* sites (underlined) using the 5'-tatatatatatatcatatggcaagctggagccacccgcagttcgaaaagggtgcaatgaaggttttagtaacatctgcatgg-3' / 5'-atatatatatatgtcgacttaccttaaagatcaggtctttcttttc-3' primers. Additional random nucleotides at the 5'-end were added for efficient restriction. A Strep-Tag II sequence was appended to the orthogonal MetRS N-terminus between two linker sequences for immunoblotting detection. See Appendix 9.6 for sequence details.
- pTEc1.1G-R/L: In addition to the rare tRNA genes provided by pTEc1, the extremely rare tRNA^{Leu} coded by the gene *leuZ* is present. This gene was PCR-amplified from genomic *E. coli* DNA using the 5'-atatatatatatgcatgctcaaaagtggtg-

aaaaatcgttg-3' / 5'-atatatatatggatcctggtagccggagcgg-3' primers and cloned into the *SphI* and *BamHI* sites (underlined) from the pTEc1 plasmid. Additional random nucleotides at the 5'-end were added for efficient restriction. pTEc2 also no longer contains the EM7 promoter, since it was substituted by the stronger constitutive *glnS'* promoter, as well as the *rho T* independent terminator in a two-step cloning procedure: i) PCR amplification of the *SpeI*-*glnS'*-*BpaRS*-*rhoT*-*SmaI* fragment using the 5'-atatatatatactagtcatcaatcatccccataatccttg-3' / 5'-atatatatatcccggg-aaaagcagaaaaacgccgc-3' primers, followed by cloning between the previously double-digested *SpeI* and *SmaI* sites (underlined) of pTEc1. This introduces the new promoter and terminator via the elimination of the old promoter and the orthogonal MetRS. Additional random nucleotides at the 5'-end were added for efficient restriction. This is followed by ii) PCR amplification of the orthogonal MetRS fragment using the 5'-atatatatatcatatggcaagctggagcc-3' / 5'-atatatatatctgcagttacctaagatcaggtctttcttttc-3' primers and its cloning between the previously double-digested *NdeI* and *PstI* sites (underlined) of pTEc1 (additional random nucleotides at the 5'-end were added for efficient restriction.) A Strep-Tag II sequence was appended to the orthogonal MetRS N-terminus between two linker sequences for immunoblotting detection. See Appendix 9.7 for sequence details.

- pTEc2: Derived from pTEc1.1G-R/L, this vector no longer contains the original sequence of the orthogonal MetRS, since it was substituted by a codon bias optimized sequence for expression in *E. coli*. The orthogonal MetRS was designed so that it contains the *NdeI*-linker-Strep-TagII-*XhoI*- sequence at its N-terminus and the -*PstI*-linker-*rhoT*-*SmaI* sequence at its C-terminus. These should allow its efficient detection by immunoblotting, as well as its efficient substitution by cloning. The entire fragment was synthesized and cloned between the previously double-digested *EcoRV* sites of the pUC57 (Genscript; New Jersey, US) vector. Finally, the whole plasmid was digested with *NdeI* and *SmaI* and the resulting fragment subcloned into pTEc1.1G-R/L. See Appendix 9.8 for sequence details.

6.1.9 Software

- Origin 6.1G (OriginLab Corporation, Northampton, MA, USA) for data analysis.
- ApE for *in silico* cloning.¹⁷⁵
- OptimumGene Codon Optimization Analysis (GeneScript, New Jersey, US).¹⁵⁴

6.2 Methods

6.2.1 Molecular biology

6.2.1.1 PCR

The Polymerase Chain Reaction (PCR) allows the amplification of specific nucleic acid sequences. For each reaction, 10 ng/ μ l target DNA sequence, 1x polymerase buffer, 250 μ M of each dNTP, 10 pmol/ μ l of forward and reverse primer and 0.02 U/ μ L of ExTaq polymerase in 50 μ l were used. The cycle is defined by a nucleic acid denaturation step at 95 °C for 5 min, followed by 25-30 cycles of DNA denaturation at 95 °C for 1 min, primer annealing at 55-60 °C for 1 min, and DNA elongation at 72 °C and 1 kb/min. A 10-min elongation period was applied.

6.2.1.2 Cloning

The DNA generated from PCR was purified with either the QIAquick PCR Purification Kit or Gel Extraction Kit from Qiagen. PCR fragments and vectors in concentrations of 0.5 to 2 μ g were double-digested with 10 U of the appropriate restriction enzymes in buffers with or without 10 μ g BSA. The reactions were performed in 50-100 μ l and incubated at 37 °C for 2-4 hrs, with the exception of reactions involving *Sma*I, for which the optimal temperature is 25 °C. After double-digestion, DNA fragments and vectors were purified with the QIAquick PCR Purification Kit and ligation was performed using 25 ng vector DNA combined with insert DNA having a 5x molar concentration with respect to the vector, 1x T4 ligase buffer, and 200 Units of T4

ligase. The ligation was performed in a 20 μ l volume and incubated at 16 °C ON.

6.2.1.3 SDS-PAGE

In Sodium Dodecyl Sulfate Poly-Acrylamide Gel Electrophoresis or SDS-PAGE, proteins are separated according to their molecular mass in a cross-linked polyacrylamide matrix. SDS denatures proteins and surrounds this with a uniform negative charge, making its migration both charge- and conformation-independent. Electrophoresis was performed at 130 V for ca. 1 hr in 12% or 17% poly-acrylamide gels. Protein bands were visualized using the Coomassie staining solution, followed by destaining at RT for 1 h (or ON).

6.2.1.4 Western Blot (Protein immunoblotting)

Western blotting exploits the specific binding of antibodies for the detection of target proteins. After SDS-PAGE, proteins are transferred to a nitrocellulose membrane and the target protein is detected using an antibody that binds specifically to it. This primary antibody is subsequently detected using a secondary antibody linked to an enzyme, typically either horseradish peroxidase (HRP) or alkaline phosphatase (AP). A substrate is then added, and forms a precipitate or a luminescent product at the sites where binding occurred. Here, the HRP-luminal system was used, and the luminescent product is detected in a light sensitive photo paper. Western blotting was performed by incubating SDS-PAGE gels with nitrocellulose membrane covered with two pieces of pre-soaked Whatman paper on both sides for 5 min in transfer buffer. Electrophoresis was then performed at 200 mA for 2 hr. The membrane was then stained with Ponceau S to check the efficiency of protein transfer. After destaining with H₂O, the membrane was incubated in TBS buffer containing 1.5% BSA for 1 h at RT to block non-specific antibody binding sites on the membrane. The membrane was subsequently incubated ON with a murine anti-Strep-Tag II antibody (1:1000 in TBS buffer) at 4 °C. The membrane was then washed with TBS buffer thrice for 10 min and incubated with the secondary anti-mouse antibody (1:4000 in TBS buffer) for

1 hr at RT. This was followed by three more washing steps. All incubation and washing steps were done with low speed shaking. The luminescent reaction was initiated by incubating the membrane with 1:1 luminol:peroxide reagent for 5 min. Detection was performed on the membrane exposed to x-film paper for 5-60 min using the X-OMAT 1000 processor.

6.2.2 Microbiology

6.2.2.1 Production and transformation of electrocompetent cells

Cells were incubated ON at 37 °C in 5 mL of LB medium. Cells were subsequently incubated with 500 mL of LB medium inoculated with a tenth of the previous culture at 37 °C, with shaking at 220 rpm. Incubation is continued until the cells reach an OD₆₀₀ between 0.6 and 0.8. The cells were then harvested, washed twice with ice-cold 10% glycerol and resuspended in 5 mL 10% glycerol. Finally, 100 µL aliquots were frozen in liquid nitrogen and kept at -80 °C until further use.

Thereafter, cells were transformed by electroporation. 50 µL of competent cells aliquot were typically mixed with ~100 ng of the desired plasmid in an electroporation cuvette. A current of 1650 V is then applied on the cell suspension. This is followed by the addition of 1 mL LB medium, and the whole is transferred to a sterile eppendorf tube, which is incubated at 37 °C for 1 h and with shaking at 1000 rpm. Finally, cells are plated on agar supplemented with the appropriate antibiotics. Single colonies that appear the next day are transferred to 5 mL antibiotic-supplemented LB medium and incubated over night at 37 °C and 200 rpm.

6.2.2.2 Limitation test

To successfully incorporate non-canonical amino acids during protein expression, it is absolutely necessary to use strains auxotrophic for the corresponding canonical amino acid. It is important to know the 'degree of auxotrophy' by determining the

required amino acid concentration to obtain high biomass production. This can be assessed using a limitation test, where different concentrations of non-canonical amino acid are used and growth is measured. For this, 5 mL NMM supplemented with the appropriate antibiotics and different concentrations of Met were inoculated with 5 μ L of pre-culture. Suspensions were incubated ON at 37 °C and 200 rpm. Cell growth was determined the next day by measuring the OD₆₀₀. The amino acid concentration that allows cells growing up to a 0.6-0.8 OD₆₀₀ was used as limiting concentration for high biomass production and are used as a reference in optimal incorporation experiments.

6.2.2.3 Small-scale expression of lipase, MetRSs, and barstar

To select the best expression clone, a small-scale protein expression test is required. For this, 5 mL of three to five ON cell LB cultures supplemented with the appropriate antibiotics are transferred to a sterile eppendorf tube, where protein expression is induced by adding 1 mM IPTG. All cell cultures were incubated at 30 °C and 200 rpm. Non IPTG-induced samples corresponding to 1 OD₆₀₀ were prepared in parallel. After 4 hours or ON incubation, 1 OD₆₀₀ of cells were harvested, resuspended in 40 μ L H₂O containing 10 μ L of 5x SDS-sample buffer and heated to 95 °C for 5 min. Protein expression is assessed by SDS-PAGE. Clones exhibiting the highest expression were selected for large-scale protein/congener expression.

6.2.2.4 Large-scale expression of lipase congeners

For the expression of lipase congeners, one tenth of the best expressing clone was inoculated into 1 L of NMM supplemented with a limiting amount of Met and the appropriate antibiotics. After Met depletion in the mid-log phase (OD₆₀₀ 0.6–0.8), which can be observed as a growth arrest, 5 mM of either Met (parent TTL expression) or Aha and Nle (congener TTL expression) were added to the media 15 min prior to induction. Gene expression was induced by the addition of 1 mM IPTG for 4-6 h at 30 °C with vigorous shaking.

6.2.2.5 Purification of lipase congeners

After soluble TTL expression, cells were harvested by low speed centrifugation (3,200 xg, 4 °C, 10 min) and the cell pellet was resuspended in Ni-NTA lysis buffer and 0.1 % Triton X-100. After addition of DNase, RNase, and lysozyme, each with a 1 mg/mL concentration, cells were ruptured by sonication and the homogenate cleared from cell debris by high speed centrifugation (30,000 xg) for 30 min at 4 °C. The clear lysate was loaded onto a 5 mL HiTrap Chelating HP column, which was then washed with 10 CV of Ni-NTA low-salt washing buffer, followed by 5 CVs of Ni-NTA high-salt washing buffer, and again 5 CVs of Ni-NTA low-salt washing buffer. Bound proteins were eluted by using an imidazole gradient (20-500 mM) with the Ni-NTA elution buffer. The elution fractions were analyzed by SDS-PAGE and those enriched in the desired congeners were pooled, dialyzed against lipase buffer, and concentrated by ultra-filtration with Vivaspin 20 having a MW cutoff of 10,000 Da. Finally, the concentrated samples were assayed for protein content using the Bradford method, with BSA as a calibration standard.

6.2.2.6 Solubility tests and large-scale expression of MetRSs

Following the small-scale expression test and protein induction and cell harvesting, a volume corresponding to 1 OD₆₀₀ is sonicated and centrifuged at high-speed for 30 min at 4 °C. The soluble phase is separated from the pellet and dissolved in the same volume of 7 M urea. To 40 µl of each fraction, 10 µL of 5x SDS-sample buffer was added. The samples were heated to 95 °C for 5 min. Protein solubility was assessed by SDS-PAGE. For expression of MetRSs, one tenth of the best expressing clone was inoculated in 1 L of LB supplemented with the appropriate antibiotics. In the mid-log phase (OD₆₀₀ 0.6–0.8), gene expression was induced by the addition of 1 mM IPTG. Cultures were maintained at 30 °C with vigorous shaking between 4 h to ON.

6.2.2.7 Purification of MetRSs proteins

After soluble MetRS expression, cells are harvested by low speed centrifugation (3,200g, 4 °C, and 10 min) and the pellet was resuspended in Ni-NTA lysis buffer. After the addition of DNase, RNase, and lysozyme, each at a concentration of 1 mg/mL, cells were ruptured by sonication. The homogenate is cleared of cell debris by high speed centrifugation (30,000 xg) for 30 min at 4 °C. The clear lysate was loaded onto a 1 mL HiTrap Chelating HP column, which was then washed with 10 CVs of Ni-NTA low-salt washing buffer. Bound proteins were eluted using an imidazole gradient (20-300 mM) with the Ni-NTA elution buffer. Elution fractions were analyzed by SDS-PAGE and those enriched in the desired congeners were pooled, dialyzed against MetRS buffer, and concentrated by ultra-filtration with Vivaspin 20 with a MW cutoff of 50,000 Da.

6.2.2.8 Large-scale expression of barstar congeners

For expression of barstar congeners, the same protocols used in lipase expression were applied (see section 6.2.2.4), with the modification of adding different concentrations of Aha:Eth (i.e. for a 3:1 ratio, 0.375 mM Aha:0.125 mM Eth; for a 1:1 ratio, 0.25 mM Aha:0.25 mM Eth; and for a 1:3 ratio, 0.125 mM Aha: 0.375 mM Eth) in a final volume of 200 mL of NMM instead.

6.2.2.9 Purification of barstar congeners

After insoluble barstar expression, cells were harvested by low-speed centrifugation (4,000 xg) for 20 min at 4 °C and the cell pellet was resuspended in barstar buffer. After addition of 1 mg/mL lysozyme, cells were ruptured by sonication for 3 min and harvested by high-speed centrifugation (30,000 xg) for 40 min at 4 °C. The supernatant was discarded and the cell pellet, which contains inclusion bodies, was dissolved in IE resuspension buffer. The suspension was separated by high-speed centrifugation (30,000 xg) for 40 min at 4 °C and the supernatant was transferred into

dialysis tubes (3500 Da cutoff). The first dialysis was performed for 3 h, the second ON and the third for 3 h at 4 °C. All dialyses were performed in IE washing buffer. Solid particles were subsequently separated by high-speed centrifugation (30, 000 xg) for 40 min at 4 °C and the supernatant was passed through a 0.22 µm filter. The clear lysate was loaded onto a 5 mL HiTrap Q Sepharose column, which was then washed with 5 CVs of IE washing buffer. Bound proteins were eluted by using a NaCl gradient (100-1000 mM) with the IE elution buffer. The elution fractions were analyzed by SDS-PAGE and those enriched in the desired congeners were pooled, dialyzed against barstar buffer and concentrated by ultra-filtration with Vivaspin 10 with a MW cutoff of 5,000 Da.

6.2.3 Biochemistry

6.2.3.1 tRNA aminoacylation assay

The tRNA aminoacylation assay is used to determine the rate of amino acid (aa) aminoacylation by an aminoacyl-tRNA synthetase (AARS).¹³⁸ In the reaction, the aminoacylated tRNA (aa-tRNA) is formed by transferring the aa, in form of aminoacyladenylate (AMP-aa), to the tRNA. In this assay, radioactively labeled aa (³⁵S-aa) was used to form [³⁵S]-aa-tRNA, which is precipitated onto a filter and separated from the eluate. The activity of the AARS with respect to its cognate aa and tRNA is detected directly by the rate of formation of [³⁵S]-aa-tRNA. The reaction mix (final volume: 30 µl) was incubated at 37 °C in 50 mM HEPES (pH 7.4), 10 mM MgCl₂, 50 mM KCl, 3 mM BME, 5 mM ATP, 1 mg/mL BSA, 5 nM [³⁵S]-Met (3 cpm/µmol), 10 -200 µM tRNA, and 1 µM of MetRS. After 15 or 20 min, 20 µl of the reaction mixture was transferred onto a filter and the tRNA was precipitated by adding 1 mL of 10% TCA, followed by washing steps with 1 mL of 5% TCA, 1 mL of absolute EtOH and 1 mL of a 1:1 solution EtOH:Ether. Filters were dried for 5 min and mixed with scintillation solution to determine the amount of radioactivity.

6.2.3.2 ATP:PPi exchange assay

This assay is used to determine the activation rate of an amino acid (aa) by an aminoacyl-tRNA synthetase (AARS).¹⁴² In the reaction, the aminoacyladenylate (AMP-aa) is formed by transferring the AMP group of ATP, accompanied by the release of pyrophosphate (PPi). In the reverse reaction, radioactively labeled PPi with ³²P will form [³²P]-ATP, the amount of which can be measured. Activated charcoal (aC), which has affinity towards ATP, is used to adsorb [³²P]-ATP and separate it from the eluate [³²P]-PPi. The activity of the AARS is detected directly by the rate of formation of [³²P]-ATP. The reaction mix was incubated at 37 °C in 100 mM Tris·HCl (pH 8.0), 80 mM MgCl₂, 5 mM KF, 700 mM BME, 5.5 mM ATP, 0.1 mg/mL BSA, 2.2 mM [³²P]-PPi (0.2 cpm/pmol), 5 μM of MetRS, and 5 mM of the L-isomer analogs of Met in a final volume of 200 μl. After 15 or 20 min, 100 μl of the reaction solution was added to 600 μl of 240 mM sodium pyrophosphate solution containing 70% (v/v) perchloric acid. [³²P]-ATP formation was followed by specific absorption of 200 μl of 7.5% (w/v) activated charcoal. The suspension was thoroughly mixed and filtered through Whatman GF/F paper. Filters were washed twice with 10 mL of water and mixed with scintillation solution to determine the amount of radioactivity.

6.2.4 Spectroscopy and spectrometry

6.2.4.1 UV/VIS-Spectroscopy

Protein concentrations were determined by the measurement of absorbance at 280 nm, and were calculated according to the Lambert-Beer-Equation $A = \epsilon d c$, where A = absorbance; ϵ = molar extinction coefficient; c = concentration; and d = path length.

6.2.4.2 Bradford protein assay

The Bradford reagent is composed of Coomassie brilliant G250 dye, which forms blue complexes with the positively charged amino groups of proteins in acidic solution. The

dye complex absorbs light at 595 nm; the dye intensity is proportional to protein concentration. All samples are measured at this wavelength and compared against a calibration curve generated using a BSA with known concentrations. For each measurement, 10 μL of sample is mixed with 990 μL of Bradford Reagent and incubated at RT for 5 min, then measured at 595 nm.

6.2.4.3 Electro Spray Ionization Mass Spectrometry (ESI-MS)

For Liquid Chromatography ESI-MS, 20 μL aliquots of the sample were pre-separated on a Waters RP C4 column (300 \AA pore size; 3.5 μm particle size; 100 x 2.1 mm) by a 20 minute elution using a gradient from 20 to 90 % 0.05 % (v/v) TFA in acetonitrile in 0.05 % (v/v) TFA in water, with a flow rate of 250 $\mu\text{L}/\text{min}$. The masses of the eluted fractions were analyzed on a MicrOTOF ESI-MS.

6.2.4.4 Spectrophotometric assay with *p*-nitrophenyl palmitate

Lipase activity was determined by measuring the hydrolysis of *p*-nitrophenyl palmitate (*p*NPP). Cleavage of *p*NPP was determined at different temperatures (40-90 $^{\circ}\text{C}$) in 25 mM Tris·HCl pH 8 according to the protocol of Winkler and Stuckmann.¹⁰¹ A buffered *p*NPP suspension containing 25 mM Tris·HCl pH 8.0, 1 mM *p*NPP and 1 mg/mL gum arabic (Acros Organics, Geel, Belgium) was homogenized at 22,000 rpm for 4 min at RT. The reaction was started by mixing 900 μL buffered *p*NPP suspension with 100 μL of the TTL preparations. Autohydrolysis was assessed by including a blank that contained the same volume of 50 mM Tris·HCl pH 8.0 instead of enzyme. The reaction mixture was incubated at the desired temperature according to the protein for 10 or 15 min with vigorous shaking. Enzymatic hydrolysis of *p*NPP was stopped by the addition of 100 μL of 1 M Na_2CO_3 and chilling on ice for 1 min. Following centrifugation at 20,000g for 10 min at RT, the absorption of the supernatant was measured at 410 nm. All values were determined in triplicates and corrected for autohydrolysis. One unit (1 U) of lipase activity is defined as the amount of enzyme necessary to liberate 1 μmol of *p*NPP (ϵ at pH 8.0 = $12.75 \times 10^6 \text{ M}^{-1} \text{ cm}^{-1}$) per minute

under the conditions described above.

6.2.4.4.1 Influence of temperature on lipase activity

The optimal temperature of lipase activity was determined with the standard *p*NPP assay at pH 8. The samples were incubated for 10 min at temperatures between 40 and 90 °C. To determine thermostability, 100 µl lipase solutions were incubated at 75, 80, 85, 90, or 95 °C at different time intervals ranging from 10 and 180 min.

6.2.4.4.2 Influence of additives on lipase activity

To investigate the effects of various substances on lipase activity, the produced congeners were incubated in solutions containing 90% organic solvent, 10% surfactant, or 10 mM inhibitor (500 mM guanidinium chloride and 2M urea) at RT for 60 min. Lipase residual activity was subsequently determined using the *p*NPP assay at the optimal temperature for 10 min at pH 8.

6.2.4.4.3 Substrate specificity for *p*-nitrophenyl esters

The reactions were performed according to the spectrophotometric assay with *p*NPP as described above but using the following *p*-nitrophenyl-derived (*p*NP) substrates (Sigma) at a concentration of 10 mM: acetate (C2:0), butyrate (C4:0), caproate (C6:0), caprylate (C8:0), caprate (C10:0), laurate (C12:0), myristate (C14:0), palmitate (C16:0), and stearate (C18:0). The reactions were incubated at the enzyme's temperature optimum and pH 8 for 10 min.

6.2.4.5 Spectrophotometric assay with tricaprylin

To determine the optimal pH of the lipase enzymes, a modified assay using the formation of copper soaps for detection of free fatty acids was used.¹⁷⁶ The substrate solution was comprised of 10 mM tricaprylin (1,2,3-trioctanoylglycerol) and 5 g/L gum

Arabic in 40 mM universal pH buffer with the desired pH 7 or 8 emulsified at maximum speed for 1 min at RT. An aqueous Copper(II)-acetate-I-hydrate solution (58 mg/mL) with pyridine at pH 6.1, was used as the copper reagent. The dye reagent contained 1 mg/mL diethyldithiocarbamate dissolved in 99.8 % (v/v) ethanol. 200 μ L substrate solution was combined with 100 μ L enzyme solution with vigorous shaking for 18 h at the optimal temperature for the specific lipase congener. This is followed by the succeeding steps, which are all performed at RT: first, the reaction was stopped by adding 125 μ L 3 M HCl. Extraction is then performed by vigorously mixing the sample with 1.5 mL isooctane for 10 min. Phases separation was achieved by spinning in a table-top centrifuge at maximum speed for 10 min. 1.25 mL of the isooctane phase were removed and mixed with 250 μ L copper reagent. The emulsion was mixed at 1400 rpm for 5 min and centrifuged again at maximum speed for 5 min. 1 mL of the organic phase was withdrawn and mixed with 200 μ L dye reagent. After 5 min, absorption at 430 nm was determined. The contribution of autohydrolysis was assessed by including a blank containing an equal volume of 40 mM universal pH buffer at the appropriate pH. All values were determined in triplicates and corrected for autohydrolysis.

6.2.4.5.1 Influence of pH in lipase activity

The influence of pH on lipase activity was assessed using the tricaprylin assay (see above) between pH 4 and 12 at the optimal temperature for 18 h.

6.2.4.5.2 Substrate specificity for triacylglycerols

The reactions were carried out according to the spectrophotometric assay with tricaprylin as described above but using the following substrates (Sigma) at a concentration of 10 mM: triacetin (C2:0), tributirin (C4:0), tricaproin (C6:0), tricaprylin (C8:0), tricaprin (C10:0), trilaurin (C12:0), trimyristin (C14:0), tripalmitin (C16:0), and tristearin (C18:0). The reactions were incubated at the enzyme's temperature optimum and pH 8 for 18 h.

6.2.4.6 Circular dichroism

Circular Dichroism (CD) is used to estimate the degree of protein folding. Additionally, the relative percentage of secondary structure elements in a sample (α -helix, β -sheet and random coil) can be estimated by comparison to reference spectra. The measurement is based on the differential absorbance of left and right circular polarized light, usually called ellipticity or Θ , by optical active substances at different wavelengths. A CD spectrum is the plot of Θ against the wavelength of circular polarized light. CD spectra of 0.2 mg/mL lipase samples were measured in 10 mM Tris·HCl pH 8.0. Measurements were performed in 110-QS Hellma quartz cells (optical path-length: 0.1 cm) under controlled temperature (Peltier type FDCD attachment, model PFD-350S/350L; JASCO International Co., Ltd., Tokyo, Japan). Ellipticity changes were recorded between 200 nm and 250 nm at an optimal temperature of 65 or 70 °C according to the congener.

6.2.4.7 N-terminal sequencing

The N-terminal sequencing method, or Edman sequencing, consists of the derivatization of N-terminal amino acids with phenylthiohydantoin (PTH), followed by a RP-HPLC step. Samples were subjected to N-terminal sequence analysis using gas-phase sequenator precise cLC (Applied Biosystems GmbH, Darmstadt, Germany) according to manufacturer instructions. Due to their hydrophobicity, the amino acid PTH derivatives display different quantifiable retention times. In this way, the intensities of all peaks were summed up to 100% and compared as in ESI-MS.

6.2.5 Informatics

6.2.5.1 Generation of a 3D structure model for TTL

The primary sequence of TTL (see Appendix 9.1 for details) was queried against the entire PDB database and compared to known 3D structures of structurally similar

proteins, such as lipases, esterases and serine proteases with aid of the software HHpred. This software provides a method for sequence database searching and structure prediction.¹⁷⁷ In addition, the sensitivity of HHpred in finding homologous sequences is comparable to the most powerful profile-profile alignment servers for structure prediction currently available, e.g. x. 100 query-template alignments were obtained from HHpred, of which four were selected according to their high score, including the esterase from the bacterium *Butyrivibrio proteoclasticus* (PDB: 2WTM)¹⁷⁸, the acylaminoacyl serine peptidase from *A. pernix* (PDB: 2HU5)¹⁷⁹, the human monoglyceride lipase (PDB: 3JW8)¹⁸⁰, and the putative serine hydrolase from *Xanthomonas campestris* (PDB: 3KSR). A multiple-sequence alignment of these templates were used to build 100 homology models, out of which the best scoring model was chosen with the aid of the software “Modeller”.¹⁸¹

7 List of figures

Figure 1. Synthetic biology.....	4
Figure 2. Radial presentation of the universal genetic code in RNA format (previous page).....	6
Figure 3. The aminoacylation reaction.....	7
Figure 4. Methionine analogs useful in X-ray crystallography.....	10
Figure 5. Methionine analogs useful as bioorthogonal reporters.....	10
Figure 6. Methionine analogs useful for probing protein hydrophathy.....	11
Figure 7. Methionine analogs useful to retain enzymatic activity.....	12
Figure 8. Methionine oxidation.....	14
Figure 9. Ribbon diagram of the 3D crystal structure of monomeric <i>EcMetRS</i>	15
Figure 10. <i>E. coli</i> tRNAs ^{Met}	16
Figure 11. The Janus face of protein synthesis.....	18
Figure 12. Structural features of lipases.....	21
Figure 13. Lipase reactions.....	22
Figure 14. Model of lipase kinetics.....	22
Figure 15. Mechanism of lipase catalysis.....	23
Figure 16. Probing the hydrophathy of lipase with two Met analogs.....	27
Figure 17. Lipase alloproteins.....	28
Figure 18. ESI-MS spectra of lipase congeners.....	29
Figure 19. Temperature and pH profiles of lipase congeners.....	31
Figure 20. Thermal stability of lipase congeners.....	32
Figure 21. Thermal activation of lipase congeners.....	34
Figure 22. 3D structure homology model for TTL.....	35
Figure 23. Secondary structure of lipase congeners.....	37
Figure 24. Two types of lipase substrates.....	38
Figure 25. Lipases substrate specificity for tryacylglycerols.....	38
Figure 26. Lipases substrate specificity for <i>p</i> -nitrophenyl alkanoate esters.....	39
Figure 27. Influence of solvents on lipase activity.....	41
Figure 28. Influence of metal ions on lipase activity.....	43
Figure 29. Influence of surfactants in lipase activity.....	45
Figure 30. Influence of inhibitors in lipase activity.....	47
Figure 31. Two types of MetRS:tRNA ^{Met} pairs.....	50
Figure 32. Expression and solubility of different MetRSs in <i>E. coli</i>	52
Figure 33. Purification of soluble MetRSs in <i>E. coli</i>	54
Figure 34. ESI-MS spectra of purified MetRSs.....	55
Figure 35. Cross-aminoacylation experiments.....	58

Figure 36. Met analogs..	60
Figure 37. Activation of Met and its analogs by host and 'orthogonal' MetRSs.....	61
Figure 38. Differential activation of Met analogs by host and 'orthogonal' MetRS.....	62
Figure 39. Tandem incorporation of Aha and Eth into barstar 1M.....	63
Figure 40. Barstar 1M alloproteins.....	64
Figure 41. Analytical characterization of barstar 1M congeners.....	65
Figure 42. Tandem incorporation of Aha and Eth into barstar 2M.....	69
Figure 43. Barstar 2M alloproteins.....	69
Figure 44. Analytical characterization of barstar 2M congeners.....	70
Figure 45. pTEc1.....	74
Figure 46. Initiator tRNAs.....	75
Figure 47. Elongator tRNAs from <i>S. acidocaldarius</i>	76
Figure 48. Intracellular expression of SaMetRS in <i>E. coli</i> transformed with pTEc1.....	77
Figure 49. <i>In silico</i> expression of EcMetRS and SaMetRS in <i>E. coli</i>	77
Figure 50. Distribution of codons present in SaMetRS whose tRNAs are the rarest in <i>E. coli</i>	78
Figure 51. pTEc1.1G-R/L.....	79
Figure 52. Expression of SaMetRS in <i>E. coli</i> transformed with pTEc1.1G-R/L.....	80
Figure 53. Expression of SaMetRS in <i>E. coli</i> transformed with pTEc1.1G-R/L after enrichment.....	80
Figure 54. Expression of SaMetRS in <i>E. coli</i> transformed with pTEc2 after enrichment.....	81
Figure 55. Making up the faces of Janus.....	82
Figure 56. MetRS sequence alignment.....	118

8 List of tables

Table 1. Identity elements that differentiate the <i>E. coli</i> initiator tRNA ^{Met} and elongator tRNA ^{Met}	17
Table 2. Enzymatic activity of lipase congeners.....	30
Table 3. Natural preference of Aha and Eth at the N-terminus of barstar 1M alloproteins.....	67
Table 4. Natural preference for Aha and/or Eth at the N-terminus and/or position 47 of barstar 2M. ...	72

9 Appendix

Met residues are indicated in red color, His-Tag residues in blue and mutated residues in green.

9.1 Primary amino acid sequence of TTL

```

1  MQKAVEITYN GKTLRGMMHL PDDVKGKVPM VIMFHGFTGN KVESHFIFVK 50
51 MSRALEKVGI GSVRFDFYGS GESDGDSESEM TFSSELEDAR QILKFKVKEQP 100
101 TTDPERIGLL GLSMGGAIAG IVAREYKDEI KALVLWAPAF NMPELIMNES 150
151 VKQYGAIM EQ LGFVDIGGHK LSKDFVEDIS KLNIFELSKG YDKKVLIVHG 200
201 TNDEAVEYKV SDRILKEVYG DNATRVTIEN ADHTFKSLEW EKKAIEESVE 250
251 FFKKELLKGG SHHHHHH

```

9.2 Primary sequence of barstar 1M (P28A/C41A/C83A)

```

1  MKKAVINGEQ IRSISDLHQT LKKELALAEY YGENLDALWD ALTGWVEYPL 50
51 VLEWRQFEQS KQLTENGAES VLQVFREKA EGADITIILS

```

9.3 Primary sequence of barstar 2M (P28A/C41A/E47M/C83A)

```

1  MKKAVINGEQ IRSISDLHQT LKKELALAEY YGENLDALWD ALTGWVEYPL 50
51 VLMWRQFEQS KQLTENGAES VLQVFREKA EGADITIILS

```

9.4 MetRS alignment

The MetRS alignment was performed with aid of the software Multalin.¹⁸²

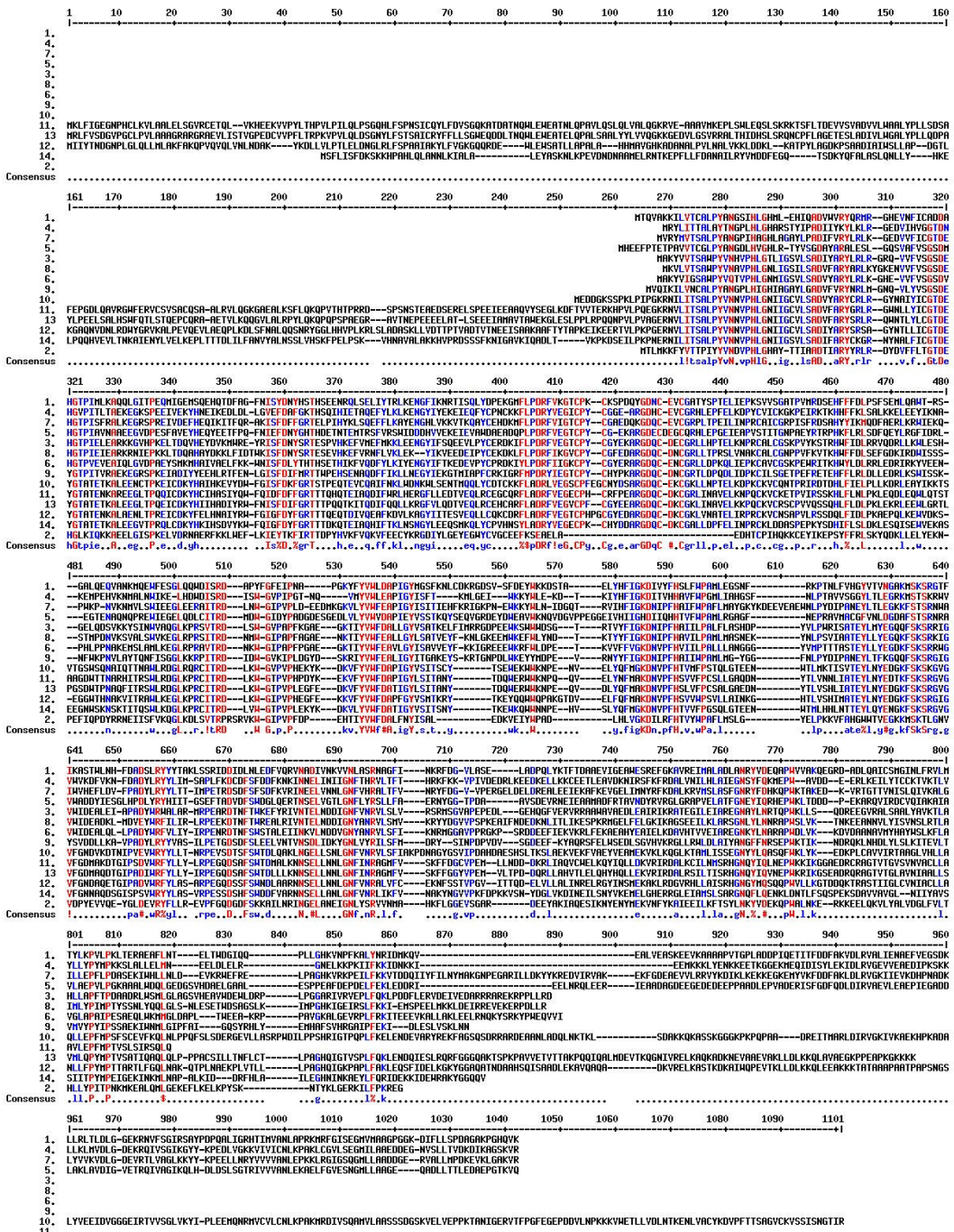


Figure 56. MetRS sequence alignment. Residues with consensus above 90% and between 50-90% are indicated in red and blue respectively. 1. *EcMetRS* WT (677aa); 2. *Aa MetRS* WT (497aa); 3. *ApMetRS* WT (572aa); 4. *MjMetRS* WT (651aa); 5. *NpMetRS* WT (698aa); 6. *PaMetRS* WT (570aa); 7. *PabMetRS* WT (722aa); 8. *SaMetRS* WT (571aa); 9. *TaMetRS* WT (547aa); 10. *AtMetRS* WT (797aa); 11. *DmMetRS* WT (1022); 12. *DmMetRS* WT (1022); 13. *HsMetRS* WT (900aa); 14. *ScMetRS* WT (751aa)

2228 MseI 2300 Tth11I
 2222 SduI 2300 DrdI
 2222 BseSI 2286 TaqI 2285 BstBI 2298 TaqI
 2221 NlaIV 2283 TspEI 2295 TspEI
 2221 AccBII 2282 ApoI 2294 ApoI
 2207 MseI
 2201 Attttttaagcagttattggtgccccttaaacgcctggttgctacgcctgataaagtgataataagcggatgaatggcagaaattcgaaagcaattcg 2300
 * * * * *
 2210 2220 2230 2240 2250 2260 2270 2280 2290 2300

>
CmR

2308 Hpy99I 2361 HpaII
 2304 BsiEI 2360 Cfr10I
 2303 HpaII 2360 BsaWI
 2303 BsiYI 2329 MseI 2356 Hpy8I 2376 HpaII
 2376 HpaII 2390 HpyCH4III
 2301 acccgtcgtcggttcaggcagggtcggttaaatagcgccttattgctattgctggtttaccggttattgactaccggaagcagtgtagcgtgtgctt 2400
 * * * * *
 2310 2320 2330 2340 2350 2360 2370 2380 2390 2400

2431 TspEI
 2429 MseI
 2428 VspI
 2427 TspEI
 2409 Bsu36I 2424 TaqI 2434 HpyCH4V 2453 HpyCH4III
 2401 ctcaaatgacctgaggtctgtttatcgaattaattgcagatataaaaaaaccaacgtaagggttggtttttcttgggatttttggcgcagagagga 2500
 * * * * *
 2410 2420 2430 2440 2450 2460 2470 2480 2490 2500

proL (tRNA(GGG)Pro EcoGene#EG30067)

2530 HpyCH4III 2553 MaeII
 2526 NlaIII 2552 BsaAI
 2526 MslI 2548 MwoI
 2523 BsiYI 2535 HhaI 2548 HhaI 2558 BsiYI 2580 HpyCH4III 2598 HpyCH4V
 2501 ttgaaacctccgacccccgacccccatgacgggtgctaccagggtgctgctacgtgcccactcgtggtgctgtaataactaccggtttccacaccgattgc 2600
 * * * * *
 2510 2520 2530 2540 2550 2560 2570 2580 2590 2600

proLp (tRNA promoter of proL operon)

proL (tRNA(GGG)Pro EcoGene#EG30067)

2631 MseI
 2630 VspI
 2629 TspEI
 2625 PsiI 2659 RsaI
 2601 aagtaagatatttcgctaaactgattataatcagtttagcagataaaacgcttctcgtacaacgctttctggtgaatggtgcccggaggcagacttga 2700
 * * * * *
 2610 2620 2630 2640 2650 2660 2670 2680 2690 2700

proLp (tRNA promoter of proL operon)

leuW (tRNA(CAA)Leu EcoGene#EG30052)

2716 SfoI
 2716 NlaIV
 2716 Nari
 2716 Kasi
 2716 HaeII
 2716 BbeI
 2716 AcyI 2726 BsiYI 2747 TspEI 2791 TaqI
 2705 MwoI 2716 AccBII 2740 Hpy8I 2790 BstBI
 2705 BstAPI 2717 HhaI 2740 AccI 2753 MwoI 2782 Hpy99I
 2701 actcgcacaccttgccgcccagacacctaactctggtgctctaccaatttcgccaactcccgcaaaaaagatggtggctacgacgggattcgacctgt 2800
 * * * * *
 2710 2720 2730 2740 2750 2760 2770 2780 2790 2800

metT (tRNA((CAU)Met EcoGene#EG30058)

leuW (tRNA(CAA)Leu EcoGene#EG30052)

2842 MaeII 2861 AccII
 2841 SnaBI 2860 NruI 2886 MwoI
 2841 BsaAI 2860 Hpy188III 2886 HhaI
 2806 MslI 2822 SduI 2838 AluI
 2822 BsiHKAI
 2801 gaccccatcattatgagtgatgctctaaccaactgagctacgtagccatcttttttgcgcatccttatcgcgcttggggcgccattatgctgtat 2900
 * * * * *
 2810 2820 2830 2840 2850 2860 2870 2880 2890 2900

metTp (tRNA promoter on pRARE)

metTp (tRNA promoter of metT-leuW-glnUW-metU-glnVX)

metT (tRNA((CAU)Met EcoGene#EG30058)


```
tyrU (tRNA(GUA)Tyr EcoGene#EG30107)
3729 Hpy188III
3728 Aval 3741 HpaII 3756 BsiYI
3723 HaeIII 3740 BsaWI 3752 NlaIV 3763 HpaII 3776 BstEII
3707 HpyCH4III 3722 CfrI 3732 NlaIV 3752 AccB1I 3769 TaqI
3701 agatttacagtctgctccctttggccgctcggaaccccaccggacttgatggtgcccactaccggaatcgaactggtgacactgattacaagtcagt 3800
* * * * *
3710 3720 3730 3740 3750 3760 3770 3780 3790 3800

tyrU (tRNA(GUA)Tyr EcoGene#EG30107)
3837 HhaI
3836 AccII
3835 HhaI
3816 MwoI 3835 Cac8I 3853 NlaIII 3865 HpyCH4V 3879 HpyCH4V
3815 AluI 3835 BssHII 3852 NspI 3863 NlaIII 3876 TspEI
3801 tgctctacctactgagcctaagtgcgcacatcaagtgcgcactctatggagacatgcgagttcatgcaactaaaaaattgcataattgtttattggtc 3900
* * * * *
3810 3820 3830 3840 3850 3860 3870 3880 3890 3900

thrUp(A52G) (tRNA promoter of thrU-tyrU-glyT-thrT o)
thrU (tRNA(UGU)Thr EcoGene#EG30102)
3940 Hpy188III
3935 RsaI
3934 NlaIV
3934 KpnI 3944 SduI
3934 AccB1I
3934 Acc65I
3931 MaeI 3944 BanII 3958 SduI
3930 StyI 3940 BspHI 3958 BanII
3930 AvrII 3941 NlaIII 3956 Cac8I
3996 HhaI
3995 SfoI
3995 NlaIV
3995 NarI
3995 KasI
3995 HaeII
3995 BbeI
3995 AcyI
3995 AccB1I
3987 MwoI 3998 Cac8I
3901 acattttatgacacagatgaagaacacagcctagtacctcatgagcccgaagtgccgagcccgatcttccccatcggtgatgctcgcgatataggcgc 4000
* * * * *
3910 3920 3930 3940 3950 3960 3970 3980 3990 4000

4020 HpaII
4019 MwoI
4019 Cfr10I
4017 HhaI
4016 SfoI
4016 NlaIV
4016 NarI 4031 HaeIII
4016 KasI 4030 CfrI
4016 HaeII 4028 NgoMIV
4016 BbeI 4028 NaeI
4016 AcyI 4028 Cfr10I
4016 AccB1I 4028 Cac8I
4008 MwoI 4018 SgrAI 4029 HpaII
4044 HpaII 4055 MboI
4068 StyI 4081 Cac8I
4001 agcaaccgcaacctgtgcccggatgcccggcaccagatgcgctccgctgagcagcctccgtcacatccaagggcgctaacgagcagatggaacatcaa 4100
* * * * *
4010 4020 4030 4040 4050 4060 4070 4080 4090 4100

4122 MwoI
4120 HhaI
4119 FspI
4118 FspAI
4110 Hpy188III 4125 TaqI
4102 Cac8I 4117 BsaBI
4140 NlaIII
4150 AluI
4162 HpyCH4V
4179 TspGWI
4187 NlaIII
4101 cgcctggtcgaggaagatgcgcacatcgacagcaagacatcctggtacagcttctcctgctgacaggaattgaagatttccgtttccatgacctcagaca 4200
* * * * *
4110 4120 4130 4140 4150 4160 4170 4180 4190 4200

4212 Cac8I
4211 AluI
4208 Cac8I
4229 AcyI
4249 Hpy188III
4273 MslI
4272 BstXI
4295 MwoI
4201 cacctggcgcaagcgtgattcagctccattatcagctcctcaggaaatggcggatggggaggcctcagaaaatggttcgtatgattgctcacc 4300
* * * * *
4210 4220 4230 4240 4250 4260 4270 4280 4290 4300

4325 NlaIII
4324 SphI
4324 NspI
4324 Cac8I
4384 TspEI
4304 HhaI
4301 ctgcccctaattcatttgacagacatgcccggaaaatagacgacattttggtgataatgtcccaaatatgtcccactctgaaattatggaggataaa 4400
* * * * *
4310 4320 4330 4340 4350 4360 4370 4380 4390 4400
```



```

                2415 AluI
                2408 HpyCH4III
                2403 HpyCH4V
2401 cgtgcatacagtcagcttggagcgaactgcctaccgggaactgagtgctcaggcgtggaatgagacaaacggcgccataacagcgggaatgacaccggtaa 2500
                2410      2420      2430      2440      2450      2460      2470      2480      2490      2500
                2474 MwoI
                2473 HaeIII
                2472 CfrI
                2470 AccII 2481 MspAI 2493 AgeI
                2494 HpaII
                2493 Cfr10I
                2493 BsaWI
                2497 Hpy8I
                2532 HhaI
                2536 BsiYI
2501 accgaaaggcaggaacaggagagcgcacgaggagcggcggggaacgcctgtatctttatagtcctgtcgggtttccaccactgatttgagcg 2600
                2510      2520      2530      2540      2550      2560      2570      2580      2590      2600
                2655 AccII
                2654 SacII
                2654 MspAI
                2608 Hpy188III
                2630 NlaIV
                2645 BceAI
                2658 HaeIII
                2676 MseI
                2697 PfoI
2601 tcagatttcgtgatgcttgcaggggcgagcctatggaaaaacggcttggcggccctctcacttccctgtaagtatcttctggcatctcca 2700
                2610      2620      2630      2640      2650      2660      2670      2680      2690      2700
                2733 Cac8I
                2749 BsiEI
                2724 MwoI
                2744 TaqI
2701 ggaatctccgccccgttcgtaagccattttccgctcggcagtcgaacgaccgagcgtagcagtcagtgagcaggaagcgaatatacctgtatca 2800
                2710      2720      2730      2740      2750      2760      2770      2780      2790      2800
                2822 HpyCH4V
                2818 HpaII
                2817 Cfr10I
                2817 BsaWI
                2817 AgeI
                2816 SgrAI
                2847 XmnI
                2844 NlaIII
                2892 Hpy8I
                2892 Bst217I
                2892 AccI
2801 catattctgctgacgcaccggtgcagcctttttctcctgccacatgaagcacttctcactgacaccctcatcagtgccaacatagtaagccagtatacact 2900
                2810      2820      2830      2840      2850      2860      2870      2880      2890      2900
                2907 HhaI
                2906 HaeII
                2906 Eco47III
                2904 MaeI
                2903 NheI
                2903 Cac8I
                2917 HpaII
                2931 BceAI
                2951 AlwNI
                2972 AluI
                2971 PvuII
                2971 MspAI
                2989 MwoI
                2996 SduI
                2996 BsiHKAI
2901 ccgctagcgtgatgtccggcgggtgcttttgccgttacgcaccaccctcagtagctgaacaggaggacagctgatagaacagaaagccactggagca 3000
                2910      2920      2930      2940      2950      2960      2970      2980      2990      3000
                3060 HhaI
                3053 MwoI
                3049 Hpy99I
                3086 MboI
                3080 TspGWI
3001 cctcaaaaacaccatcatacactaaatcagtaagttggcagcatcaccgcagcactttgcccgaataaatacctgtgacggaagatcacttcgcagaa 3100
                3010      3020      3030      3040      3050      3060      3070      3080      3090      3100
                3144 PflMI
                3144 BsiYI
                3129 HpaII
                3142 HaeIII
                3177 MaeII
                3170 MboI
                3185 NlaIV
                3165 MaeII
                3176 BsaAI
                3197 MslI
3101 taaataaatcctggtgctccctgttgataccgggaagccctggccaacttttggcgaataatgagacgttgatcggcagcgttaagaggttccaactttcacc 3200
                3110      3120      3130      3140      3150      3160      3170      3180      3190      3200
                CmR promoter

```


5568 HhaI
5567 AccII
5566 HhaI
5547 MwoI 5566 Cac8I 5584 NlaIII 5596 HpyCH4V
5546 AluI 5566 BssHII 5583 NspI 5594 NlaIII
5507 BstEII
5501 cgaactggcgactactgattacaagtcagttgctctacctaactgagctaaagtcggatcaagttagcgcactctatggagacatgagcagtccatgcaa 5600
* * * * *
5510 5520 5530 5540 5550 5560 5570 5580 5590 5600

thrUp(A52G) (tRNA promoter of thrU-tyrU-glyT-thrT o

thrU (tRNA (UGU) Thr EcoGene#EG30102)

5671 Hpy188III
5666 RsaI
5665 NlaIV
5665 KpnI 5675 SduI
5665 AccBII
5665 Acc65I
5615 TspEI 5662 MaeI 5675 BanII 5695 MboI
5610 HpyCH4V 5661 StyI 5671 BspHI 5689 SduI
5607 TspEI 5661 AvrII 5672 NlaIII 5689 BanII
5601 ctaaaaaattgcataattgtttattggtcaccattttatgcgacacgatgaagaaacagccctagttacctcatgagcccgaaagtggcagccgatctt 5700
* * * * *
5610 5620 5630 5640 5650 5660 5670 5680 5690 5700

thrUp(A52G) (tRNA promoter of thrU-tyrU-glyT-thrT o

5751 HpaII
5750 MwoI
5750 Cfr10I
5727 HhaI 5748 HhaI
5726 SfoI 5747 SfoI
5726 NlaIV 5747 NlaIV
5726 NarI 5747 NarI 5762 HaeIII
5726 KasI 5747 KasI 5761 CfrI
5726 HaeII 5747 HaeII 5759 NgoMIV 5788 TspGWI
5726 BbeI 5747 BbeI 5759 NaeI 5785 XhoII
5726 AcyI 5747 AcyI 5759 Cfr10I 5785 NlaIV
5726 AccBII 5739 MwoI 5749 SgrAI 5760 HpaII 5785 BamHI
5718 MwoI 5729 Cac8I 5747 AccBII 5759 Cac8I 5775 HpaII 5786 MboI 5799 StyI
5701 cccatcggtgatgtcggcgatataggcgcagcaaccgcaactgtggcggcggtgatgccccacgatgctcggcgttagagatcccgccacatacc 5800
* * * * *
5710 5720 5730 5740 5750 5760 5770 5780 5790 5800

5853 MwoI
5851 HhaI
5850 FspI
5812 Cac8I 5841 Hpy188III 5856 TaqI 5881 AluI 5893 HpyCH4V
5807 MwoI 5833 Cac8I 5848 BsaBI 5871 NlaIII 5888 Hpy99I
5807 BlpI
5801 aaggcgctaagcggcagatggaacatcaacgctcggtcaggaagatgcatgagacagacacacatcattgagccttgcctgctgctgcaggaa 5900
* * * * *
5810 5820 5830 5840 5850 5860 5870 5880 5890 5900

5943 Cac8I
5942 AluI
5918 NlaIII
5939 Cac8I
5910 TspGWI
5960 AcyI
5980 Hpy188III
5901 ttgaagatttccggttccatgacctgacacacactggcgaagctggcgtattcagtcaggcgtccctattcagtcctcaggaatggcggtatggga 6000
* * * * *
5910 5920 5930 5940 5950 5960 5970 5980 5990 6000

6056 NlaIII
6055 SphI
6055 NspI
6055 Cac8I
6008 XmnI
6004 MslI
6003 BstXI
6026 MwoI
6035 HhaI
6001 gtccatagaaaatggttcgtaggtatgctcaccttgccgctaatacttggacagagcatgcagggaataatagcagcatttttggtgataatgtcccacaa 6100
* * * * *
6010 6020 6030 6040 6050 6060 6070 6080 6090 6100

6168 HpyCH4V
6167 PstI
6167 BfmI
6166 SbfI
6162 HhaI
6160 MwoI
6160 HhaI
6160 Cac8I
6160 BssHII
6159 AscI
6115 TspEI 6150 TspEI 6161 AccII 6175 BstBI 6186 HaeIII
6101 atgtcccaactctgaaatttgaggatataaagaaggcgtaactgattgaattgtaagtcggcgccctgaggattcgaacctggcggccacgacttaga 6200
* * * * *
6110 6120 6130 6140 6150 6160 6170 6180 6190 6200

argU (tRNA (UCU) Arg EcoGene#EG30014)



4347 TspEI
4345 MseI
4344 VspI
4343 TspEI
4306 HpyCH4III 4325 Bsu36I 4340 TaqI 4350 HpyCH4V 4369 HpyCH4III 4389 SmlI
4388 Hpy188III
4301 gtgtgacocgtgtgctttctcaaatgcctgaggtotgtttatcgaattaattgcagataaaaaaaccgtaagggttggtttttcttgagattttt 4400
* * * * *
4310 4320 4330 4340 4350 4360 4370 4380 4390 4400

<
G Exchanged for A

EcoGene#EG30067)

proL (tRNA (GGG) Pro

4446 HpyCH4III 4469 MaeII
4442 NlaIII 4468 BsaAI
4442 MslI 4464 MwoI
4439 BsiYI 4451 HhaI 4464 HhaI 4474 BsiYI 4496 HpyCH4III
4401 ggtcgccacgagagatttgaacctccgaccccccaccccatgacggtgcgctaccaggctgctacgtgcccactcgtggctgctaatactaccgt 4500
* * * * *
4410 4420 4430 4440 4450 4460 4470 4480 4490 4500

proLp (tRNA promoter of proL operon)

proL (tRNA (GGG) Pro EcoGene#EG30067)

4547 MseI
4546 VspI
4545 TspEI
4514 HpyCH4V 4541 PsiI 4575 RsaI
4501 ttccacaccgattgcaagtaagattttcgctaaactgatttataaattaatcagttagcgataaaacgcttctcgtacaacgctttctggatgggtgc 4600
* * * * *
4510 4520 4530 4540 4550 4560 4570 4580 4590 4600

proLp (tRNA promoter of proL operon)

LeuW (tRNA (CAA) Leu

EcoGene#EG30052)

4632 SfoI
4632 NlaIV
4632 NarI
4632 KasI
4632 HaeII
4632 BbeI
4632 AcyI 4642 BsiYI
4621 MwoI 4632 AccB1I
4621 BstAPI 4633 HhaI
4663 TspEI
4663 Hpy8I
4656 AccI 4669 MwoI
4698 AccII
4697 SacII
4697 MspAI
4694 BsiYI
4690 NlaIV
4690 AccB1I
4601 gggagcgagacttgaaactcgacaccttgcggcgcagaaactaactctgtgctctaccacttttccactcccgcaaaaaaatggatggcgcgagc 4700
* * * * *
4610 4620 4630 4640 4650 4660 4670 4680 4690 4700

LeuW (tRNA (CAA) Leu EcoGene#EG30052)

Sa-tRNAMetI

4759 BceAI
4722 HpaII 4738 HhaI 4756 MwoI 4778 AccII
4721 BsaWI 4737 HaeII 4755 AluI 4777 NruI
4714 HpaII 4735 HpaII 4751 BlpI 4777 Hpy188III
4701 ggggatttgaaaccggacaaccggattatgagtccggcgtctaaccaggtgagctacggcggcatcttttttcgcgataccttatcggcgtgtgcg 4800
* * * * *
4710 4720 4730 4740 4750 4760 4770 4780 4790 4800

metTp (tRNA promoter on pRARE)

metTp (tRNA promoter of metT-leuW-glnUW-

metU-glnVX

Sa-tRNAMetI

4831 Hpy8I
4803 MwoI 4831 HincII 4858 TaqI
4803 HhaI 4825 HpyCH4V 4852 TspEI 4867 HpyCH4III 4896 NlaIII
4801 gggcgattatgcgtatagacgttcagcgtcaacctcttttcaaggaaatgtcgtcaaaagtactgtttggttaggtgcaaacagcgaaccatga 4900
* * * * *
4810 4820 4830 4840 4850 4860 4870 4880 4890 4900

metTp (tRNA promoter on pRARE)

metTp (tRNA promoter of metT-leuW-glnUW-metU-glnVX

10 References

1. Gibson, D. et al. Complete chemical synthesis, assembly, and cloning of a *Mycoplasma genitalium* genome. *Science* **319**, 1215-20 (2008).
2. Knight, T. Idempotent Vector Design for Standard Assembly of Biobricks. in *IT Synthetic Biology Working Group* (2003).
3. Basu, S., Gerchman, Y., Collins, C., Arnold, F. & Weiss, R. A synthetic multicellular system for programmed pattern formation. *Nature* **434**, 1130-4 (2005).
4. Lu, T. & Collins, J. Dispersing biofilms with engineered enzymatic bacteriophage. *Proc Natl Acad Sci U S A* **104**, 11197-202 (2007).
5. Ro, D. et al. Production of the antimalarial drug precursor artemisinic acid in engineered yeast. *Nature* **440**, 940-3 (2006).
6. Anderson, J., Clarke, E., Arkin, A. & Voigt, C. Environmentally controlled invasion of cancer cells by engineered bacteria. *J Mol Biol* **355**, 619-27 (2006).
7. Martin, C., Nielsen, D., Solomon, K. & Prather, K. Synthetic metabolism: engineering biology at the protein and pathway scales. *Chem Biol* **16**, 277-86 (2009).
8. Voloshchuk, N. & Montclare, J. Incorporation of unnatural amino acids for synthetic biology. *Mol Biosyst* **6**, 65-80 (2010).
9. Dong, H., Nilsson, L. & Kurland, C. Co-variation of tRNA abundance and codon usage in *Escherichia coli* at different growth rates. *J Mol Biol* **260**, 649-63 (1996).
10. Giegé, R., Sissler, M. & Florentz, C. Universal rules and idiosyncratic features in tRNA identity. *Nucleic Acids Res* **26**, 5017-35 (1998).
11. Walsh, C., Garneau-Tsodikova, S. & Gatto, G.J. Protein posttranslational modifications: the chemistry of proteome diversifications. *Angew Chem Int Ed Engl* **44**, 7342-72 (2005).
12. Budisa, N. *Engineering the Genetic Code*, 312 (Wiley-VCH Verlag GmbH & Co. KGaA, 2005).

13. Dougherty, D. Unnatural amino acids as probes of protein structure and function. *Curr Opin Chem Biol* **4**, 645-52 (2000).
14. Hohsaka, T. & Sisido, M. Incorporation of non-natural amino acids into proteins. *Curr Opin Chem Biol* **6**, 809-15 (2002).
15. Link, A., Mock, M. & Tirrell, D. Non-canonical amino acids in protein engineering. *Curr Opin Biotechnol* **14**, 603-9 (2003).
16. Budisa, N. Prolegomena to future experimental efforts on genetic code engineering by expanding its amino acid repertoire. *Angewandte Chemie International Edition in English* **43**, 6426-6463 (2004).
17. Hendrickson, T., de Crécy-Lagard, V. & Schimmel, P. Incorporation of nonnatural amino acids into proteins. *Annu Rev Biochem* **73**, 147-76 (2004).
18. Wang, L. & Schultz, P. Expanding the genetic code. *Angew Chem Int Ed Engl* **44**, 34-66 (2004).
19. Budisa, N. et al. Toward the experimental codon reassignment in vivo: protein building with an expanded amino acid repertoire. *FASEB J* **13**, 41-51 (1999).
20. Wang, L., Brock, A., Herberich, B. & Schultz, P. Expanding the genetic code of *Escherichia coli*. *Science* **292**, 498-500 (2001).
21. Young, T. & Schultz, P. Beyond the canonical 20 amino acids: expanding the genetic lexicon. *J Biol Chem* **285**, 11039-44 (2010).
22. Liu, C. & Schultz, P. Adding New Chemistries to the Genetic Code. *Annu Rev Biochem* (2010).
23. Neumann, H., Peak-Chew, S. & Chin, J. Genetically encoding N(epsilon)-acetyllysine in recombinant proteins. *Nat Chem Biol* **4**, 232-4 (2008).
24. Yanagisawa, T. et al. Multistep engineering of pyrrolysyl-tRNA synthetase to genetically encode N(epsilon)-(o-azidobenzyloxycarbonyl) lysine for site-specific protein modification. *Chem Biol* **15**, 1187-97 (2008).
25. Nguyen, D. et al. Genetic encoding and labeling of aliphatic azides and alkynes in recombinant proteins via a pyrrolysyl-tRNA Synthetase/tRNA(CUA) pair and click chemistry. *J Am Chem Soc* **131**, 8720-1 (2009).

26. Rodriguez, E., Lester, H. & Dougherty, D. In vivo incorporation of multiple unnatural amino acids through nonsense and frameshift suppression. *Proc Natl Acad Sci U S A* **103**, 8650-5 (2006).
27. LEVINE, M. & TARVER, H. Studies on ethionine. III. Incorporation of ethionine into rat proteins. *J Biol Chem* **192**, 835-50 (1951).
28. COWIE, D. & COHEN, G. Biosynthesis by *Escherichia coli* of active altered proteins containing selenium instead of sulfur. *Biochim Biophys Acta* **26**, 252-61 (1957).
29. van Hest, J. & Tirrell, D. Efficient introduction of alkene functionality into proteins in vivo. *FEBS Lett* **428**, 68-70 (1998).
30. Budisa, N. et al. High-level biosynthetic substitution of methionine in proteins by its analogs 2-aminohexanoic acid, selenomethionine, telluromethionine and ethionine in *Escherichia coli*. *Eur J Biochem* **230**, 788-96 (1995).
31. Hendrickson, W., Horton, J. & LeMaster, D. Selenomethionyl proteins produced for analysis by multiwavelength anomalous diffraction (MAD): a vehicle for direct determination of three-dimensional structure. *EMBO J* **9**, 1665-72 (1990).
32. Budisa, N. et al. High-level biosynthetic substitution of methionine in proteins by its analogs 2-aminohexanoic acid, selenomethionine, telluromethionine and ethionine in *Escherichia coli*. *European Journal of Biochemistry* **230**, 788-96 (1995).
33. Garner, D. et al. Reduction potential tuning of the blue copper center in *Pseudomonas aeruginosa* azurin by the axial methionine as probed by unnatural amino acids. *J Am Chem Soc* **128**, 15608-17 (2006).
34. Boles, J. et al. Bio-incorporation of telluromethionine into buried residues of dihydrofolate reductase. *Nat Struct Biol* **1**, 283-4 (1994).
35. van Hest, J., Kiick, K. & Tirrell, D. Efficient incorporation of unsaturated methionine analogues into proteins in vivo. *Journal of the American Chemical Society* **122**, 1282-8 (2000).

36. Kiick, K., Saxon, E., Tirrell, D. & Bertozzi, C. Incorporation of azides into recombinant proteins for chemoselective modification by the Staudinger ligation. *Proc Natl Acad Sci U S A* **99**, 19-24 (2002).
37. Merkel, L., Cheburkin, Y., Wiltschi, B. & Budisa, N. In vivo chemoenzymatic control of N-terminal processing in recombinant human epidermal growth factor. *Chembiochem* **8**, 2227-32 (2007).
38. Tornøe, C., Christensen, C. & Meldal, M. Peptidotriazoles on solid phase: [1,2,3]-triazoles by regiospecific copper(i)-catalyzed 1,3-dipolar cycloadditions of terminal alkynes to azides. *J Org Chem* **67**, 3057-64 (2002).
39. Kolb, H., Finn, M. & Sharpless, K. Click Chemistry: Diverse Chemical Function from a Few Good Reactions. *Angew Chem Int Ed Engl* **40**, 2004-2021 (2001).
40. Jewett, J.C. & Bertozzi, C.R. Cu-free click cycloaddition reactions in chemical biology. *Chemical Society Reviews* **39**, 1272-1279 (2010).
41. Merkel, L., Beckmann, H.S.G., Wittmann, V. & Budisa, N. Efficient N-terminal glycoconjugation of proteins by the N-end rule. *Chembiochem* **9**, 1220-1224 (2008).
42. Link, A. & Tirrell, D. Cell surface labeling of Escherichia coli via copper(I)-catalyzed [3+2] cycloaddition. *J Am Chem Soc* **125**, 11164-5 (2003).
43. Beatty, K. et al. Fluorescence visualization of newly synthesized proteins in mammalian cells. *Angew Chem Int Ed Engl* **45**, 7364-7 (2006).
44. Dieterich, D., Link, A., Graumann, J., Tirrell, D. & Schuman, E. Selective identification of newly synthesized proteins in mammalian cells using bioorthogonal noncanonical amino acid tagging (BONCAT). *Proc Natl Acad Sci U S A* **103**, 9482-7 (2006).
45. Strable, E. et al. Unnatural Amino Acid Incorporation into Virus-Like Particles. *Bioconjug Chem* (2008).
46. Moroder, L. & Budisa, N. Synthetic Biology of Protein Folding. *Chemphyschem* (2010).
47. Wolschner, C. et al. Design of anti- and pro-aggregation variants to assess the effects of methionine oxidation in human prion protein. *Proc Natl Acad Sci U S A* **106**, 7756-61 (2009).

48. Budisa, N. et al. Atomic mutations in annexin V--thermodynamic studies of isomorphous protein variants. *Eur J Biochem* **253**, 1-9 (1998).
49. Yuan, T. & Vogel, H. Substitution of the methionine residues of calmodulin with the unnatural amino acid analogs ethionine and norleucine: biochemical and spectroscopic studies. *Protein Sci* **8**, 113-21 (1999).
50. Anfinsen, C. & Corley, L. An active variant of staphylococcal nuclease containing norleucine in place of methionine. *J Biol Chem* **244**, 5149-52 (1969).
51. Duewel, H., Daub, E., Robinson, V. & Honek, J. Incorporation of trifluoromethionine into a phage lysozyme: implications and a new marker for use in protein 19F NMR. *Biochemistry* **36**, 3404-16 (1997).
52. Holzberger, B., Rubini, M., Möller, H. & Marx, A. A highly active DNA polymerase with a fluorine core. *Angew Chem Int Ed Engl* **49**, 1324-7 (2010).
53. Budisa, N. et al. Efforts towards the design of 'teflon' proteins: in vivo translation with trifluorinated leucine and methionine analogues. *Chem Biodivers* **1**, 1465-75 (2004).
54. Cirino, P., Tang, Y., Takahashi, K., Tirrell, D. & Arnold, F. Global incorporation of norleucine in place of methionine in cytochrome P450 BM-3 heme domain increases peroxygenase activity. *Biotechnol Bioeng* **83**, 729-34 (2003).
55. Gilles, A. et al. Conservative replacement of methionine by norleucine in *Escherichia coli* adenylate kinase. *J Biol Chem* **263**, 8204-9 (1988).
56. Ring, M. & Huber, R. The properties of beta-galactosidases (*Escherichia coli*) with halogenated tyrosines. *Biochem Cell Biol* **71**, 127-32 (1993).
57. Brooks, B., Phillips, R. & Benisek, W. High-efficiency incorporation in vivo of tyrosine analogues with altered hydroxyl acidity in place of the catalytic tyrosine-14 of Delta 5-3-ketosteroid isomerase of *Comamonas* (*Pseudomonas*) *testosteroni*: effects of the modifications on isomerase kinetics. *Biochemistry* **37**, 9738-42 (1998).
58. Budisa, N., Wenger, W. & Wiltschi, B. Residue-specific global fluorination of *Candida antarctica* lipase B in *Pichia pastoris*. *Mol Biosyst* (2010).

59. YOSHIDA, A. & YAMASAKI, M. Studies on the mechanism of protein synthesis; incorporation of ethionine into alpha-amylase of *Bacillus subtilis*. *Biochim Biophys Acta* **34**, 158-65 (1959).
60. Cirino, P.C., Tang, Y., Takahashi, K., Tirrell, D.A. & Arnold, F.H. Global incorporation of norleucine in place of methionine in cytochrome P450 BM-3 heme domain increases peroxygenase activity. *Biotechnology and Bioengineering* **83**, 729-734 (2003).
61. Walasek, P. & Honek, J. Nonnatural amino acid incorporation into the methionine 214 position of the metzincin *Pseudomonas aeruginosa* alkaline protease. *BMC Biochem* **6**, 21 (2005).
62. Schoffelen, S., Lambermon, M., van Eldijk, M. & van Hest, J. Site-specific modification of *Candida antarctica* lipase B via residue-specific incorporation of a non-canonical amino acid. *Bioconjug Chem* **19**, 1127-31 (2008).
63. Budisa, N. Prolegomena to future experimental efforts on genetic code engineering by expanding its amino acid repertoire. *Angew Chem Int Ed Engl* **43**, 6426-63 (2004).
64. Gellman, S. On the role of methionine residues in the sequence-independent recognition of nonpolar protein surfaces. *Biochemistry* **30**, 6633-6 (1991).
65. Shacter, E. Quantification and significance of protein oxidation in biological samples. *Drug Metab Rev* **32**, 307-26 (2000).
66. Berlett, B. & Stadtman, E. Protein oxidation in aging, disease, and oxidative stress. *J Biol Chem* **272**, 20313-6 (1997).
67. Vogt, W. Oxidation of methionyl residues in proteins: tools, targets, and reversal. *Free Radic Biol Med* **18**, 93-105 (1995).
68. Mechulam, Y. et al. Crystal structure of *Escherichia coli* methionyl-tRNA synthetase highlights species-specific features. *J Mol Biol* **294**, 1287-97 (1999).
69. Serre, L. et al. How methionyl-tRNA synthetase creates its amino acid recognition pocket upon L-methionine binding. *J Mol Biol* **306**, 863-76 (2001).

70. Brunie, S., Zelwer, C. & Risler, J. Crystallographic study at 2.5 Å resolution of the interaction of methionyl-tRNA synthetase from *Escherichia coli* with ATP. *J Mol Biol* **216**, 411-24 (1990).
71. Cory, S., Marcker, K., Dube, S. & Clark, B. Primary structure of a methionine transfer RNA from *Escherichia coli*. *Nature* **220**, 1039-40 (1968).
72. Dube, S., Marcker, K., Clark, B. & Cory, S. Nucleotide sequence of N-formyl-methionyl-transfer RNA. *Nature* **218**, 232-3 (1968).
73. Schmitt, E. et al. Molecular recognition governing the initiation of translation in *Escherichia coli*. A review. *Biochimie* **78**, 543-54 (1996).
74. Laursen, B., Sørensen, H., Mortensen, K. & Sperling-Petersen, H. Initiation of protein synthesis in bacteria. *Microbiol Mol Biol Rev* **69**, 101-23 (2005).
75. Old, I., Phillips, S., Stockley, P. & Saint Girons, I. Regulation of methionine biosynthesis in the Enterobacteriaceae. *Prog Biophys Mol Biol* **56**, 145-85 (1991).
76. Waller, J. The NH₂-terminal residues of the proteins from cell-free extracts of *E. coli*. *J Mol Biol* **7**, 483-96 (1963).
77. Kennell, D. & Riezman, H. Transcription and translation initiation frequencies of the *Escherichia coli* lac operon. *J Mol Biol* **114**, 1-21 (1977).
78. Tang, W. & Zhao, H. Industrial biotechnology: tools and applications. *Biotechnol J* **4**, 1725-39 (2009).
79. Benkovic, S. & Hammes-Schiffer, S. A perspective on enzyme catalysis. *Science* **301**, 1196-202 (2003).
80. Farinas, E., Bulter, T. & Arnold, F. Directed enzyme evolution. *Curr Opin Biotechnol* **12**, 545-51 (2001).
81. Arnold, F. Combinatorial and computational challenges for biocatalyst design. *Nature* **409**, 253-7 (2001).
82. Burton, S., Cowan, D. & Woodley, J. The search for the ideal biocatalyst. *Nat Biotechnol* **20**, 37-45 (2002).
83. Davis, B. Chemical modification of biocatalysts. *Curr Opin Biotechnol* **14**, 379-86 (2003).
84. Ollis, D. et al. The alpha/beta hydrolase fold. *Protein Eng* **5**, 197-211 (1992).

85. Nardini, M. & Dijkstra, B. Alpha/beta hydrolase fold enzymes: the family keeps growing. *Curr Opin Struct Biol* **9**, 732-7 (1999).
86. SARDA, L. & DESNUELLE, P. [Actions of pancreatic lipase on esters in emulsions.]. *Biochim Biophys Acta* **30**, 513-21 (1958).
87. Rathi, P., Bradoo, S., SAXena, R. & Gupta, R. A hyper-thermostable, alkaline lipase from *Pseudomonas* sp. with the property of thermal activation *Biotechnology Letters* **22**, 495-498 (2000).
88. Jaeger, K., Ransac, S., Koch, H., Ferrato, F. & Dijkstra, B. Topological characterization and modeling of the 3D structure of lipase from *Pseudomonas aeruginosa*. *FEBS Lett* **332**, 143-9 (1993).
89. Jaeger, K. et al. Bacterial lipases. *FEMS Microbiol Rev* **15**, 29-63 (1994).
90. Noble, M., Cleasby, A., Johnson, L., Egmond, M. & Frenken, L. The crystal structure of triacylglycerol lipase from *Pseudomonas glumae* reveals a partially redundant catalytic aspartate. *FEBS Lett* **331**, 123-8 (1993).
91. Uppenberg, J., Hansen, M., Patkar, S. & Jones, T. The sequence, crystal structure determination and refinement of two crystal forms of lipase B from *Candida antarctica*. *Structure* **2**, 293-308 (1994).
92. Verger, R. Interfacial enzyme kinetics of lipolysis. *Annu Rev Biophys Bioeng* **5**, 77-117 (1976).
93. Verger, R. & De Haas, G. Enzyme reactions in a membrane model. 1. A new technique to study enzyme reactions in monolayers. *Chem Phys Lipids* **10**, 127-36 (1973).
94. Royter, M. Technical University Hamburg-Harburg (2006).
95. Reis, P., Holmberg, K., Watzke, H., Leser, M. & Miller, R. Lipases at interfaces: a review. *Adv Colloid Interface Sci* **147-148**, 237-50 (2009).
96. Zaks, A. & Klibanov, A. Enzymatic catalysis in organic media at 100 degrees C. *Science* **224**, 1249-51 (1984).
97. Reetz, M. Lipases as practical biocatalysts. *Curr Opin Chem Biol* **6**, 145-50 (2002).
98. Jaeger, K. & Eggert, T. Lipases for biotechnology. *Curr Opin Biotechnol* **13**, 390-7 (2002).

99. Houde, A., Kademi, A. & Leblanc, D. Lipases and their industrial applications: an overview. *Appl Biochem Biotechnol* **118**, 155-70 (2004).
100. Royter, M. et al. Thermostable lipases from the extreme thermophilic anaerobic bacteria *Thermoanaerobacter thermohydrosulfuricus* SOL1 and *Caldanaerobacter subterraneus* subsp. *tengcongensis*. *Extremophiles* **13**, 769-83 (2009).
101. Winkler, U. & Stuckmann, M. Glycogen, hyaluronate, and some other polysaccharides greatly enhance the formation of exolipase by *Serratia marcescens*. *J Bacteriol* **138**, 663-70 (1979).
102. Verger, R. 'Interfacial activation' of lipases: facts and artifacts. *Trends in Biotechnology* **15**, 32-38 (1997).
103. Brzozowski, A. et al. A model for interfacial activation in lipases from the structure of a fungal lipase-inhibitor complex. *Nature* **351**, 491-4 (1991).
104. Blow, D. Enzymology. Lipases reach the surface. *Nature* **351**, 444-5 (1991).
105. van Tilbeurgh, H. et al. Interfacial activation of the lipase-procolipase complex by mixed micelles revealed by X-ray crystallography. *Nature* **362**, 814-20 (1993).
106. Turner, N., Needs, E., Khan, J. & Vulfson, E. Analysis of conformational states of *Candida rugosa* lipase in solution: implications for mechanism of interfacial activation and separation of open and closed forms. *Biotechnol Bioeng* **72**, 108-18 (2001).
107. Agarwal, P., Billeter, S., Rajagopalan, P., Benkovic, S. & Hammes-Schiffer, S. Network of coupled promoting motions in enzyme catalysis. *Proc Natl Acad Sci U S A* **99**, 2794-9 (2002).
108. Svendsen, A. Lipase protein engineering. *Biochim Biophys Acta* **1543**, 223-238 (2000).
109. Yang, J., Koga, Y., Nakano, H. & Yamane, T. Modifying the chain-length selectivity of the lipase from *Burkholderia cepacia* KWI-56 through in vitro combinatorial mutagenesis in the substrate-binding site. *Protein Eng* **15**, 147-52 (2002).

110. Colton, I., Ahmed, S. & Kazlaukskas, R. Isopropanol Treatment Increases Enantioselectivity of *Candida rugosa* Lipase toward Carboxylic Acid Esters. *J. Org. Chem* **60**, 212-217 (1995).
111. Kitagawa, M. & Tokiwa, Y. Synthesis of polymerizable sugar ester possessing long spacer catalyzed by lipase from *Alcaligenes* sp. and its chemical polymerization. *Biotechnology Letters* **20**, 627–630 (1998).
112. Fritz. Enhancement of Selectivity and Reactivity of Lipases by Additives. *Tetrahedron* **56**, 2905-2919 (2000).
113. Okamoto, T., Yasuhito, E. & Ueji, S. Metal ions dramatically enhance the enantioselectivity for lipase-catalysed reactions in organic solvents. *Org Biomol Chem* **4**, 1147-53 (2006).
114. Finkelstein, A., Strawich, E. & Sonnino, S. Characterization and partial purification of a lipase from *Pseudomonas aeruginosa*. *Biochim Biophys Acta* **206**, 380-91 (1970).
115. Pandey, A. et al. The realm of microbial lipases in biotechnology. *Biotechnol Appl Biochem* **29 (Pt 2)**, 119-31 (1999).
116. Mozaffar, Z., Weete, J.D. & Dute, R. Influence of surfactants on an extracellular lipase from *Pythium ultimum*. *Journal of the American Oil Chemists' Society* **71**, 75-79 (1994).
117. Freeman, K.S., Tang, T.T., Shah, R.D.E., Kiserow, D.J. & McGown, L.B. Activity and Stability of Lipase in AOT Reversed Micelles with Bile Salt Cosurfactant. *The Journal of Physical Chemistry* **104**, 9312–9316 (2000).
118. Zhang, J., Lin, S. & Zeng, R. Cloning, expression, and characterization of a cold-adapted lipase gene from an antarctic deep-sea psychrotrophic bacterium, *Psychrobacter* sp 7195. *J Microbiol Biotechnol* **17**, 604-10 (2007).
119. Nam, K., Kim, S., Priyadarshi, A., Kim, H. & Hwang, K. The crystal structure of an HSL-homolog EstE5 complex with PMSF reveals a unique configuration that inhibits the nucleophile Ser144 in catalytic triads. *Biochem Biophys Res Commun* **389**, 247-50 (2009).
120. Kwon, I., Kirshenbaum, K. & Tirrell, D. Breaking the degeneracy of the genetic code. *J Am Chem Soc* **125**, 7512-3 (2003).

121. Schimmel, P. & Söll, D. When protein engineering confronts the tRNA world. *Proc Natl Acad Sci U S A* **94**, 10007-9 (1997).
122. Kwok, Y. & Wong, J. Evolutionary relationship between *Halobacterium cutirubrum* and eukaryotes determined by use of aminoacyl-tRNA synthetases as phylogenetic probes. *Can J Biochem* **58**, 213-8 (1980).
123. Petrissant, G., Boisnard, M. & Puissant, C. [Purification of a methionine tRNA from rabbit liver]. *Biochim Biophys Acta* **213**, 223-5 (1970).
124. RajBhandary, U. & Ghosh, H. Studies on polynucleotides. XCI. Yeast methionine transfer ribonucleic acid: purification, properties, and terminal nucleotide sequences. *J Biol Chem* **244**, 1104-13 (1969).
125. Gillemaut, P. & Weil, J. Aminoacylation of *Phaseolus vulgaris* cytoplasmic, chloroplastic and mitochondrial tRNAs^{Met} and of *Escherichia coli* tRNAs^{Met} by homologous and heterologous enzymes. *Biochim Biophys Acta* **407**, 240-8 (1975).
126. Blanquet, S., Petrissant, G. & Waller, J. The mechanism of action of methionyl-tRNA synthetase. 2. Interaction of the enzyme with specific and unspecific tRNAs. *Eur J Biochem* **36**, 227-33 (1973).
127. Schneller, J., Schneider, C. & Stahl, A. Distinct nuclear genes for yeast mitochondrial and cytoplasmic methionyl-tRNA synthetases. *Biochem Biophys Res Commun* **85**, 1392-9 (1978).
128. Carias, J., Mouricout, M. & Julien, R. Chloroplastic methionyl-tRNA synthetase from wheat. *Biochem Biophys Res Commun* **98**, 735-42 (1981).
129. Schwob, E., Sanni, A., Fasiolo, F. & Martin, R. Purification of the yeast mitochondrial methionyl-tRNA synthetase. Common and distinctive features of the cytoplasmic and mitochondrial isoenzymes. *Eur J Biochem* **178**, 235-42 (1988).
130. Mirande, M., Cirakoğlu, B. & Waller, J. Seven mammalian aminoacyl-tRNA synthetases associated within the same complex are functionally independent. *Eur J Biochem* **131**, 163-70 (1983).

131. Meinnel, T., Mechulam, Y., Fayat, G. & Blanquet, S. Involvement of the size and sequence of the anticodon loop in tRNA recognition by mammalian and *E. coli* methionyl-tRNA synthetases. *Nucleic Acids Res* **20**, 4741-6 (1992).
132. Wang, L. & Schultz, P. Expanding the genetic code. *Chem Commun (Camb)*, 1-11 (2002).
133. Crepin, T., Schmitt, E., Blanquet, S. & Mechulam, Y. Structure and function of the C-terminal domain of methionyl-tRNA synthetase. *Biochemistry* **41**, 13003-11 (2002).
134. Link, A. et al. Discovery of aminoacyl-tRNA synthetase activity through cell-surface display of noncanonical amino acids. *Proc Natl Acad Sci U S A* **103**, 10180-5 (2006).
135. Tanrikulu, I., Schmitt, E., Mechulam, Y., Goddard, W.r. & Tirrell, D. Discovery of *Escherichia coli* methionyl-tRNA synthetase mutants for efficient labeling of proteins with azidonorleucine in vivo. *Proc Natl Acad Sci U S A* **106**, 15285-90 (2009).
136. Schmitt, E. et al. Switching from an induced-fit to a lock-and-key mechanism in an aminoacyl-tRNA synthetase with modified specificity. *J Mol Biol* **394**, 843-51 (2009).
137. Kiick, K., CM, J., Hest, v. & Tirrell, D. Expanding the Scope of Protein Biosynthesis by Altering the Methionyl-tRNA Synthetase Activity of a Bacterial Expression Host. *Angew Chem Int Ed Engl* **39**, 2148-2152 (2000).
138. Hartman, M., Josephson, K. & Szostak, J. Enzymatic aminoacylation of tRNA with unnatural amino acids. *Proc Natl Acad Sci U S A* **103**, 4356-61 (2006).
139. Hartman, M., Josephson, K., Lin, C. & Szostak, J. An expanded set of amino acid analogs for the ribosomal translation of unnatural peptides. *PLoS ONE* **2**, e972 (2007).
140. Yoo, T. & Tirrell, D. High-throughput screening for methionyl-tRNA synthetases that enable residue-specific incorporation of noncanonical amino acids into recombinant proteins in bacterial cells. *Angew Chem Int Ed Engl* **46**, 5340-3 (2007).

141. Hirel, P., Schmitter, M., Dessen, P., Fayat, G. & Blanquet, S. Extent of N-terminal methionine excision from *Escherichia coli* proteins is governed by the side-chain length of the penultimate amino acid. *Proc Natl Acad Sci U S A* **86**, 8247-51 (1989).
142. Lawrence, F., Blanquet, S., Poirer, M., Robert-Gero, M. & Waller, J. The mechanism of action of methionyl-tRNA synthetase. 3. Ion requirements and kinetic parameters of the ATP-PPi exchange and methionine-transfer reactions catalyzed by the native and trypsin-modified enzymes. *Eur J Biochem* **36**, 234-43 (1973).
143. Grogan, D. Exchange of genetic markers at extremely high temperatures in the archaeon *Sulfolobus acidocaldarius*. *J Bacteriol* **178**, 3207-11 (1996).
144. Richmond, M. The effect of amino acid analogues on growth and protein synthesis in microorganisms. *Bacteriol Rev* **26**, 398-420 (1962).
145. Hartley, R. Barnase and barstar: two small proteins to fold and fit together. *Trends Biochem Sci* **14**, 450-4 (1989).
146. Golbik, R., Fischer, G. & Fersht, A. Folding of barstar C40A/C82A/P27A and catalysis of the peptidyl-prolyl cis/trans isomerization by human cytosolic cyclophilin (Cyp18). *Protein Sci* **8**, 1505-14 (1999).
147. Kiick, K. University of Massachusetts Amherst (2001).
148. Kadner, R. Regulation of methionine transport activity in *Escherichia coli*. *J Bacteriol* **122**, 110-9 (1975).
149. Old, J. & Jones, D. A comparison of ethionine with methionine in *Escherichia coli* in vitro polypeptide chain initiation and synthesis. *FEBS Lett* **66**, 264-8 (1976).
150. Wang, A., Winblade Nairn, N., Johnson, R., Tirrell, D. & Grabstein, K. Processing of N-terminal unnatural amino acids in recombinant human interferon-beta in *Escherichia coli*. *Chembiochem* **9**, 324-30 (2008).
151. Chang, A. & Cohen, S. Construction and characterization of amplifiable multicopy DNA cloning vehicles derived from the P15A cryptic miniplasmid. *J Bacteriol* **134**, 1141-56 (1978).

152. Juhling, F. et al. tRNAdb 2009: compilation of tRNA sequences and tRNA genes. *Nucleic Acids Research* **37**, D159-D162 (2009).
153. Schmidt, T. & Skerra, A. The Strep-tag system for one-step purification and high-affinity detection or capturing of proteins. *Nat Protoc* **2**, 1528-35 (2007).
154. http://www.genscript.com/cgi-bin/tools/rare_codon_analysis. GenScript Rare Codon Analysis Tool.
155. Osawa, S., Jukes, T., Watanabe, K. & Muto, A. Recent evidence for evolution of the genetic code. *Microbiol Rev* **56**, 229-64 (1992).
156. Burgess-Brown, N. et al. Codon optimization can improve expression of human genes in Escherichia coli: A multi-gene study. *Protein Expr Purif* **59**, 94-102 (2008).
157. Ryu, Y. & Schultz, P. Efficient incorporation of unnatural amino acids into proteins in Escherichia coli. *Nat Methods* **3**, 263-5 (2006).
158. Richardson, J. Rho-dependent transcription termination. *Biochim Biophys Acta* **1048**, 127-38 (1990).
159. Young, T., Ahmad, I., Yin, J. & Schultz, P. An enhanced system for unnatural amino acid mutagenesis in E. coli. *J Mol Biol* **395**, 361-74 (2010).
160. Taki, M. et al. Leucyl/Phenylalanyl-tRNA-protein transferase-mediated chemoenzymatic coupling of N-terminal Arg/Lys units in post-translationally processed proteins with non-natural amino acids. *Chembiochem* **7**, 1676-9 (2006).
161. Watanabe, T., Miyata, Y., Abe, R., Muranaka, N. & Hohsaka, T. N-terminal specific fluorescence labeling of proteins through fourbase codon-mediated incorporation of fluorescent hydroxy acid. *Nucleic Acids Symp Ser (Oxf)*, 363-4 (2007).
162. Muranaka, N., Miura, M., Taira, H. & Hohsaka, T. Incorporation of unnatural non-alpha-amino acids into the N terminus of proteins in a cell-free translation system. *Chembiochem* **8**, 1650-3 (2007).
163. Goto, Y. et al. Reprogramming the Translation Initiation for the Synthesis of Physiologically Stable Cyclic Peptides. *ACS Chem Biol* (2008).

-
164. Connor, R., Piatkov, K., Varshavsky, A. & Tirrell, D. Enzymatic N-terminal Addition of Noncanonical Amino Acids to Peptides and Proteins. *Chembiochem* (2008).
 165. Heal, W. et al. Site-specific N-terminal labelling of proteins in vitro and in vivo using N-myristoyl transferase and bioorthogonal ligation chemistry. *Chem Commun (Camb)*, 480-2 (2008).
 166. Watanabe, T., Miyata, Y., Abe, R., Muranaka, N. & Hoshida, T. N-terminal specific fluorescence labeling of proteins through incorporation of fluorescent hydroxy acid and subsequent ester cleavage. *Chembiochem* **9**, 1235-1242 (2008).
 167. Goto, Y., Murakami, H. & Suga, H. Initiating translation with D-amino acids. *RNA* **14**, 1390-8 (2008).
 168. Hotelier, T. et al. ESTHER, the database of the alpha/beta-hydrolase fold superfamily of proteins. *Nucleic Acids Res* **32**, D145-7 (2004).
 169. Lepthien, S., Merkel, L. & Budisa, N. *In vivo* double and triple labeling of proteins using synthetic amino acids. *Angewandte Chemie International Edition in English* (in press).
 170. Abdeljabbar, D., Klein, T., Zhang, S. & Link, A. A single genomic copy of an engineered methionyl-tRNA synthetase enables robust incorporation of azidonorleucine into recombinant proteins in *E. coli*. *J Am Chem Soc* **131**, 17078-9 (2009).
 171. Hausmann, C.D. & Ibba, M. Aminoacyl-tRNA synthetase complexes: molecular multitasking revealed. *Fems Microbiology Reviews* **32**, 705-721 (2008).
 172. Conti, E. & Izaurralde, E. Nonsense-mediated mRNA decay: molecular insights and mechanistic variations across species. *Curr Opin Cell Biol* **17**, 316-25 (2005).
 173. Hirao, I. et al. An unnatural base pair for incorporating amino acid analogs into proteins. *Nat Biotechnol* **20**, 177-82 (2002).
 174. Dong, S., Merkel, L., Moroder, L. & Budisa, N. Convenient syntheses of homopropargylglycine. *J Pept Sci* **14**, 1148-50 (2008).
 175. <http://www.biology.utah.edu/jorgensen/wayned/ape/>.

-
176. Schmidt-Dannert, C., Sztajer, H., Stöcklein, W., Menge, U. & Schmid, R. Screening, purification and properties of a thermophilic lipase from *Bacillus thermocatenulatus*. *Biochim Biophys Acta* **1214**, 43-53 (1994).
 177. Söding, J., Biegert, A. & Lupas, A. The HHpred interactive server for protein homology detection and structure prediction. *Nucleic Acids Res* **33**, W244-8 (2005).
 178. Goldstone, D. et al. Structural and functional characterization of a promiscuous feruloyl esterase (Est1E) from the rumen bacterium *Butyrivibrio proteoclasticus*. *Proteins* **78**, 1457-69 (2010).
 179. Kiss, A. et al. The acylaminoacyl peptidase from *Aeropyrum pernix* K1 thought to be an exopeptidase displays endopeptidase activity. *J Mol Biol* **368**, 509-20 (2007).
 180. Bertrand, T. et al. Structural basis for human monoglyceride lipase inhibition. *J Mol Biol* **396**, 663-73 (2010).
 181. Eswar, N. et al. Comparative protein structure modeling using Modeller. *Curr Protoc Bioinformatics* **Chapter 5**, Unit 5.6 (2006).
 182. Corpet, F. Multiple sequence alignment with hierarchical clustering. *Nucleic Acids Res* **16**, 10881-90 (1988).